The Pennsylvania State University

The Graduate School

College of Engineering

ELASTO-PLASTIC ANALYSIS OF CORRUGATED SANDWICH STEEL PANELS

A Thesis in

Civil Engineering

by

Wan-Shu Chang

Submitted in Partial Fulfillment
of the Requirements
for the Degree of

Doctor of Philosophy

August 2004

The thesis of Wan-Shu Chang was reviewed and approved* by the following:

Theodor Krauthammer
Professor of Civil Engineering
Thesis Advisor
Chair of Committee

Eduard S. Ventsel
Professor of Engineering Science and Mechanics
Thesis Co-Advisor

Sabih I. Hayek
Distinguished Professor Emeritus of Engineering Mechanics

Vijay K. Varadan
University Distinguished Professor of Engineering Science and Mechanics

Andrew Scanlon
Professor of Civil Engineering
Head of the Department of Civil Engineering

*Signatures are on file in the Graduate School

ABSTRACT

In this study, the elasto-plastic analysis of a corrugated-core sandwich plate has been developed. The developed study based on generalized Galerkin method (or Navior method for simply supported edges) and incremental theory of plasticity with the initial incremental plastic moments calculated by an iterative procedure can be applied in both elastic perfectly-plastic and strain-hardening behaviors. However, due to currently absent experimental data of the post yield behavior of corrugated-core sandwich plates, in these numerical studies, only the behaviors of elastic perfectly-plastic cases were analyzed in this work.

Also, a comprehensive stress analysis for corrugated-core plates is developed. The effects of geometric parameters and various lengths and widths of corrugated-core sandwich plates with all simply supported boundary conditions on the plate behavior and strength were studied. Some new phenomena observed in experimental investigations of corrugated-core sandwich plates, but not found in previous numerical analysis, have been confirmed and reported. In particular, our investigation has strengthened some experimental results obtained in (Tan et al. 1989) which lacked supported from 3D FEM, and the other analytical solutions.

TABLE OF CONTENTS

LIST OF FIGURES

LIST OF TABLES

ACKNOWLEDGEMENTS

I would like to express my sincere gratitude and profound thanks to my advisors, Professor Ted Krauthammer and Professor Edward S. Ventsel, for their remarkable patience, valuable encouragement and advice throughout all the stages of this work. The great care with which they have read the manuscript, their numerous suggestions for improvements of the English style, as well as helpful technical comments, are greatly appreciated.

I would also like to thank the members of my doctoral committee, Dr. Sabih I Hayek, Dr. Andrew Scanlon, and Dr. Vijay K. Varadan, for their valuable advice and review during the course of research. I also want to express my gratefulness to all the members of the Protective Technology Center at the Penn State University for their help and support.

Finally, I wish to thank my wife, Ching-Yi, for the full support she gave to me. This work would not have been possible without the affection and sacrifice of my family; my parents in Taiwan and lovely son, Ethan. This study is dedicated to them.

Chapter 1

Introduction

1.1 Background and Problem Statement

A close-to-analytic solution is proposed for the elasto-plastic analysis of corrugated-core sandwich plate bending. The 3-dimensional (3D) sandwich panel will be reduced to an equivalent 2D structurally orthotropic thick plate continuum. In this analysis, the Galerkin method and the incremental method with initial plastic moments are employed to solve the elasto-plastic problem.

For many years, the analysis and design of structures have been based on the linear theory of elasticity with the assumption of isotropic material properties, but it is well known that this approach is unduly conservative because it fails to take advantage of the ability of many materials to carry stresses above their yield stresses. The main difficulty of plastic analysis is the mathematical complexity. However, that difficulty has been overcome by the advent of high-speed computers and the efficient use of computational methods.

A sandwich plate shown in Figure **1-1** is a three-layer structure, comprised of a thick core between two thin, flat face sheets. Generally, the face plates are made of high-strength materials and the core is made of a low strength and density. Due to the high-

strength faces and low-weight core, the significant feature of this structure is its high strength to weight ratio.

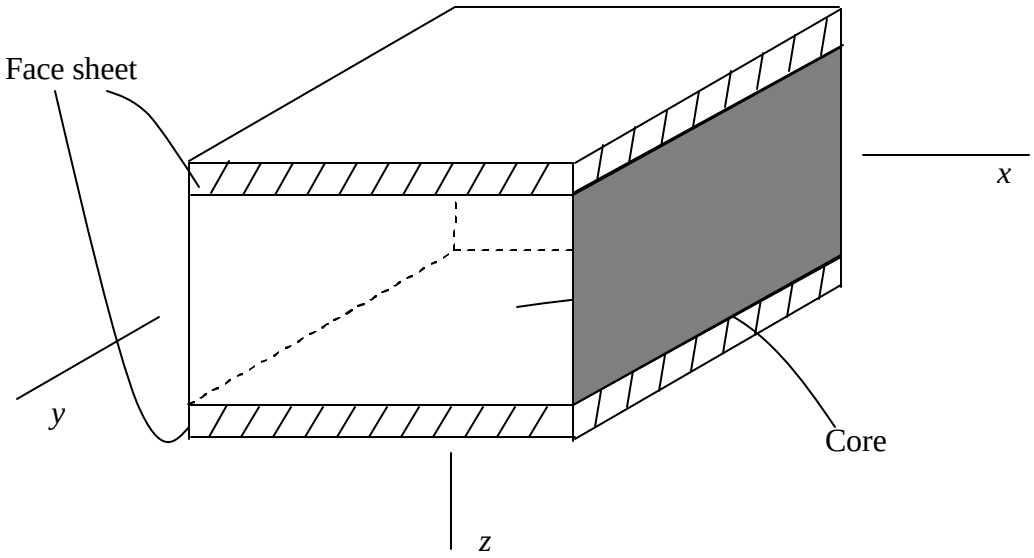

Fig. 1-1: A sandwich plate

The advantages of sandwich plates are summarized as follows:

1. High stiffness and strength to weight ratios.
2. The good surface finish reduces an aerodynamic resistance.
3. Good thermal and acoustic insulation.
4. High energy absorption capability with different fillers and cores.
5. Increase the interior space and ease of equipment installation.

A corrugated-core sandwich plate is shown in Figure **1-2**. To analyze the bending behavior of the corrugated-core sandwich plate, the following assumptions are made:

1. The plate is symmetrical type corrugated-core sandwich plate shown in Figure **1-2**. Therefore, both face plates are identical in material and thickness.
2. The material of the corrugated-core sandwich plate is isotropic.
3. The deformation of this plate is small.
4. Facing plates are thin compared with the corrugation depth. Consequently, the local bending stiffness of the face sheets is negligible.
5. The core contributes to the panel flexural stiffness in the *x*-direction but not in the *y*-direction.
6. The elastic modulus of the plate in the *z*-direction is assumed to be infinite.
7. The core can resist the transverse shear stresses and also contribute to the flexural and extensional stiffness.
8. The transverse shortening of the core is ignored.

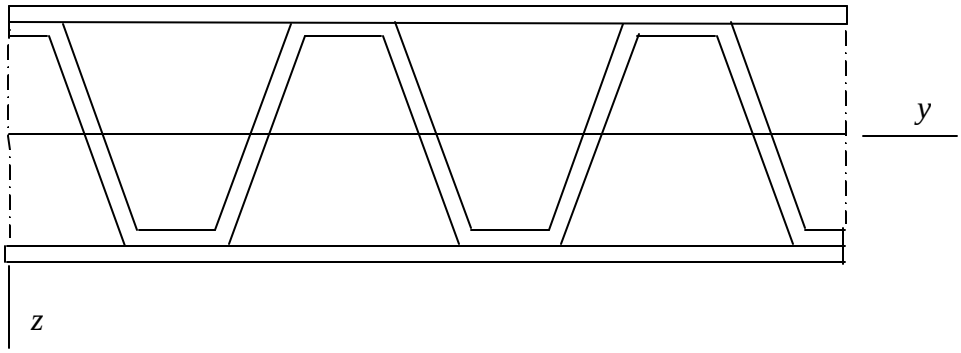

Fig. 1-2: Symmetrical type of a corrugated-core sandwich plate

The basis for this corrugated-core sandwich plate bending problem is the Reissner-Mindlin plate theory. In this theory, straight material lines normal to the middle surface are assumed to remain straight, but not necessarily normal to the middle surface during distortion of the plate. Namely, the three independent degrees of freedom correspond to the deflection w and the slopes q_x and q_y. w is the deflection in z-direction (i.e. the direction of thickness). q_x and q_y are the slopes of the xz- and yz-planes, respectively.

Due to several elastic constants derived by Libove and Hubka (1951), the 3D corrugated-core flat sandwich plate here can be regarded as a 2D equivalent continuum. The governing equations for the elasto-plastic analysis of corrugated-core sandwich plates are made by approximating them with continuous structurally orthotropic structures. The Galerkin method and the incremental theory of plasticity approach with initial plastic moments are employed to solve this problem. An iterative method is then used to evaluate the incremental plastic moments in each stage. In this elasto-plastic analysis, the material maintains a linear elastic behavior until yield. Then, yield condition, flow rule, and strain-hardening rule are used to calculate stress and plastic strain increments.

It can be seen in literature reviews that recently the finite element method (FEM) is widely used in the elasto-plastic analysis. FEM is now firmly accepted as the most powerful numerical technique in engineering. Tan et al. (1989) showed experimentally that for the 3D corrugated-core sandwich plate, the 3D FEM model agreed well with

measured deflections in linear elastic range. However, in the moment analysis, there are discrepancies between the 3D FEM and experimental results (Tan et al. 1989). In the experimental results, the signs of moments in *x*- and *y*-directions are opposite, but the 3D FEM showed the same signs in the studied case. In addition, it is very difficult to modify the boundary conditions where using the 3D FEM.

1.2 Importance

The theory of elasticity cannot be used to address the behavior after material yielding occurs. Furthermore, an elasto-plastic analysis of corrugated-core sandwich plates is currently unavailable. Therefore, the procedure for the elasto-plastic analysis of sandwich plates was developed in this study.

Also, the yield criteria for naturally isotropic and anisotropic materials have been developed and applied previously. However, because the corrugated-core sandwich plate is a structurally orthotropic system, there is no yield criterion for such a structure. Therefore, a yield criterion for structurally orthotropic constructions was developed in this study. Hill's and Ilyushin's yield criteria were modified and extended to include structurally orthotropic constructions.

1.3 Objectives

The main goal of this study is to enable the development of plastic analysis of corrugated-core sandwich plates. The three key issues that need to be considered in this elasto-plastic analysis are reliable elastic analysis, yield criterion, and appropriate constitutive descriptions. Hill's yield criterion developed for the naturally anisotropic material will be extended to include structurally orthotropic constructions.

The results obtained from linear elastic analysis by the above-developed solution of the corrugated-core plate with all simply supported boundaries are compared with the results provided by other authors (e.g. Tan et al. 1989) before proceeding to analyze the elasto-plastic problem. The elasto-plastic solution begins on a linear elastic analysis. The linear analysis is also developed and is mainly to check the results.

The behavior of a plate is related to its' stiffness. Several geometric parameters might contribute to the stiffness of the corrugated sandwich panel. The effects of geometric parameters such as ratio of face to core thickness, ratio of pitch to core depth, the core depth to core thickness ratio, and corrugation angle and the length in corrugation direction and the width in the direction normal to corrugation are analyzed.

1.4 Scope

This research is limited to only the elastic perfectly-plastic analysis of rectangular corrugated-core sandwich plates with all simply supported edges. The theoretical

formulation can be adapted to elastic perfectly-plastic and strain-hardening problems; however, in this study, only elastic perfectly-plastic problem will be considered.

Furthermore, it is also very important to know what geometric parameters in the corrugated-core sandwich plate will affect the behaviors of that plate significantly. Different geometric parameters such as the corrugation angle (α), the ratio of core to facing sheet thickness (t_c/t_f), the ratio of corrugation pitch to core depth (p/h_c), and the core depth to core thickness ratio (h_c/t_c) and various lengths and widths are investigated.

1.5 Thesis Layout

This thesis has five chapters. Chapter One is a brief introduction to the concept, and also lists the scope and objectives. Chapter Two is the review of previous work for sandwich plates, elasto-plastic analysis, and numerical methods. The theoretical methodology is presented in Chapter Three. Chapter Four contains analysis and numerical examples to compare and investigate the effects of different geometric parameters. Chapter Five contains the conclusion and recommendations for future work in this work.

Chapter 2

Literature Review

2.1 Plate Bending Theories

Several plate bending theories have been developed in the past decades. Two widely used theories of these plate bending theories are Kirchhoff's theory also well known as the classical theory (or thin plate theory) and Reissner theory. The linear Kirchhoff theory assumed that there is no deformation in the middle plane of the plate and the straight line normal to the middle plane remains the normal to the middle surface after deformation. According to the Kirchhoff assumption, the transverse shear strains and stresses, as well as stress normal to the plate midsurface are neglected in the classical plate theory.

Reissner (1945) modified the classical theory (or Kirchhoff's theory). He proposed that the rotations of normal to the plate midsurface in the *xz*- and *yz*- plane could be introduced as independent variable in the plate theory. Mindlin (1951) simplified Reissner's assumption that normal to the plate midsurface before deformation remains straight but not necessary normal to the plate after deformation and the stress normal to the plate midsurface is disregarded as in the Kirchhoff theory. This plate bending theory modified by Reissner and Mindlin is well known as the Reissner-Mindlin plate theory. The Reissner-Mindlin plate theory is suitable to analyze both thin and

moderately thick plates. The analysis of the corrugated-core sandwich plates in this thesis is based on this theory.

2.2 Sandwich Plates

2.2.1 Development of Sandwich Constructions

Sandwich panels are extensively and increasingly used due to its lightweight advantage in civil engineering, aerospace engineering, and shipbuilding industry where weight is an important design issue. With the variety of faces and cores, the sandwich panels have wide applications in many fields such as acoustic and thermal insulation and fire safety. Therefore, the sandwich panels have been used commercially in exterior walls and internal partition walls in architectural engineering. The detail introduction of applying sandwich panels in engineering is directly in (Davies 2001; Karbhari 1997)

With the advent of high-speed flight, sandwich plates were widely used in airplane design because of the promised high strength and the well-finish surface maintaining aerodynamically smooth surface. Also, the sandwich construction can be a possible substitute for sheet-stringer to reduce the weight of an aircraft. Recently, the US Navy has been studying application of the laser-welded corrugated-core sandwich constructions (Marsico et al. 1993; Wiernicki et al. 1991). These applications cover bulkheads and decks on accommodation areas, deckhouses, deck edge elevator doors, and hangar by division doors.

The advantage of using two faces separated by a distance is thought to have been first discussed by Duleau, French, in 1820. This concept was first applied commercially after 100 years. After World War Two, due to the blossoming of aviation, there was an increased interest in sandwich construction. In the late 1940s, Gough et al. (1940) and Williams et al. (1941) published the pioneer theoretical works on structural sandwich constructions.

The core of the sandwich construction keeps the faces apart and stabilizes them by resisting vertical deformations, and also enables the whole structure to act as a single thick plate as a virtue of its shear strength. The second feature that characterizes the sandwich construction is its outstanding strength. In addition, the core carries a portion of the bending load. Therefore, sandwich panels are commonly used in aviation, aerospace, civil engineering and other applications where weight is an important design issue due to its exceptionally high flexural stiffness-to-weight ratio.

Development of core materials has continued from 1940s through to today in an effort to reduce the weight of sandwich panels. Many sandwich-type configurations employing different production techniques have been suggested. In general, sandwich cores could be classified into four types: (a) foam or solid core, (b) honeycomb core, (c) web core, and (d) corrugated or truss core. Most popular materials of sandwich cores are soft and light. In most foam and honeycomb core sandwich panels all the in-plane and bending loads are assumed to be carried by the faces only. However, in web and

corrugated-core constructions, a portion of the in-plane and bending loads are also carried by the core.

Plate theories applicable to general sandwich plates for small deflection have been developed by Libove and Batdorf (1948) for flat panels and by Stein and Mayers (1950) for curved panels. In these two papers, deflections due to transverse shear are taken into account and sandwich plates are regarded as structurally orthotropic panels because the face sheets or core (or both) may have orthotropic stretching properties in general. To reduce a 3D sandwich construction to a 2D equivalent continuum, seven physical constants are introduced in flat plates. They include the transverse shear stiffness D_{Qx} and D_{Qy}, the bending stiffness D_x and D_y, a twisting stiffness D_{xy}, and the Poisson ratios u_x and u_y.

In 1960s, studies in sandwich construction had spread widely. Plantema (1966) published the first book on sandwich construction in 1966. In 1969, the book by Allen (1969) followed. In the early work up through the 1960s, including these two books written by Plantema and Allen, a nomenclature and analytical presentation of sandwich panels was developed.

A book by Zenkert (1995) supplements with more examples and solved problems contained in the Plantema and Allen books. A review by Noor et al. (1996) provided over 800 relevant references that were all discussed in that review and another 559 references as a supplemental bibliography. In this review recent developments in the computational

modeling of sandwich plates and shells are introduced. Vinson (1999) published a textbook for sandwich structural analysis. Later, Vinson (2001) had given an extensive list of 179 references to provide a review of several aspects of sandwich structures. Almost all important literatures on the subject of sandwich structures can be found in that review.

2.2.2 Corrugate-Core Sandwich Plates

Most popular materials of sandwich cores are soft and light such as balsa wood and foam. Conventional forms of sandwich cores are honeycomb-shaped. Honeycomb cores currently provide the greatest shear strength and stiffness to weight ratios but require special care in ensuring adequate bonding to the facing sheets.

In the early literature on the instability of sandwich constructions, much attention was devoted to wrinkling phenomena. This type of failure is made possible by the finite resistance of the core to deformations perpendicular to the faces and is of special importance when the core is made of an expanded material. However, modern sandwich cores are made of high strength materials that have a high resistance in this respect, such as a corrugated steel sheet. For the purposes of an analysis it can be assumed that the transverse normal stiffness of the core is infinitely large. The innovative corrugated-core sandwich plate consists of a corrugated sheet laser welded between two face sheets. Unlike soft honeycomb-shaped core, a corrugated core resists not only vertical shear but also bending and twisting. In this thesis, a corrugated-core sandwich plate is analyzed. A

corrugated-core sandwich plate is consisted of two facing plates and a corrugation core shown in Figure **2-1**. In general, both facing plates and corrugation are made of the same material. The corrugated core is often stiff enough to contribute to the flexural rigidity.

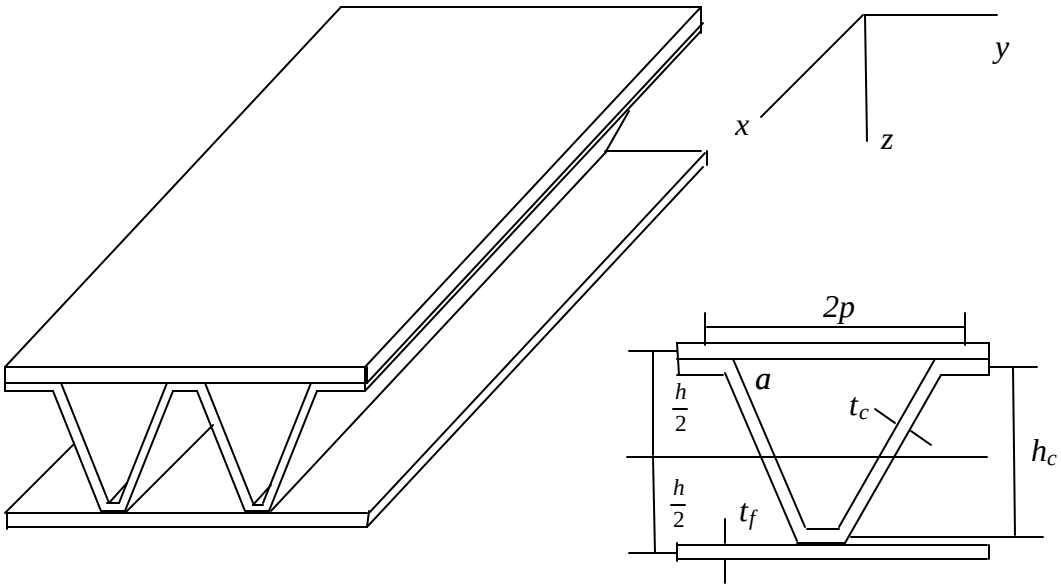

Fig. 2-1: **Corrugated-Core sandwich panel and a panel unit**

2.2.3 Previous Works on Corrugate-Core Sandwich Panels

In 1951, Libove and Hubka (1951) derived formulas for evaluating elastic constants of a corrugated-core sandwich plate. These elastic constants are necessary for the analysis of flat sandwich plate theory derived by Libove and Batdorf (1948). Also, those formulas for evaluating elastic constants are used in this elasto-plastic analysis in this thesis.

In the 1980s, through the early 1990s, several experiments of sandwich panels have been conducted in UK. Montague and Norris (1987) and Norris et al. (1989) studied the structural behavior of spot-welded and corrugated-core steel panels. Tan et al. (1989) published a paper on experimental testing of corrugated-core sandwich panels and compared the results with finite element method and the closed solution developed from the work of Libove and Bandorf (1948).

In these papers, various dimensional panels were analyzed. In the all around simply supported plate, both finite element analysis and the closed solution predicted the deflection well; however, in the predictions of bending stresses and moments, both solutions predicted the same sign on the facing plates in both x- and y-directions. These results conflicted with the experimental investigations that bending moment M_x and M_y have the opposite sign in some cases.

It is believed that the production difficulties prevent the wide use of steel corrugated-core sandwich panels. The main manufactured difficult is firmly joining face sheet to the corrugated core. Laser welding enables construction of steel corrugated-core sandwich constructions by welding from one side only. In 1989, configurations of laser-welded corrugated-core steel sandwich panels were tested by Forbes (1989) to illustrate behavior of the structure under compression, bending and shear. In that experiment, before extreme post-buckling deformation, no sample failed due to the failure of the laser-welded connection. Therefore, the laser weld shows the excellent capacity of joining faces to the core.

Recently, the corrugated-core sandwich panels are widely employed in the shipbuilding industry. The US Navy has studied application of the laser-welded corrugated-core sandwich panels since the 1990's (Marsico, 1993; Eiernicki, 1991). Also, in UK in 1991, Bird (1991) conducted several experiments to study static strength, fatigue, and blast trials on laser-welded steel sandwich panels. In these tests the properties of laser-welded steel sandwich panels have been shown to be adequate for ship construction. Also the corrugated-core panels have shown good blast characteristics and could be excellent for resisting fragmentation damage with incorporation of appropriate absorbent materials.

The third international conference on sandwich construction was held at Southampton, UK, in 1995. Couple papers were presented in that conference about the application and analysis of corrugated-core sandwich panels. Kattan (1995) and Kujala and Tuhkuri (1995) presented the capability of using laser-welded corrugated-core sandwich panels in shipbuilding. Those structures were found to be up to 40-50% lighter than the conventional steel grillages.

More recently, several different types of core have been investigated. Fung et al. studied the C-core (1993; 1996) and Z-core (Fung et al., 1994) sandwich panels. In 2001, Lok et al. (2000) introduced a truss-core sandwich panel and studied its elastic stiffness properties and behavior. A truss core is very similar to a corrugated-core in the outlook. The difference between those two structures is that the corrugation is a continuous structure but the truss core is assembled by two inclined plates in a panel unit.

2.3 Elasto-Plastic Analysis

Hill (1950) introduced the further concept of plastic anisotropy into the theory of plasticity by Mises. He also proposed a yield criterion constituting a generalization of the Huber-Mises criterion. Olszak and Urbanowski (1956) introduced the anisotropic parameters, the tensor moduli of plasticity, into the plastic potential and yield criterion for perfectly plastic materials. Hu (1956) extended the theory for strain-hardening materials. These anisotropic parameters vary as the material strain-hardens as was first pointed out by Hill (1950) and was later used by Jensen et al. (1966) for a shear lag problem.

The nonlinear difficulty created by mathematical complexity has been overcome by the advent of high-speed computers and the efficient use of computational methods. The formulation and solution of the incremental problem in elastic-plastic solids is a fundamental problem in plasticity. Finite element method and boundary element method are well-known for the solution of this type of problems and solutions can be carried out in standard finite element and boundary element codes.

Beginning with the 1970s, the advent of structural mechanics dealing with laminated structures shifted attention of researchers to orthotropic plates and much work has been done in characterizing elasto-plastic analysis of these plates. All sandwich panels can be regard as laminated structures. One face is the lamina 1, the core is lamina

2, and the other face is lamina 3. The theory of laminate can be applied in all sandwich structures. Those idea and advantages have been discussed by Vinson (1999).

Many papers in elasto-plastic analysis of composite plates were published. In these studies, two approximate approaches, finite element method (Marcal and King 1967; Owen and Figueiras 1983a; Owen and Figueiras 1983b; Valliappan et al. 1976) and boundary element method (Karam and Telles 1992; Telles and Brebbia 1979; Telles 1983; Telles and Carrer 1991), were employed.

2.3.1 Finite Element Method

The finite element solution of elastic-plastic problems has been intensely developed since the 1960s and a number of different approaches have been proposed. A considerable literature exists on the elasto-plastic analysis using finite element method. Oden (1969) had given an extensive list of references that include the various investigations in the fields of material, geometric and combined nonlinear behavior of structures in 1969.

In the same year, Whang (1969) published a paper on elasto-plastic orthotropic plates and shells using finite element method. In that paper, a finite element method was developed for the elasto-plastic analysis for bi-linear strain-hardening orthotropic plates and shells. Two approaches, the initial stiffness approach and tangent stiffness approach, were presented and compared. Both applied the Huber-Mises yield function and the

Prandtl-Reuss flow rule. A generalized yield function for anisotropic material with the anisotropic parameters was used.

In 1980, Owen and Hinton (1980) published the book of finite elements in plasticity. In that book, the two-dimensional layer and non-layer structures were analyzed. The FEM procedures and programming dealing with the elastic-plastic materials were introduced.

2.3.2 Boundary Element Method

The boundary element method has been developed for several kinds of non-linear problems such as elasto-plasticity, viscoplasticity and creep. A book on boundary elements by Banerjee and Butterfield (1981) provided solutions for elasto-plastic problems of two or three dimensions by means of initial strain or stress. In 1986, Moshaiov and Vorus (1986) published a paper on plate bending problem by boundary element method and incremental theory with initial plastic moments.

Whether using finite element or boundary element methods to solve elasto-plastic problems, an incremental approach must be applied in which the loading is divided into increments after the yielding occurs.

2.4 Yielding Criteria

An accurate yielding function is the key factor for the accuracy of the plastic analysis. The yield criterion determines the stress level at which plastic deformation begins. Numerous criteria have been proposed for the yielding of materials. The most widely used criteria are the Tresca maximum shear criterion and the von Mises yield criterion. Those two criteria have the significant agreement with experimental predictions and closely approximate metal plastic behavior. In this section, those two criteria are briefly introduced. The detail of those yielding surfaces can be found in several references (e.g. Lubliner 1990; Mendelson 1983; Shames and Cozzarelli 1992).

The projections of Tresca and von Mises yield surfaces in the π-plane are regular hexagon and circle, respectively, as shown in Figure **2-2**(a). In (σ_1-σ_3) and (σ_2-σ_3)-plane those are irregular hexagon and ellipse, respectively, as shown in Figure **2-2**(b). Generally, the Tresca yield surface is a regular hexagon inscribed within the von Mises yield surface.

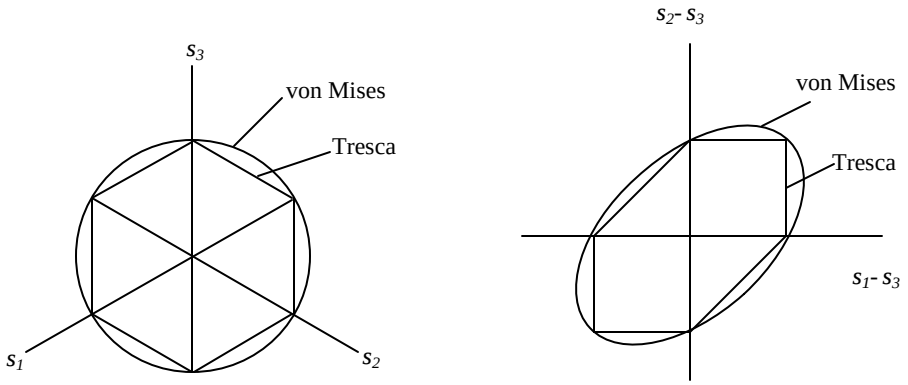

(a) p-plane (b) (s_1-s_3) (s_2-s_3)-plane

Fig. 2-2: Projections of the von Mises and Tresca yield surfaces

In Figure **2-2**, it can be seen that the Tresca yield criterion is linear between segments. The singularities on the principal axes make the plasticity difficult. Some difficulties regarding the direction of plastic flow arise at the corners of the hexagon. Singular yield surface with corners has been discussed by Koiter (1953, 1960). Generally, the plastic analysis as based on the smooth von Mises yield surface seems to be more appropriate for the numerical discussion. Also, the von Mises yield criterion usually fits the experimental data better than other criteria.

2.4.1 Tresca Criterion (Maximum Shear Theory) (Doltsinis 2000; Kachanov 1971)

The Tresca criterion is the historically oldest. This theory assumes that the plastic deformation occurs when the magnitude of the maximum shear stress over all planes reaches a critical value. The limit value can be determined by simple tension experiment. This criterion may be written in the following:

$$\begin{aligned} 2|t_1| &= |s_2 - s_3| \le 2k \\ 2|t_2| &= |s_3 - s_1| \le 2k \\ 2|t_3| &= |s_1 - s_2| \le 2k \end{aligned} \qquad \textbf{(2.1)}$$

Where

f some function

k a material parameter to be determined experimentally

s_1, s_2, s_3 principal stresses

t_1, t_2, t_3 shear stresses

The forms Eq. **2.1** are not unique and not an analytic function. It can be rewritten as:

$$f = \left[(s_1 - s_2)^2 - 4k^2\right]\left[(s_2 - s_3)^2 - 4k^2\right]\left[(s_1 - s_3)^2 - 4k^2\right] \qquad \textbf{(2.2)}$$

The above form has the advantage of being analytic and, moreover, it can be expressed in terms of the principal stress-deviator invariants J_2 and J_3.

$$f = 4J_2^3 - 27J_3^2 - 36k^2J_2^2 + 96k^4J_2 - 64k^6 \qquad \textbf{(2.3)}$$

According to Eq. **2.3**, to apply the Tresca criterion, one major difficulty of is that it is necessary to know in advance the maximum and minimum principal stresses. Or it will suffer from the great complexity of the Tresca criterion in its general form, Eq. **2.3**. Only in the case that the maximum and minimum principal stresses are known a priori can the Tresca criterion be reduced into a simple form.

2.4.2 von Mises Criterion (Distortion Energy Theory)

von Mises suggested that yielding occurs when the second deviatoric stress invariant, J_2, reaches a critical value. Or it is called the distortion energy theory. This theory assumes that yielding begins when the distortion energy equals the distortion energy at yielding in simple tension. An analytic form of the Mises yield function (Calcote, 1968) is

$$f = J_2 - k^2 \qquad (\mathbf{2.4})$$

Or

$$f = \frac{1}{6}\left[(s_1 - s_2)^2 + (s_2 - s_3)^2 + (s_3 - s_1)^2\right] - k^2 \qquad (\mathbf{2.5})$$

Where

f some function

J_2 the second deviatoric stress invariant

s_1, s_2, s_3 principal stresses

k a material parameter to be determined experimentally

A physical meaning of the constant k can be obtained by considering the yielding of materials under simple stress states. In terms of the stress component referred to the x-, y-, and z- axes, the von Mises yield criterion may be written as:

$$(s_x - s_y)^2 + (s_y - s_z)^2 + (s_z - s_x)^2 + 6(t_{xy}^2 + t_{yz}^2 + t_{xz}^2) = 6k^2 \qquad (\mathbf{2.6})$$

Where

s_x, s_y, s_z stresses in x-, y-, and z- directions, respectively

t_{xy}, t_{yz}, t_{xz} shear stresses

Hill (1950) generalized the von Mises yield criterion for isotropic materials to include anisotropic materials. He assumed the yield criterion to be a quadratic in the stress components as given by

$$2f(s_{ij}) = F(s_y - s_z)^2 + G(s_z - s_x)^2 + H(s_x - s_y)^2 + 2Lt_{yz}^2 + 2Mt_{zx}^2 + 2Nt_{xy}^2 = 1 \quad (\mathbf{2.7})$$

Where

F, G, H, L, M, N material anisotropic parameters

For most metals von Mises criterion fits the experimental result more closely that Tresca criterion. Throughout the elasto-plastic analysis in this thesis, the von Mises yield criterion is employed.

It should be noted that there is no yield criterion for structurally orthotropic plates. In the previous research, both von Mises and Tresca yield criteria deal with the naturally isotropic and aniosotropic materials. However, in this study, the structure is made of the isotropic material but the behavior of the structure is orthotropic. The Ilyushin yield surface, shown in Eq. **2.8** and expressed in terms of dimensionless stress resultant, is considered and modified to the structurally orthotropic plate.

$$\left(\frac{M_1}{M_0}\right)^2 + \left(\frac{M_2}{M_0}\right)^2 - \left(\frac{M_1}{M_0}\right)\left(\frac{M_2}{M_0}\right) + 3\left(\frac{M_{12}}{M_0}\right)^2 = 1 \quad (\mathbf{2.8})$$

Because of the structural type, the behaviors of the structurally orthotropic plate are different in both the corrugation direction and the direction normal to the corrugation. The yield criteria developed for the naturally anisotropic material are not appropriate in this analysis. However, it seems that the empirical data of structurally orthotropic plates for the post yield behaviors are not available. Therefore, several physical assumptions are reasonably made in this study and introduced in Chapter three and these assumptions coincide with the naturally anisotropic material.

2.5 Plastic Stress-Strain Relations

A more complicated distinction between elastic and plastic stress-strain relations arises from the fact that in the elastic range, the strains are unique and can be determined by the stress; therefore, for a given set of stresses we can calculate the strains by using Hooke's law without any regard as to how the stress state was reached; however, in general, in the plastic range, the strains are not uniquely determined by the stresses but depend on the history of loading or the stresses state.

Because of the dependence of the plastic strains on the loading path, it is necessary to calculate the increments of plastic strain throughout the loading history and then obtain the total strains by summation. However, there is at least one important class of loading paths for which the plastic strains are independent of the loading path and depend only on the final state of stress. These are called proportional loading paths, in which all the stresses increase in the same ratio. These will be discussed subsequently.

2.5.1 Incremental Theory of Plasticity (Plastic Flow Rule) (Mendelson 1983)

In general, the incremental theory is considered as the correct phenomenological theory of plasticity. The process of deformation in plastic stage is irreversible. The equations of the theory of plastic flow establish a connection between infinitesimal increments of strain and stress, the stresses themselves and certain parameters of plastic state. The total strain increments are combined the increments in elastic strains and plastic strains and shows as follow:

$$de = de^{e} + de^{p} \qquad (\mathbf{2.9})$$

Where de^{e} is the increment in elastic strain components and is connected with the increment in elastic stress according to Hooke's law. de^{p} is the increment in plastic strain components and can be expressed by the flow rule:

$$de_{ij}^{p} = \frac{\partial g}{\partial s_{ij}} dl \qquad (\mathbf{2.10})$$

Where dl is a positive scalar that depends on the stress increment. The function g, defining the ratios of the components of the plastic strain increment, is known as the plastic potential. In the view of the similarity of the properties of the yield function and the plastic potential, it is generally assumed that they are actually identical.

The flow rule obtained on the basis of identity of plastic potential and yield function is known as the associated flow rule for the given yield criterion. There are two particular stress-strain relations associated with von Mises yield criterion and known as: (a) Levy-Mises equations and (b) Prandtl-Reuss equations.

(a) Levy-Mises Equations

Levy first introduced the general three-dimensional equations relating the increments of total strain to the stress deviations in 1870. Also, in 1913, these equations were given independently by von Mises. These are known as the Levy-Mises equations. These equations are shown as follows:

$$\frac{de_x}{S_x} = \frac{de_y}{S_y} = \frac{de_z}{S_z} = \frac{de_{yz}}{t_{yz}} = \frac{de_{zx}}{t_{zx}} = \frac{de_{xy}}{t_{xy}} = dl \qquad (\mathbf{2.11})$$

or

$$de_{ij} = S_{ij}\, dl \qquad (\mathbf{2.12})$$

Where

S_{ij} the stress deviator tensor

dl nonnegative constant which may vary through out the loading history

In these equations the elastic strains are assumed to be ignored and the total strain increments are assumed to be equal to the plastic strain increments. Therefore, these equations can be applied to large plastic flow so that the elastic strains can be neglected and cannot be used in the elasto-plastic transitional range.

(b)Prandtl-Reuss-Equations

Instead of the Levy-Mises equations, Prandtl and Ruess included both elastic and plastic components of strains in the generalization of Eq. **2.11**. Reuss assumed that the plastic strain increment is proportional to the instantaneous stress deviation at any instant of loading. The equations are as follows:

$$\frac{de_x^p}{S_x} = \frac{de_y^p}{S_y} = \frac{de_z^p}{S_z} = \frac{de_{xy}^p}{t_{xy}} = \frac{de_{yz}^p}{t_{yz}} = \frac{de_{zx}^p}{t_{zx}} = dl \qquad (\mathbf{2.13})$$

or

$$de_{ij}^p = S_{ij}\, dl \qquad (\mathbf{2.14})$$

Eq. **2.11** can be regarded as a special case of Eq. **2.13** where the elastic strains are neglected. The theory in which the plastic strains are governed by Eq. **2.12** or Eq. **2.14** is known as the incremental or flow theory of plasticity. We can apply von Mises yield criterion, the equivalent or effective stress s_e, and the equivalent or effective plastic strain increment de_p into the Prandtl-Ruess equations. Then, the constant dl can be written as:

$$dl = \frac{3}{2}\frac{de_p}{s_e} \qquad (\mathbf{2.15})$$

and the stress-strain relations become:

$$de_x^p = \frac{de_p}{s_e}\left[s_x - \frac{1}{2}(s_y + s_z)\right]$$

$$de_y^p = \frac{de_p}{s_e}\left[s_y - \frac{1}{2}(s_z + s_x)\right] \qquad (\mathbf{2.16})$$

$$de_z^p = \frac{de_p}{s_e}\left[s_z - \frac{1}{2}(s_x + s_y)\right]$$

$$de_{xy}^{p} = \frac{3}{2}\frac{de_{p}}{s_{e}} t_{xy}$$

$$de_{yz}^{p} = \frac{3}{2}\frac{de_{p}}{s_{e}} t_{yz} \qquad (\mathbf{2.17})$$

$$de_{zx}^{p} = \frac{3}{2}\frac{de_{p}}{s_{e}} t_{zx}$$

or

$$de_{ij} = \frac{3}{2}\frac{S_{ij}}{s_{e}} de_{p} \qquad (\mathbf{2.18})$$

The Prandtl-Ruess stress-strain relation is well known as the most satisfactory basis for dealing with plastic analysis when anisotropy and Bauschinger effect are secondary importance (Chakrabarty, 1987); however, the incremental theory generally leads to mathematical complexities.

2.5.2 Deformation Theory

In contrast to the incremental or flow theories, Hencky proposed total stress-strain relations in 1924. Considerable simplifications are often achieved by using the deformation theory. The components of the total plastic strain are taken to be proportional to the corresponding deviatoric stresses. The plastic strain relation proposed by Hencky can be written as:

$$e_{ij}^{p} = lS_{ij} \qquad (\mathbf{2.19})$$

Where l is positive during loading and zero during unloading. From Eq. **2.19**, the plastic strain is a function only of the current state of stress and is independent of the loading path.

It can easily be proved that for the case of proportional loading, i.e., if all the stresses are increasing in a ratio, the incremental theory described previously can reduce to the deformation theory. The verification can be found in (Kachanov 1971; Mendelson 1983). Furthermore, Budiansky (1959) proposed that there are a range of loading paths other than proportional loading for which the general requirements of plasticity theory are satisfied by deformation theories.

2.6 Methods of Analysis

The main difficulty of plastic analysis is the mathematic complexity. However, that difficulty has been overcome by advent of high-speed computers and the efficient use of computational methods. In this numerical analysis, the general Galerkin method, direct iteration, and initial stiffness approach are employed.

2.6.1 The Galerkin method

The Galerkin method can be employed successfully to diverse types of plate bending problems. The main idea of this method is minimizing errors by orthogonalizing with respect to the assigned set of trial functions and reducing the system of differential

equations into a system of algebraic equations (Giri and Smitses 1980; Niyogi 1973). By applying the Galerkin method, Bennett (1971) studied the nonlinear vibration of unsymmetrical angle-ply plates. This method can yield a very easy and fast solution. The detail treatment can be found in (Ventsel and Krauthammer 2001) or any plate bending theory monograph.

2.6.2 Initial stiffness approach

The mathematical programming concepts to incremental elastic-plastic analysis have been discussed by Martin et al. (1987). There are two approaches, initial stress and initial strain approaches. The initial stiffness approach (Owen and Figueiras 1983a; Owen and Figueiras 1983b) has been developed and extensively used for elasto-plastic problem. Zienkiewicz et al. (1969) developed the finite element programming using the initial stress method. The initial plastic moment method developed by Moshaiov et al. (1986) has been adopted as the computational process in the proposed elasto-plastic analysis.

Chapter 3

Methodology

3.1 Introduction

In this chapter the elasto-plastic analysis of a corrugated-core sandwich plate is addressed. In general, the corrugated-core sandwich plate is made of an isotropic material. To develop a mathematical theory of plasticity, several idealizations of yield criterion are taken into account. First, it is assumed that the conditions of loading are such that all strain rate and thermal effects can be neglected. Secondly, the Bauschinger effect is disregarded. Finally, the material is assumed to be isotropic.

As mentioned previously, the 3D corrugated-core sandwich plate can be reduced to a 2D structurally orthotropic continuum using several elastic constants. The basic elasto-plastic material behavior in the two-dimensional structurally orthotropic plate must be presented before the numerical aspects. The Reissner-Mindlin plate theory is applied to this analysis; namely, the transverse shear deformation effects are taken into account for a sandwich plate subjected to static loads. Also, the von Mises' and Ilyushin's yield surfaces are considered and modified in this analysis.

The analysis is based on the Reissner-Mindlin plate theory. Therefore, three hypotheses of this theory are as follows:

1. The straight line normal to the middle plane of the plate remains straight but not necessarily normal to the middle plane when the plate is subjected to bending.
2. The transverse normal stress, s_z, is small when compared with the stresses s_x and s_y, i.e. the s_z can be neglected.
3. The middle plane remains unstrained subsequent to bending.

An elastic-plastic analysis based on the incremental theory of plasticity can be carried out into two stages, elastic and elasto-plastic steps. The elastic step is that the elastic solution where internal stresses and strains follow Hook's law and the elasto-plastic step is that this elastic system is modified to combine plastic strains. The plastic strain is defined as the difference between the total strain and the elastic strain. Unlike elastic solids, in which the state of strain depends only on the final state of stress, the plastic deformation is determined by the complete history of the loading. Therefore, the plastic problems are essentially incremental in nature. The detail will be discussed in the following sections.

3.2 Elastic Analysis

Before the onset of plasticity the relationship between stress and strain remains in the linear elastic stage. In elastic range, the strains are linearly related to the stresses by

Hook's law. We consider the corrugated-core sandwich plates with thin faces under the assumptions stated in Section **1.1**. It is assumed that the sheet faces work as membranes; namely, only the direct stresses that are uniformly distributed over the thickness act in the faces. The core contributes to the flexural stiffness in the corrugation direction, *x*-direction, but not in the direction normal to the corrugation, *y*-direction. The shear strain deformations of this plate are taken into account. Due to these elastic constants introduced by Libove and Batdorf (1948), the 3D corrugated-core sandwich plate can be reduced to a 2D structurally orthotropic plate.

3.2.1 Equilibrium Equations

A positive bending moment results in tensile stresses forming in the bottom fibers. Accordingly, all the moments and shear forces acting on the element in Figure **3-1** are positive. Consider the equilibrium of an infinitesimal element with length *dx* and width *dy* cut from the plate subjected to vertical distributing load of intensity $q(x, y)$ applied to an upper surface of the plate shown in Figure **3-1**. Since the stress resultants and the stress couples are assumed to be applied to the middle plane of this element, a distributed load $q(x,y)$ is transferred to the middle plane.

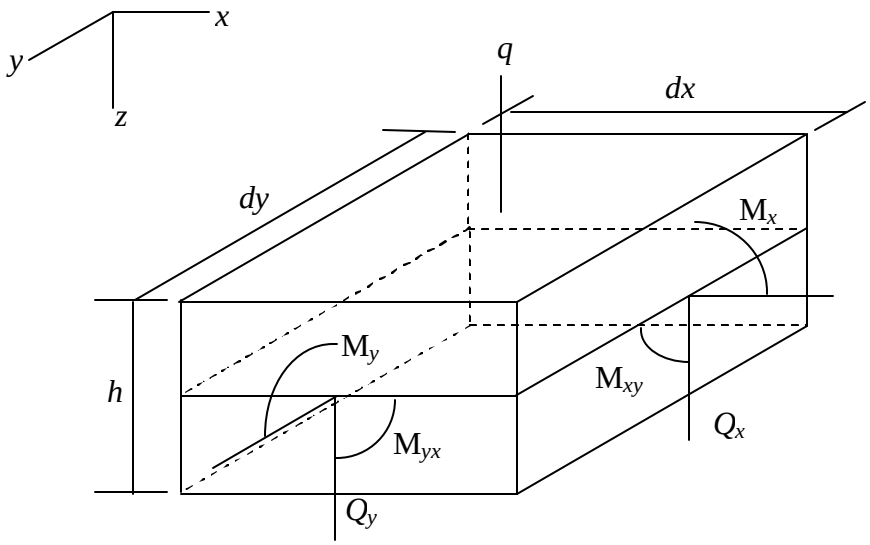

Fig. 3-1: Sign convention used in the plate analysis

We can take the equilibriums of moments about *x* axis and *y* axis and the sum of forces in *z* direction. Therefore, the following three independent conditions of equilibrium can be formed, respectively.

$$\frac{\partial M_x}{\partial x}+\frac{\partial M_{yx}}{\partial y}-Q_x=0 \qquad (\mathbf{3.1})$$

$$\frac{\partial M_{xy}}{\partial x}+\frac{\partial M_y}{\partial y}-Q_y=0 \qquad (\mathbf{3.2})$$

$$\frac{\partial Q_x}{\partial x}+\frac{\partial Q_y}{\partial y}+q=0 \qquad (\mathbf{3.3})$$

Where

M_x bending moment in the x-direction

M_y bending moment in the *y*-direction

M_{xy} twisting moment and $M_{yx}=M_{xy}$

Q_x transverse shear force in the *x*-*z* plane

Q_y transverse shear force in the *y*-*z* plane

q transverse load intensity

3.2.2 Curvature-Displacement Relations

According to the first Mindlin plate hypothesis in Section **3.1**, three independent degrees of freedom corresponding to the deflection *w* in *z*-direction and the angles of rotation q_x and q_y, which are not related to the deflection *w* are acquired for the plate problem. Therefore, we can obtain the curvature-displacement relationship as follows:

$$c_x = -\frac{\partial q_x}{\partial x},\ c_y = -\frac{\partial q_y}{\partial y} \tag{3.4}$$

$$c_{xy} = -\frac{1}{2}\left(\frac{\partial q_x}{\partial y} + \frac{\partial q_y}{\partial x}\right) \tag{3.5}$$

Where:

q_x and q_y slopes of the normal to the middle plane of the sandwich plate about the *y* and *x* axes, respectively. The above angles are assumed to be independent variables with respect to *w*

c_x curvature along the *x* axis

c_y curvature along the *y* axis

c_{xy} twisting curvature with respect to the *x* and *y* axes

3.2.3 Constitutive Equations

The 3D corrugated-core sandwich plate can be considered as a 2D structurally orthotropic construction due to several elastic constants. Thus, we can obtain the following bending moments, Eq. 3.6 and Eq. 3.7, and twisting moment relation, Eq. 3.8, for orthotropic plates by substituting curvature-displacement relations, Eq. 3.4 and Eq. 3.5, as follows:

$$M_x = \frac{D_x}{1-u_x u_y}\left(c_x + u_y c_y\right) = D_{xx}\left(c_x + u_y c_y\right) = -D_{xx}\left(\frac{\partial q_x}{\partial x} + u_y \frac{\partial q_y}{\partial y}\right) \tag{3.6}$$

$$M_y = \frac{D_y}{1-u_x u_y}\left(u_x c_x + c_y\right) = D_{yy}\left(u_x c_x + c_y\right) = -D_{yy}\left(\frac{\partial q_y}{\partial y} + u_x \frac{\partial q_x}{\partial x}\right) \tag{3.7}$$

$$M_{xy} = D_{xy} c_{xy} = -\frac{D_{xy}}{2}\left(\frac{\partial q_y}{\partial x} + \frac{\partial q_x}{\partial y}\right) \tag{3.8}$$

Where:

D_x and D_y flexural stiffnesses of the sandwich plate as a whole in the *xz* and *yz* planes, respectively.

D_{xy} twisting stiffness of the sandwich plate as a whole in the *xy* plane.

u_x and u_y Poinson's ratios in *x* and *y* axes, respectively.

Here $D_x u_y = D_y u_x$ and this has been derived by Libove and Batdorf (1951), and

$D_{xx} = \frac{D_x}{1 - u_x u_y}$ and $D_{yy} = \frac{D_y}{1 - u_x u_y}$, thus, $D_{xx} u_y = D_{yy} u_x$.

The shear forces can be expressed as Eq. 3.9 and Eq. 3.10:

$$Q_x = D_{Qx} g_{xz} = D_{Q_x} \left(-q_x + \frac{\partial w}{\partial x} \right) \quad \textbf{(3.9)}$$

$$Q_y = D_{Qy} g_{yz} = D_{Q_y} \left(-q_y + \frac{\partial w}{\partial y} \right) \quad \textbf{(3.10)}$$

Where

w deflection in *z*-direction.

D_{Qx} and D_{Qy} shear stiffnesses of plates in *xz* and *yz* planes, respectively.

As described previously, a 3D sandwich construction can reduce to a 2D structurally equivalent orthotropic plate due to the above elastic constants. These elastic constants, D_x, D_y, D_{xy}, D_{Qx}, and D_{Qy}, of corrugated-core sandwich plates were derived by

Libove and Hubka (1951). D_x and D_y are the flexural stiffness of the sandwich plate as a whole in the *xz* and *yz* coordinate planes, respectively, and D_{xy} is the twisting stiffness of the sandwich plate as a whole in the *xy* plane. They can be defined as Eq. **3.11**:

$$D_x = -\frac{M_x}{\partial^2 w / \partial x^2}; D_y = -\frac{M_y}{\partial^2 w / \partial y^2}; D_{xy} = \frac{M_{xy}}{\partial^2 w / \partial x \partial y} \qquad (\mathbf{3.11})$$

D_{Qx} and D_{Qy} are the shear stiffness of the sandwich plate as a whole in the *xz* and *yz* planes, respectively. They are defined as Eq. **3.12**:

$$D_{Qx} = \frac{Q_x}{g_{xz}}; D_{Qy} = \frac{Q_y}{g_{yz}} \qquad (\mathbf{3.12})$$

The detailed expressions of these elastic constants can be found in Appendix A.

3.2.4 Governing Equations

Substituting for the stress resultants and stress couples from Eq. **3.4** to Eq. **3.8** into Eq. **3.1** to Eq. **3.3**, we obtain the following system of governing differential equations for an orthotropic sandwich plate:

$$\left(D_{xx}\frac{\partial^2}{\partial x^2} + \frac{D_{xy}}{2}\frac{\partial^2}{\partial y^2} - D_{Q_x}\right)q_x + \left(\frac{D_{xy}}{2} + D_{xx}u_y\right)\frac{\partial^2 q_y}{\partial x \partial y} + D_{Q_x}\frac{\partial w}{\partial x} = 0 \qquad (\mathbf{3.13})$$

$$\left(\frac{D_{xy}}{2} + D_{yy}u_x\right)\frac{\partial^2 q_x}{\partial x \partial y} + \left(D_{yy}\frac{\partial^2}{\partial y^2} + \frac{D_{xy}}{2}\frac{\partial^2}{\partial x^2} - D_{Q_y}\right)q_y + D_{Q_y}\frac{\partial w}{\partial y} = 0 \qquad (\mathbf{3.14})$$

$$-D_{Q_x}\frac{\partial q_x}{\partial x} - D_{Q_y}\frac{\partial q_y}{\partial y} + \left(D_{Q_x}\frac{\partial^2}{\partial x^2} + D_{Q_y}\frac{\partial^2}{\partial y^2}\right)w + q = 0 \qquad (\mathbf{3.15})$$

The above system can be represented in the following operator form:

$$L(\{J\}) = \{F\} \tag{3.16}$$

Where:

$$L = \begin{bmatrix} L_{11} & L_{12} & L_{13} \\ L_{21} & L_{22} & L_{23} \\ L_{31} & L_{32} & L_{33} \end{bmatrix} \tag{3.17}$$

$$\{J\} = \begin{Bmatrix} q_x \\ q_y \\ w \end{Bmatrix} \tag{3.18}$$

$$\{F\} = \begin{Bmatrix} 0 \\ 0 \\ -q \end{Bmatrix} \tag{3.19}$$

$$\begin{aligned} L_{11} &= D_{xx}\frac{\partial^2(\ )}{\partial x^2} + \frac{D_{xy}}{2}\frac{\partial^2(\ )}{\partial y^2} - D_{Qx} \\ L_{12} &= \left(\frac{D_{xy}}{2} + D_{xx}u_y\right)\frac{\partial^2(\ )}{\partial x \partial y} \\ L_{13} &= D_{Qx}\frac{\partial(\ )}{\partial x} \end{aligned}$$

$$\begin{aligned} L_{21} &= L_{12}\,,\ L_{22} = D_{yy}\frac{\partial^2(\ )}{\partial y^2} + \frac{D_{xy}}{2}\frac{\partial^2(\ )}{\partial x^2} - D_{Qy} \\ L_{23} &= D_{Qy}\frac{\partial(\ )}{\partial y} \end{aligned} \tag{3.20}$$

$$\begin{aligned} L_{31} &= -L_{13}\,,\ L_{32} = -L_{23} \\ L_{33} &= D_{Qx}\frac{\partial^2(\ )}{\partial x^2} + D_{Qy}\frac{\partial^2(\ )}{\partial y^2} \end{aligned}$$

q intensity of lateral loading

3.3 Theory of Plasticity

The objective of the theory of plasticity is to obtain a theoretical relationship between stress and strain for an elastic-plastic behavior of materials. There are three requirements in order to formulate a theory that models elasto-plastic material behavior:

1. An explicit relationship between stress and strain must be formulated to describe material behavior under elastic conditions, i.e., before the onset of plastic deformation.
2. A yield criterion, which specifies the state of the multiaxial stresses corresponding to the occurrence of plastic flow.
3. A flow rule, which determines the relations between plastic strain increments and stresses increments after yielding.

The second requirement the Huber-Mises yield criterion, with isotropic hardening extended for naturally anisotropic materials by Hill, and Ilyushin's dimensionless yield surface, will be modified to a structurally orthotropic plate for this analysis. To achieve the elasto-plastic analysis, the yield criterion should be determined first. As mentioned previously, this corrugated-core sandwich plate is approximated by a 2D structurally orthotropic plate. The material of that plate is isotropic material; however, the structural behavior of that plate is orthotropic. No yield criterion was used in previous studies for

structurally orthotropic behavior of plates. Therefore, in this study, the yield criterion will be modified for a structurally orthotropic.

To derive the governing differential equations for the elastic-plastic analysis of corrugated-core sandwich plates, the following assumptions will be made:

1. The yield function f is a function of the direct stresses associated with flexure of the plate only, but not of the transverse shear stresses.
2. All assumptions regarding the behavior and mechanical response of the corrugated-core sandwich plate adapted in mechanics of sandwich plates and discussed previously are valid here except for the constitutive equations. In what follows, it is also assumed that displacements are small, and the material of the plate is isotropic.
3. When the bending moment reaches the yield moment, the whole cross section of the reduced plate plastifies simultaneously, namely, the whole cross section of the plate is assumed to become plastic instantaneously.

The third assumption is however a convenient fiction as in reality there is always a gradual plastification of the whole cross-section of the plate with the outer fibers becoming initially plastic. The plastic zone then spreads inward until the whole section ultimately yields shown in Figure **3-2**. Moreover, this assumption can reduce a significant difficulty in calculation.

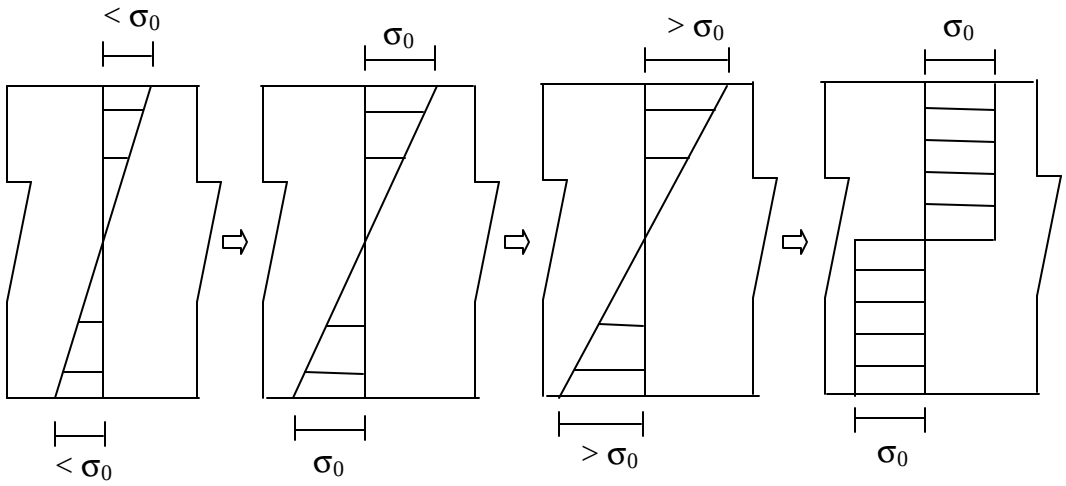

Fig. 3-2: Yielding of non-layered cross-section

According to the above conditions, the development of the elasto-plastic analysis is introduced in the following sections. Essentially, plastic behavior is characterized by an irreversible strain, which can only be obtained once a certain level of stress has been reached.

3.3.1 The Yield Criterion

It is supposed that a solid continuum is subjected to gradually increasing stresses. The initial deformation of the solid is entirely elastic and recoverable on completely unloading. For certain critical combinations of applied stresses, plastic deformation first occurs in the element. A rule that defines the limit of elastic behavior under any possible stress combinations is called yield criterion.

An accurate yield function is the key factor for the accuracy of the elasto-plastic analysis. Because of the assumption that the whole cross section yields simultaneously in Section **3.3**, the yield function in terms of stress couples is considered here. For Mindlin plates we may assume that the yield function F is expressed as a function of the bending moments $\{M\}$, but not of the shear forces $\{Q\}$ (Karam 1992). During yielding it is assumed that the bending and twisting moments must remain on the yield surface so that:

$$f\left(\{M\}\right) = k(x) \tag{3.21}$$

Where f is some function and k is a material parameter that is determined experimentally. The term k may be a function of a hardening parameter, x.

Rearrange Eq. **3.21**:

$$F\left(\{M\}, x\right) = f\left(\{M\}\right) - k(x) = 0 \tag{3.22}$$

The von Mises yield surface for the bending of structurally orthotropic sandwich plates can be obtained by modifying Ilyushin's yield surface expressed in terms of dimensionless stress resultants for isotropic plates and shells (Shi and Voyiadjis 1992) or the plate yield criteria for isotropic plate in (Lubliner 1990) as follows:

$$m_{11}^2 - m_{11}m_{22} + m_{22}^2 + 3m_{12}^2 = 1 \tag{3.23}$$

Where:

$$m_{ab} = M_{ab} / M_U \tag{3.24}$$

$$M_U = s_0 h^2 / 4 \qquad (\mathbf{3.25})$$

$a, b = 1,2$

h = the thickness of plate

s_0 = yield stress

Using the same dimensionless idea as Eq. **3.23** and introducing the anisotropic parameters into the von Mises yield function, we can obtain:

$$\frac{A_{11}}{2} m_x^2 + \frac{A_{22}}{2} m_y^2 - A_{12} m_x m_y + 3A_{33} m_{xy}^2 - 1 = 0 \qquad (\mathbf{3.26})$$

The terms m_x, m_y, and m_{xy} are dimensionless bending and twisting moments, respectively defined as:

$$m_x = \frac{M_x}{M_{x0}}, \; m_y = \frac{M_y}{M_{y0}}, \; m_{xy} = \frac{M_{xy}}{M_{xy0}} \qquad (\mathbf{3.27})$$

Where :

M_x and M_y bending moments in the x (the corrugation direction) and y (perpendicular to the corrugation) directions, respectively

M_{xy} twisting moment for the structurally orthotropic sandwich plate

M_{x0} and M_{y0} uniaxial yield bending moments in the x (the corrugation direction) and y (perpendicular to the corrugation) directions, respectively

M_{xy0} yield twisting moment for the structurally orthotropic sandwich plate

A_{11}, A_{12}, A_{22}, and A_{33} Anisotropic parameters depend on the structural orthotropy of the sandwich plate. The formulas of these anisotropic parameters are given in Appendix B.

Accordingly, the yield criterion for structurally orthotropic sandwich plates can be formulated. Since the corrugated-core sandwich plate is regarded as a structurally orthotropic plate, the yield moments in each *x*- and *y*-direction should be different. In an elastic perfectly-plastic material, the effects of strain hardening are disregarded. That means once the yield moment M_0 is reached the material could not take more strength. The strain hardening provides an increase in the strength of the material. Figure **3-3** is the behaviors of elastic perfectly-plastic and strain-hardening structures.

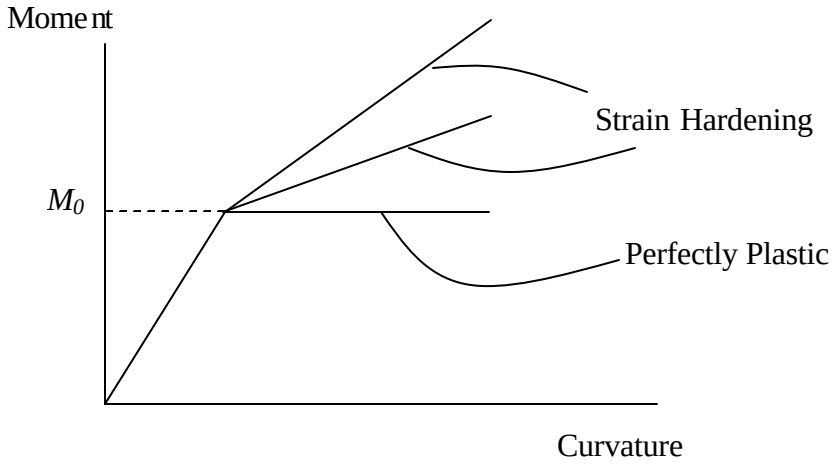

Fig. 3-3: Material behavior

Next, let us define the uniaxial yield moment. According to the third assumption in Section **3.3**, the whole cross section yields simultaneously. Geometric parameters of a plate unit are defined in Figure **3-4**. Therefore, referring to Figure **3-4**, this moment in the direction of corrugation, M_{x0}, can be calculated as follows:

$$\begin{aligned} M_{x0} &= s_0 t_f h + \int_{-h_c/2}^{h_c/2} s_0 z dA_c \\ &= s_0 t_f \left(h_c + t_c + t_f\right) + 2\int_0^{h_c/2} s_0 z dA_c \\ &= s_0 \left[t_f \left(h_c + t_c + t_f\right) + 2Z\right] \end{aligned} \qquad \textbf{(3.28)}$$

Where:

Z first moment of area of one-half of the corrugation about the central axis of the plate per unit length

σ_0 the yield stress of the material in a tension test

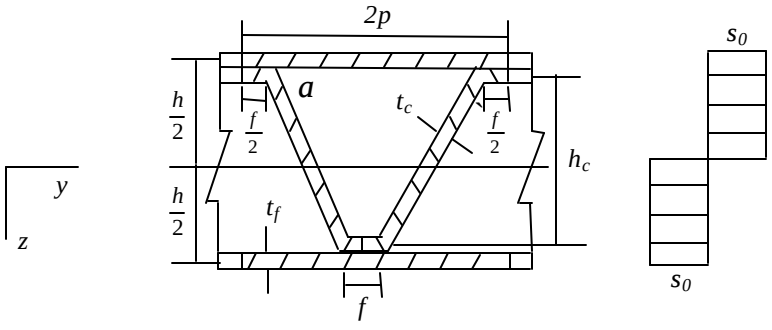

Fig. 3-4: the cross section and stress distribution in *x* direction

Where:

t_c, t_f thicknesses of core and face sheets, respectively.

a corrugation angle

h_c depth of corrugation measured from the center line at crest to center line at trough

h distance between middle surfaces of face sheets

$2p$ corrugation pitch, the distance between two crowns

f length of corrugation flat segment

The flexural contribution of core in the direction normal to the corrugation is significantly smaller than the face sheets. Furthermore, the position of the core varies in different cross section selected in the y-direction. Therefore, according to the basic assumption of the corrugated-core sandwich plate in Section **1.1**, the corrugation gives no contribution into the flexural resistance in the *y*-direction, i.e. the direction normal to the corrugation. Hence, referring to Figure **3-5**, the yield moment M_{y0} can be defined as:

$$M_{y0} = 2s_0 t_f \left(\frac{h_c}{2} + \frac{t_c + t_f}{2} \right) = s_0 t_f \left(h_c + t_c + t_f \right) \qquad (\mathbf{3.29})$$

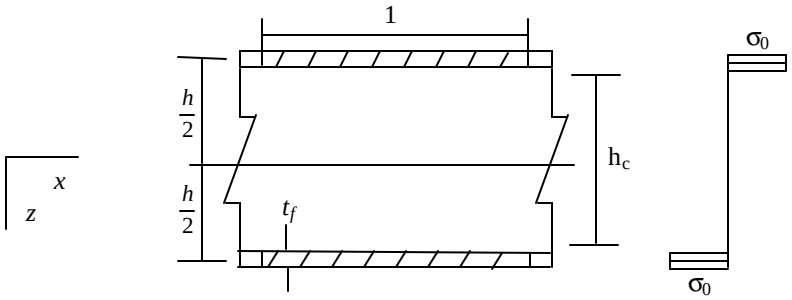

Fig. 3-5: the cross section and stress distribution in *y* direction

The same reason of moment resistance for twisting moment as that in *y*-direction, the corrugation also gives no contribution into the twisting resistance to flexure. Thus:

$$M_{xy0} = t_0 t_f \left(h_c + t_c + t_f\right) \qquad \textbf{(3.30)}$$

Since $\tau_0 = \sigma_0 / \sqrt{3}$, we have: Eq. **3.31**

$$M_{xy0} = \frac{s_0}{\sqrt{3}} t_f \left(h_c + t_c + t_f\right) \qquad \textbf{(3.31)}$$

3.3.2 Elasto-Plastic Analysis

The process of plastic deformation is irreversible. Most of the work of deformation is transformed into heat. A more complicated distinction between elastic and plastic stress-strain relations is that in the elastic stage the stains are uniquely determined by the stresses, whereas in plastic range the strains are generally not uniquely determined by the stresses, but depend on the whole history of loading. To analyze the elasto-plastic

behavior, the modified yield criterion based on von Mises and Ilyushin criteria and associated flow rule (Prandtl-Reuss equations) are used.

3.3.2.1 Incremental Form of Elastic Constitutive Equations

The definitions of those symbols in the incremental form are the same as previous sections. The symbol, *d*, in front of the term is defined as the increment of that term. The total curvature increments are considered to be the components of elastic and plastic curvature increments and can be written as:

$$\{dc\} = \{dc^{e}\} + \{dc^{p}\} \tag{3.32}$$

Where the superscripts *e* and *p* are the elastic and plastic curvature components, respectively.

According to the kinematic assumptions, the increments of the total bending strain are given in terms of the deflection and slope increments as follows:

$$dc_{x} = -\frac{\partial(dq_{x})}{\partial x}, \quad dc_{y} = -\frac{\partial(dq_{y})}{\partial y} \tag{3.33}$$

$$dc_{xy} = -\frac{1}{2}\left(\frac{\partial(dq_{x})}{\partial y} + \frac{\partial(dq_{y})}{\partial x}\right) \tag{3.34}$$

$$dy_{x}^{e} = -dq_{x} + \frac{\partial(dw)}{\partial x} \quad , \quad dy_{x}^{e} = -dq_{y} + \frac{\partial(dw)}{\partial y} \tag{3.35}$$

The elastic strain increments are related to the moments through the orthotropic Hooke's law as follows:

$$dM_x = D_{xx}\left(dc_x^e\right) + D_{xx}u_y\left(dc_y^e\right)$$

$$dM_y = D_{yy}u_x\left(dc_x^e\right) + D_{yy}\left(dc_y^e\right)$$

$$dM_{xy} = D_{xy}\left(dc_{xy}^e\right) \qquad \textbf{(3.36)}$$

$$dQ_x = D_{Qx}\left(dy_x^e\right)$$

$$dQ_y = D_{Qy}\left(dy_y^e\right)$$

Or in matrix form:

$$\{dM\} = \left[C^e\right]\{dc^e\} \qquad \textbf{(3.37)}$$

$$\{dQ\} = \left[C^s\right]\{dy^e\} \qquad \textbf{(3.38)}$$

$$\{dc^e\} = \left[C^e\right]^{-1}\{dM\} \qquad \textbf{(3.39)}$$

Where:

$$\left[C^e\right] = \begin{bmatrix} D_{xx} & D_{xx}u_y & 0 \\ D_{yy}u_x & D_{yy} & 0 \\ 0 & 0 & D_{xy} \end{bmatrix}$$

$$\left[C^s\right] = \begin{bmatrix} D_{Qx} & 0 \\ 0 & D_{Qy} \end{bmatrix}$$

$$\{dc^e\} = \begin{Bmatrix} dc_x^e \\ dc_y^e \\ dc_{xy}^e \end{Bmatrix}, \quad \{dy^e\} = \begin{Bmatrix} dy_x^e \\ dy_y^e \end{Bmatrix}$$

$$\{dM\} = \begin{Bmatrix} dM_x \\ dM_y \\ dM_{xy} \end{Bmatrix}, \quad \{dQ\} = \begin{Bmatrix} dQ_x \\ dQ_y \end{Bmatrix}$$

According to the Prandtl-Ruess theory (Valliappan 1976), the plastic strain incremental components (curvatures) can be expressed as:

$$\{dc^p\} = \begin{Bmatrix} dc_x^p \\ dc_y^p \\ dc_{xy}^p \end{Bmatrix} = \begin{Bmatrix} \frac{1}{2}\left(A_{11}M_x - A_{12}M_y\right)\frac{d\bar{c}^p}{\bar{M}} \\ \frac{1}{2}\left(-A_{12}M_x + A_{22}M_y\right)\frac{d\bar{c}^p}{\bar{M}} \\ 3A_{33}M_{xy}\frac{d\bar{c}^p}{\bar{M}} \end{Bmatrix} \qquad (\mathbf{3.40})$$

$$\bar{M}^2 = \frac{A_{11}}{2}M_x^2 - A_{12}M_xM_y + \frac{A_{22}}{2}M_y^2 + 3A_{33}M_{xy}^2 \qquad (\mathbf{3.41})$$

Where the equivalent moment, $\bar{M}$, is defined by the Huber-Mises yield function. $d\bar{c}^p$ is the incremental equivalent plastic strain associated with $d\bar{M}$, which is obtained by implicit differentiation of Eq. **3.41** as shown:

$$d\bar{M} = \left(A_{11}M_x - A_{12}M_y\right)\frac{dM_x}{2\bar{M}} + \left(-A_{12}M_x + A_{22}M_y\right)\frac{dM_y}{2\bar{M}} + 3A_{33}M_{xy}\frac{dM_{xy}}{\bar{M}} \qquad (\mathbf{3.42})$$

If H is defined as the slope of equivalent moment vs. equivalent plastic strain curve as shown in Figure **3-6** , then $d\bar{c}^{p}$ is related to $d\bar{M}$ as follows:

$$d\bar{c}^{p} = \frac{d\bar{M}}{H} \qquad (\mathbf{3.43})$$

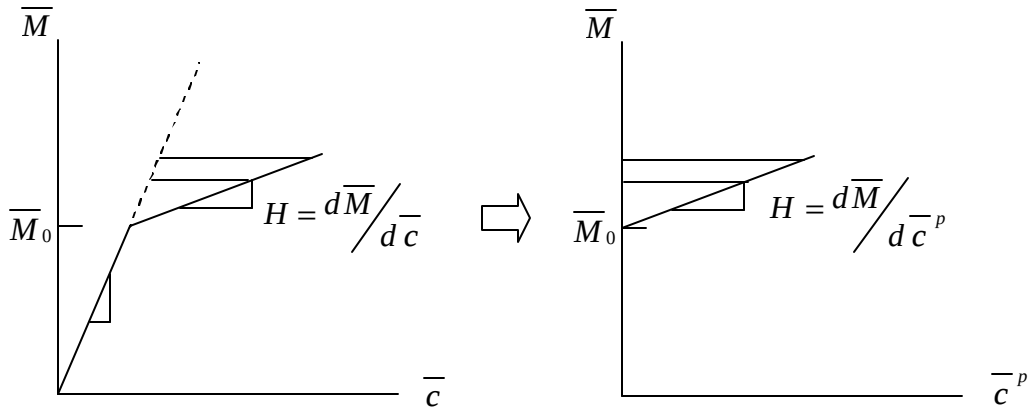

Fig. 3-6: Equivalent Stress-Strain Curve

For example, consider a strip-beam cut from the plate in the x direction. For this particular case, since the only moment occurs in x-direction, it can be shown that the equivalent moment and equivalent plastic strain increment reduce to:

$$\begin{aligned} d\bar{M} &= dM_x \\ d\bar{c}^{p} &= dc_x^{p} \end{aligned} \qquad (\mathbf{3.44})$$

Therefore, Eq. **3.43** for the above case can be considered as the following form:

$$H = \frac{d\overline{M}}{d\overline{c}^{p}} = \frac{dM_x}{dc_x^{p}} = \frac{dM_x}{dc_x - dc_x^{e}} = \frac{1}{\frac{dc_x}{dM_x} - \frac{dc_x^{e}}{dM_x}} = \frac{1}{\left(\frac{1}{EI_x}\right)_p - \frac{1}{EI_x}} = \frac{(EI_x)_p}{1 - \frac{(EI_x)_p}{EI_x}} \tag{3.45}$$

Where:

EI_x, $(EI_x)_p$ the elastic and elasto-plastic response slopes, respectively

E the modulus of elasticity of the plate material.

It can be shown that H is the slope of the uniaxial stress versus the uniaxial plastic strain as obtained in a uniaxial yield test. Obviously, for structurally orthotropic sandwich plates, the values of H will be different in the x and y directions.

Let us write Eq. **3.40** in the matrix form as:

$$\{dc^{p}\} = \{a\} d\overline{c}^{p} \tag{3.46}$$

Where:

$$\{a\} = \begin{Bmatrix} \frac{1}{2}\frac{(A_{11}M_x - A_{12}M_y)}{\overline{M}} \\ \frac{1}{2}\frac{(-A_{12}M_x + A_{22}M_y)}{\overline{M}} \\ 3A_{33}\frac{M_{xy}}{\overline{M}} \end{Bmatrix} \tag{3.47}$$

Then the incremental equivalent moment, $d\overline{M}$, given by Eq. **3.42**, can be also written in the matrix form as:

$$d\overline{M} = \{a\}^T \{dM\} \tag{3.48}$$

Rewriting the elastic relations i.e. Eq. **3.37** in the form:

$$\{dM\} = [C^e]\{dc^e\} = [C^e](\{dc\} - \{dc^p\}) \tag{3.49}$$

and substituting Eq. **3.46** into Eq. **3.49**, we can get:

$$\{dM\} = [C^e](\{dc\} - \{a\}d\overline{c}^p) \tag{3.50}$$

But because of Eq. **3.43**:

$$d\overline{M} = H(d\overline{c}^p) \tag{3.51}$$

Substituting Eq. **3.49** into Eq. **3.48** and using Eq. **3.51**, yields:

$$d\overline{M} = \{a\}^T [C^e](\{dc\} - \{a\}d\overline{c}^p) = Hd\overline{c}^p \tag{3.52}$$

Now the incremental equivalent plastic strain $d\overline{c}^p$ can be expressed as:

$$d\overline{c}^p = \frac{\{a\}^T [C^e]\{dc\}}{\{a\}^T [C^e]\{a\} + H} \tag{3.53}$$

Substituting Eq. **3.53** into Eq. **3.49**, we obtain:

$$\{dM\} = [C^e]\left[\{dc\} - \frac{\{a\}\{a\}^T [C^e]\{dc\}}{\{a\}^T [C^e]\{a\} + H}\right] \tag{3.54}$$

We can represent the above equation in the following form:

$$\{dM\} = [C^{ep}]\{dc\} \tag{3.55}$$

$$[C^{ep}] = \left[[C^e] - \frac{[C^e]\{a\}\{a\}^T[C^e]}{\{a\}^T[C^e]\{a\} + H} \right] \tag{3.56}$$

The elasto-plasticity matrix $[C^{ep}]$ takes the place of the elasticity matrix $[C^e]$ in the incremental analysis. It is evident that the elasto-plastic matrix is symmetric and positive definite. Furthermore, the Eq. **3.55** is valid whether or not '*H*' takes on a zero value.

3.3.2.2 The Incremental Form of the Governing Equations

The incremental form of the equilibrium equations is given by:

$$[T]\{d\Xi\} = \{dR\} \tag{3.57}$$

Where:

$$\{d\Xi\} = \{dM_x, dM_y, dM_{xy}, dQ_x, dQ_y\}^T = \begin{Bmatrix} \{dM\} \\ \{dQ\} \end{Bmatrix}$$

$$\{dR\} = \begin{Bmatrix} 0 \\ 0 \\ -dq \end{Bmatrix}$$

$$[T]=\begin{bmatrix} \frac{\partial}{\partial x} & 0 & \frac{\partial}{\partial y} & -1 & 0 \\ 0 & \frac{\partial}{\partial y} & \frac{\partial}{\partial x} & 0 & -1 \\ 0 & 0 & 0 & \frac{\partial}{\partial x} & \frac{\partial}{\partial y} \end{bmatrix}$$

Using Eq. **3.54** the moments may be expressed as follows:

$$\{dM\}=\{dM^{e}\}-\{dM^{p}\} \tag{**3.58**}$$

$$\{dM^{e}\}=[C^{e}]\{dc\}=\begin{Bmatrix} dM_{x}^{e} \\ dM_{y}^{e} \\ dM_{xy}^{e} \end{Bmatrix} \tag{**3.59**}$$

$$\{dM^{p}\}=[C^{e}]\frac{\{a\}\{a\}^{T}[C^{e}]\{dc\}}{\{a\}^{T}[C^{e}]\{a\}+H}=\begin{Bmatrix} dM_{x}^{p} \\ dM_{y}^{p} \\ dM_{xy}^{p} \end{Bmatrix} \tag{**3.60**}$$

Substituting Eq. **3.58** into Eq. **3.57** , we can get:

$$\frac{\partial\left(dM_{x}^{e}-dM_{x}^{p}\right)}{\partial x}+\frac{\partial\left(dM_{xy}^{e}-dM_{xy}^{p}\right)}{\partial y}-dQ_{x}=0$$

$$\frac{\partial\left(dM_{xy}^{e}-dM_{xy}^{p}\right)}{\partial x}+\frac{\partial\left(dM_{y}^{e}-dM_{y}^{p}\right)}{\partial y}-dQ_{y}=0 \tag{**3.61**}$$

$$\frac{\partial\left(dQ_{x}\right)}{\partial x}+\frac{\partial\left(dQ_{y}\right)}{\partial y}=-dq$$

Rearrange the above Eq. **3.61**, we can obtain:

$$\frac{\partial\left(dM_x^e\right)}{\partial x}+\frac{\partial\left(dM_{xy}^e\right)}{\partial y}-dQ_x=\frac{\partial\left(dM_x^p\right)}{\partial x}+\frac{\partial\left(dM_{xy}^p\right)}{\partial y}$$

$$\frac{\partial\left(dM_{xy}^e\right)}{\partial x}+\frac{\partial\left(dM_y^e\right)}{\partial y}-dQ_y=\frac{\partial\left(dM_{xy}^p\right)}{\partial x}+\frac{\partial\left(dM_y^p\right)}{\partial y} \qquad (\mathbf{3.62})$$

$$\frac{\partial\left(dQ_x\right)}{\partial x}+\frac{\partial\left(dQ_y\right)}{\partial y}=-dq$$

Substituting Eq. **3.59** and Eq. **3.33** to Eq. **3.36** into Eq. **3.62**, after some transformation the following equation is obtained:

$$[L]\{dJ\}=\{dR\}+\Delta\{dR\} \qquad (\mathbf{3.63})$$

Where:

$$\Delta\{dR\}=\begin{Bmatrix}\dfrac{\partial\left(dM_x^p\right)}{\partial x}+\dfrac{\partial\left(dM_{xy}^p\right)}{\partial y}\\ \dfrac{\partial\left(dM_{xy}^p\right)}{\partial x}+\dfrac{\partial\left(dM_y^p\right)}{\partial y}\\ 0\end{Bmatrix} \qquad (\mathbf{3.64})$$

$$\{dJ\}=\begin{Bmatrix}dq_x\\ dq_y\\ dw\end{Bmatrix}$$

$$\{dR\}=\begin{Bmatrix}0\\ 0\\ -dq\end{Bmatrix}$$

$$[L]=\begin{bmatrix} L_{11} & L_{12} & L_{13} \\ L_{21} & L_{22} & L_{23} \\ L_{31} & L_{32} & L_{33} \end{bmatrix}$$

The differential operators L_{ij} $(i,j=1,2,3)$ are identical to Eq. **3.20**. It is evident that the governing equations of sandwich plate bending, Eq. **3.63**, include lateral loading and plastic moment effects. The plastic moment vector, $\{dM^p\}$, which is unknown at any increment, simply appears in the equations as an additional lateral load.

3.4 Boundary Conditions

For most common types of supports, in practice, the boundary conditions are simply supported, clamped, and free. Let us consider the appropriate boundary conditions prescribed on an edge of a sandwich, rectangular, orthotropic plate. Unlike the classical theory, the governing differential equations, Eq. **3.63**, have the sixth order not fourth order; therefore, three boundary conditions should be prescribed at any point of the sandwich plate side. The discussions for the different boundary conditionsis presented next.

(a) Simply supported edge

The principal boundary conditions for a simply supported edge are that the deflections in *z*-direction and bending moments, M_x or M_y, are zero. There are two different types of conditions that may be regarded as the third boundary condition (Folie 1971), illustrated in Figure **3-7**. One may set the twisting moment, M_{xy}, to zero thus

permitting the edge to shear, e.g. on this edge parallel to the x-axis g_{xz}?0. In most practical cases, there will be an edge stiffener or some symmetric constraint to prevent such shear deformation. Therefore, the boundary condition should rather allow the existence of a twisting moment along the edge but restrict the shear deformation of the edge. The former boundary condition, where the twisting moment along the edge is zero, is called the soft boundary condition. The latter, preventing shear deformations, is called the hard boundary condition.

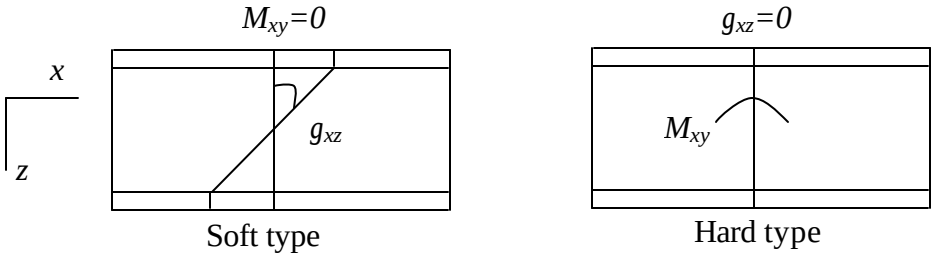

Fig. 3-7: Definition of boundary conditions (for y=0 or b)

Two boundary conditions for a simply supported edge, say x=constant are:

$$w = 0, M_x = 0 \qquad (\mathbf{3.65})$$

(1) Hard type boundary:

The third condition will be represented for the hard type of simply supported boundary condition. Then the following boundary condition takes place:

$$g_{yz} = -q_y + \frac{\partial w}{\partial y} = 0 \qquad (\mathbf{3.66})$$

From Eq. **3.10**, because D_{Qy} is the elastic constant of corrugated-core sandwich plates, therefore, we can obtain:

$$Q_y = D_{Qy} g_{yz} = D_{Q_y}\left(-q_y + \frac{\partial w}{\partial y}\right) = 0 \qquad (\mathbf{3.67})$$

From Eq. **3.6**, we can obtain:

$$M_x = -D_{xx}\left(\frac{\partial q_x}{\partial x} + u_y \frac{\partial q_y}{\partial y}\right) = 0 \qquad (\mathbf{3.68})$$

Since D_{xx} is the material constant, hence:

$$\frac{\partial q_x}{\partial x} + u_y \frac{\partial q_y}{\partial y} = 0 \qquad (\mathbf{3.69})$$

Thus, the boundary conditions at $x = 0$, a in this case can be formulated in terms of the principal unknowns of the problem, as follows:

$$w = 0$$

$$\frac{\partial q_x}{\partial x} + u_y \frac{\partial q_y}{\partial y} = 0 \qquad (\mathbf{3.70})$$

$$-q_y + \frac{\partial w}{\partial y} = 0$$

Since $w = 0$ on the edge $x = \text{constant}$, $\partial w/\partial y = 0$. Therefore, the third equation of Eq. **3.70** is of the form $q_y = 0$ and thus $\partial q_y / \partial y = 0$. Finally, we can represent the above boundary conditions in the form:

For $x = 0, a$

$$w = 0, \frac{\partial q_x}{\partial x} = 0, q_y = 0 \quad \textbf{(3.71)}$$

Meanwhile, the boundary conditions for hard type simply support on the edges y = constant can be defined as follows:

For $y = 0, b$

$$w = 0, \frac{\partial q_y}{\partial y} = 0, q_x = 0 \quad \textbf{(3.72)}$$

(2) Soft type boundary:

For $x = 0, a$

$$w = 0, M_x = 0, M_{xy} = 0 \quad \textbf{(3.73)}$$

For $y = 0, b$

$$w = 0, M_y = 0, M_{xy} = 0 \quad \textbf{(3.74)}$$

From Eq. **3.4** to Eq. **3.8**, the boundary conditions, Eq. **3.73** and Eq. **3.74**, can be expressed in terms of the deflection and slopes, therefore,

For $x = 0, a$

$$w = 0, \frac{\partial q_x}{\partial x} + u_y \frac{\partial q_y}{\partial y} = 0, \frac{\partial q_x}{\partial y} + \frac{\partial q_y}{\partial x} = 0 \quad \textbf{(3.75)}$$

For $y = 0, b$

$$w = 0, \frac{\partial q_y}{\partial y} + u_x \frac{\partial q_x}{\partial x} = 0, \frac{\partial q_x}{\partial y} + \frac{\partial q_y}{\partial x} = 0 \qquad (\mathbf{3.76})$$

(b) Clamped edge

The boundary conditions characterizing a clamped edge are no displacements of the neutral surface and no rotation of the cross-section in the boundary. These boundary conditions are shown as follows: Eq. **3.77**

$$q_x = q_y = w = 0 \qquad (\mathbf{3.77})$$

(c) Free edge

There are no force and stress couples on a free edge. Therefore, the boundary conditions for a free edge can be expressed as:

For $x = 0, a$

$$M_x = M_{xy} = Q_x = 0 \qquad (\mathbf{3.78})$$

For $y = 0, b$

$$M_y = M_{xy} = Q_y = 0 \qquad (\mathbf{3.79})$$

Or the boundary conditions can be expressed all in terms of deflection and slopes as followings:

For $x=0, a$

$$\frac{\partial q_x}{\partial x} + u_y \frac{\partial q_y}{\partial y} = 0, \frac{\partial q_x}{\partial y} + \frac{\partial q_y}{\partial x} = 0, -q_x + \frac{\partial w}{\partial x} = 0 \qquad (\mathbf{3.80})$$

For y=0, b

$$\frac{\partial q_y}{\partial y} + u_x \frac{\partial q_x}{\partial x} = 0, \frac{\partial q_x}{\partial y} + \frac{\partial q_y}{\partial x} = 0, -q_y + \frac{\partial w}{\partial y} = 0 \qquad (\mathbf{3.81})$$

3.5 Research Approach

For elastic analysis, the general Galerkin method and double Fourier's expressions are applied. The trial functions satisfying the boundary conditions are selected for this analysis. We substitute the selected trial functions into the governing Eq. **3.16** and solve simultaneous equation system for the unknown coefficients in double Fourier's series of these unknown displacements until the yielding occurs. Thus, the deflection, w, and rotated angles, q_x and q_y, can be found by substituting these coefficients into the Fourier's expressions. Furthermore, the corresponding moments and curvatures in x- and y-direction can be calculated.

After the yielding occurs, the elasto-plastic analysis begins. Except the methods used in elastic analysis, in addition, the iteration procedure and incremental theory of plasticity are employed to solve the governing equations, Eq. **3.63**, in the elasto-plastic analysis. Because in the elasto-plastic analysis the incremental theory of plasticity is employed, the trial functions are employed in an incremental style. The most difficulty of the elasto-plastic analysis is that in Eq. **3.63** the $D\{dR\}$ is unknown and relates to the incremental plastic moments $\{dM^p\}$. In each increment the incremental plastic moments

are unknown. Therefore, it is necessary to employ iterative to find the plastic moments and *D{dR}*. The procedure is discussed in Chapter Four.

Chapter 4

Numerical Analysis and Results

4.1 Introduction

The mathematical model of the elasto-plastic analysis of corrugated-core sandwich plates was proposed in previous Chapter. The numerical procedure for the elasto-plastic analysis is presented in this Chapter. In this analysis, Double Fourier expansions are employed to analyze plate bending problems. The linear elastic analysis is fairly straightforward. Each load corresponds to displacements. Thus, according to the constitutive equations, the stress couples can be obtained.

The elasto-plastic analysis begins on a reliable elastic linear analysis. Only a significant result of elastic linear analysis can induce an accurate elasto-plastic analysis. Therefore, the present analytical solution with simply supported edges is corroborated by experimental results, the analytical solution, and 3D finite element analysis of corrugated-core sandwich plate reported in (Tan et al. 1989).

The difficulty of the elasto-plastic analysis is the mathematical complexity. The general Galerkin and incremental methods are employed to solve the elasto-plastic bending problem. The double iterations are applied to the load increment and the plastic

incremental moment determination. The outer loop is the load increment and the inner loop is to obtain the plastic incremental moments. Numerical simulations are done by using MATLAB (2000).

4.2 Linear Elastic Analysis

4.2.1 Numerical Algorithm

Double Fourier series solutions have been widely applied in plate problems especially for simply supported boundary conditions (e.g., Whitney 1969; Whitney and Leissa 1970; Holston 1971; Pagano 1970). Hence, in this rectangular plate, as shown in Figure **4-1** with all simply-supported edges, the solutions of the governing differential equations, Eq. **3.16,** can be sought in the form of an infinite double Fourier expansion, as follows:

$$w = \sum_{m=1}^{\infty}\sum_{n=1}^{\infty} w_{mn} \sin\left(\frac{mp\,x}{a}\right)\sin\left(\frac{np\,y}{b}\right)$$
$$q_x = \sum_{m=1}^{\infty}\sum_{n=1}^{\infty} A_{mn} \cos\left(\frac{mp\,x}{a}\right)\sin\left(\frac{np\,y}{b}\right) \qquad (\mathbf{4.1})$$
$$q_y = \sum_{m=1}^{\infty}\sum_{n=1}^{\infty} B_{mn} \sin\left(\frac{mp\,x}{a}\right)\cos\left(\frac{np\,y}{b}\right)$$

$$q = \sum_{m=1}^{\infty}\sum_{n=1}^{\infty} q_{mn} \sin\left(\frac{mp\,x}{a}\right)\sin\left(\frac{np\,y}{b}\right) \qquad (\mathbf{4.2})$$

Where w_{mn}, A_{mn}, and B_{mn} are represent coefficients to be determined. q_{mn} can be determined by the external load using double Fourier expansion. a is the length in the

direction of corrugation and b is the width in the direction perpendicular to the corrugation.

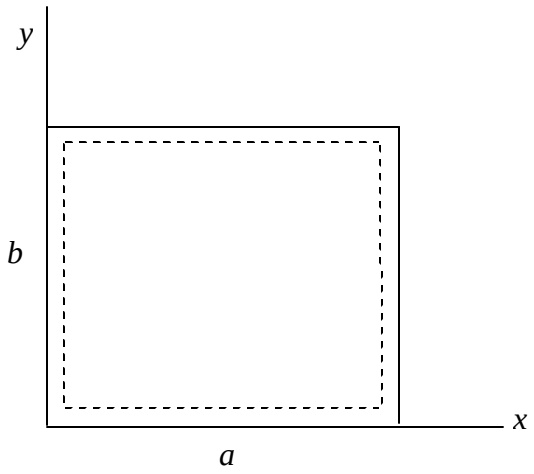

Fig. 4-1: Rectangular simply supported plate

The external load over a rectangular plate can be any type of functions. In the subsequent example the uniformly distributed load is discussed. Let q be the intensity of the uniformly distributed load. Then, the coefficients of the double Fourier expansion, q_{mn} in Eq. **4.2**, can be determined as:

$$q_{mn} = \frac{4}{ab}\int_0^a\int_0^b q \sin\frac{mp\,x}{a}\sin\frac{np\,y}{b}\,dxdy$$

$$= \frac{4q}{p^2 ab}\left(1-\cos(mp)\right)\left(1-\cos(np)\right) \qquad \textbf{(4.3)}$$

$$= \frac{4q}{p^2 ab}\left[1-(-1)^m\right]\left[1-(-1)^n\right]$$

In Eq. **4.3**, only when the terms, *m* and *n*, are equal to odd numbers the q_{mn} is a non-zero value. Otherwise, it equals to zero. Furthermore, it can be easily verified that the expressions for the deflection and two rotations, Eq. **4.1**, automatically satisfy the prescribed boundary conditions Eq. **3.71** and Eq. **3.72**.

The general Galerkin method is not necessary for solving the linear elastic analysis of a rectangular plate with all simply supported boundary edges. The Navior method is employed, instead. Substituting Eq. **4.1** and Eq. **4.2** into Eq. **3.13** to Eq. **3.15**, the system of equations in terms of the above unknown coefficients is in the following form:

$$[K]\{U\}=\{R\} \tag{4.4}$$

Where:

$$[K]=\begin{bmatrix} K_{11} & K_{12} & K_{13} \\ K_{21} & K_{22} & K_{23} \\ K_{31} & K_{32} & K_{33} \end{bmatrix}$$

$$\begin{aligned} K_{11} &= D_{xx}\left(\frac{mp}{a}\right)^2+\frac{D_{xy}}{2}\left(\frac{np}{b}\right)^2+D_{Qx};\ K_{12}=\left[\frac{D_{xy}}{2}+D_{xx}u_y\right]\left(\frac{mnp^2}{ab}\right) \\ K_{13} &= -D_{Qx}\left(\frac{mp}{a}\right) \end{aligned} \tag{4.5}$$

$$K_{21}=K_{12};\ K_{22}=D_{yy}\left(\frac{np}{b}\right)^2+\frac{D_{xy}}{2}\left(\frac{mp}{a}\right)^2+D_{Qy};\ K_{23}=-D_{Qy}\left(\frac{np}{b}\right) \tag{4.6}$$

$$K_{31} = K_{13}\,;\; K_{32} = K_{23}\,;\; K_{33} = \left[D_{Qx}\left(\frac{mp}{a}\right)^2 + D_{Qy}\left(\frac{np}{b}\right)^2 \right] \qquad (\mathbf{4.7})$$

$$\{U\} = \begin{Bmatrix} w_{mn} \\ A_{mn} \\ B_{mn} \end{Bmatrix}; \{R\} = \begin{Bmatrix} 0 \\ 0 \\ q_{mn} \end{Bmatrix}$$

Solving Eq. **4.4**, the coefficients of the deflection, w, and the slopes, q_x and q_y, in Eq. **4.1** can be obtained. Therefore, substituting the known solutions in Eq. **4.1** into the curvature-displacement relations, Eq. **3.4** and Eq. **3.5**, and the constitutive relations, Eq. **3.6** to Eq. **3.8**, the moments of this plate can be obtained. Figure **4-2** is the programming flow chart for the elastic analysis.

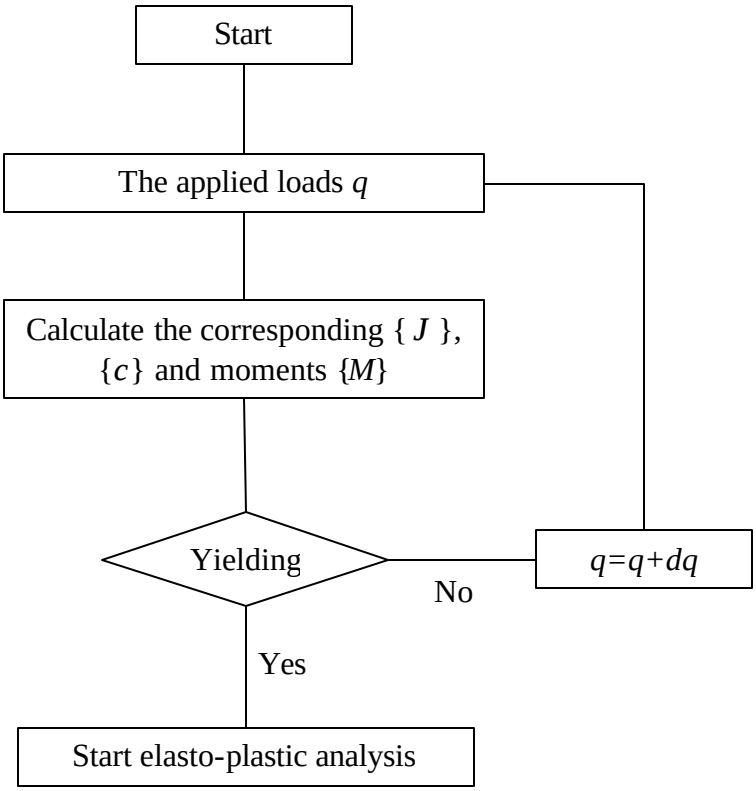

Fig. 4-2: Flow chart for elastic analysis

4.2.2 Elastic Analysis Comparison with Experimental Results

In this section, the behavior of the 6m by 2.1m corrugated-core sandwich plate studied by Tan et al. (1989) is analyzed. The material properties of the corrugated-core sandwich plate are the same as the plate in (Tan et al. 1989). In this case, the uniform distributed loading intensity is taken to be 5520 N/m^2. The modulus of elasticity is 208 GPa and the Poisson's ratio is assumed to be 0.3. These stiffness values shown in

Table **4-1** which are obtained from the formulas by (Libove and Hubka 1951) are from (Lok and Cheng 2000).

Table 4-1: Geometric Parameters and Elastic Constants

p (mm)	h_c (mm)	f (mm)	t_f (mm)	t_c (mm)
265	107.5	82.5	2.5	2.5
D_x (N-m)	D_y (N-m)	D_{xy} (N-m)	D_{Qx} (N/m)	D_{Qy} (N/m)
4.1×10^6	3.22×10^6	2.31×10^6	2.83×10^7	1.59×10^5

Table **4-2** shows the comparisons of the maximum deflection at the central point with classical analysis developed by Libove and Batdorf (1948), 3D corrugated-core sandwich plate finite element analysis (3D FEM) both reported in (Tan et al. 1989), and the present solution based on Reissner-Mindlin plate theory. As can be seen, the difference between the 3D FEM and the present solution in this thesis is 0.37% and between the solution by Tan et al. and the 3D FEM is 1.19%. Figure **4-3** is the deflection diagram of the whole plate, with a complete deflects downward.

Table 4-2: Comparison of central deflection

Maximum Deflection, w_{max} (mm)			Difference (%) between the present solution and 3D FEM	Difference (%) between solution by Tan and 3D FEM
Tan et al. 1989		Present solution		
solution By Tan	3D FEM analysis			
6.86	6.779	6.754	0.37	1.19

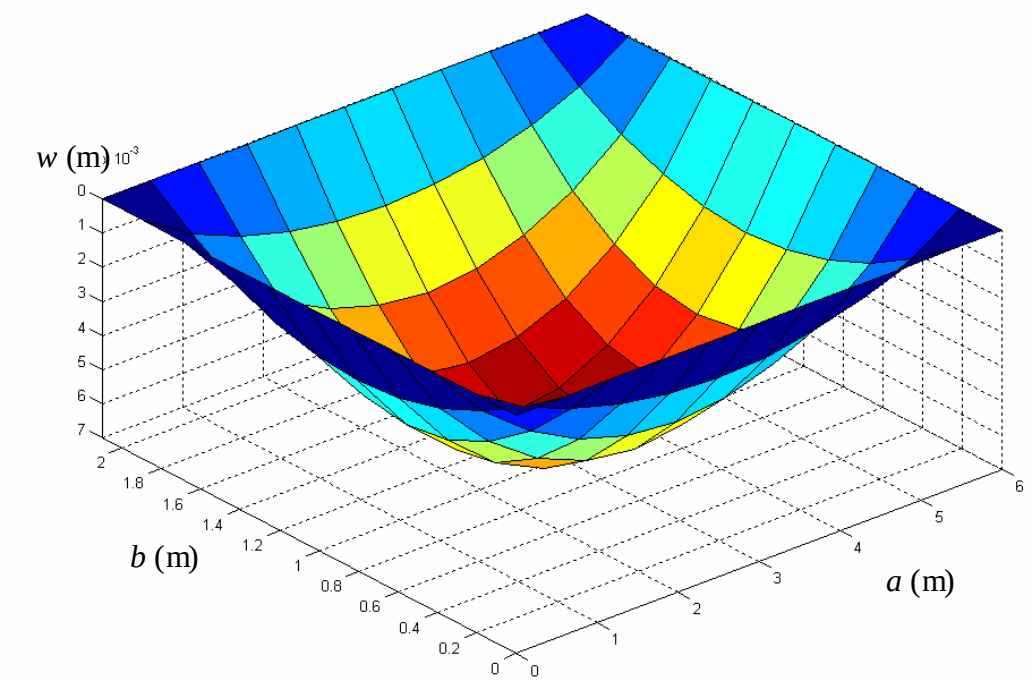

Fig. 4-3: Deflection of the corrugated-core sandwich plate

Figure **4-4** shows the central deflection of the panel from this solution, the 3D FEM, and the experimental investigations. It is noted that although the present solution is closed to the experimentally obtained deflections, and it agrees closely with that given by the 3D FEM and provides adequate predictions.

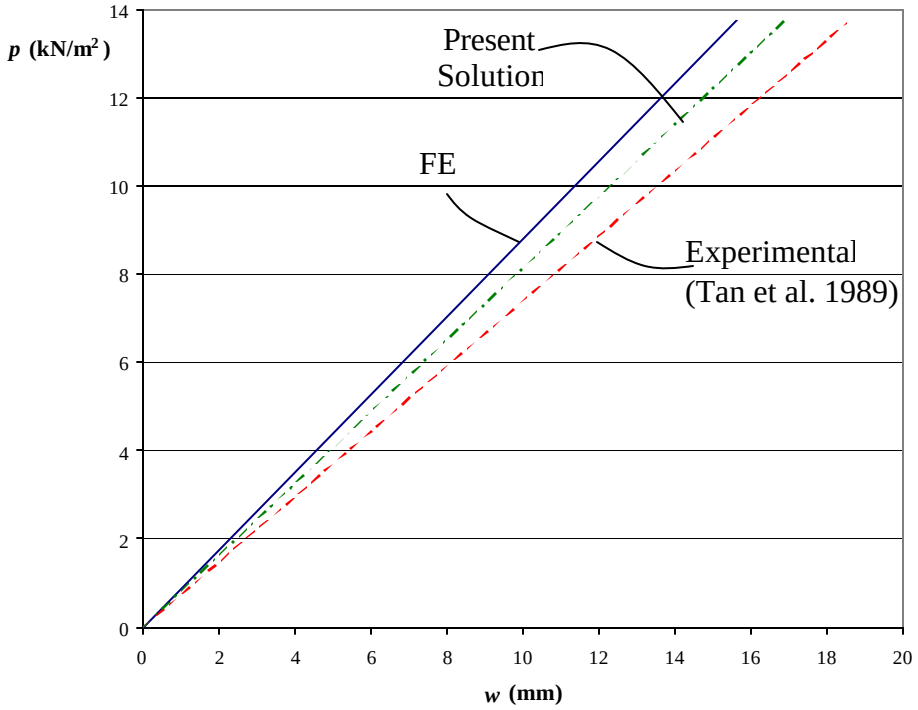

Fig. 4-4: Central deflection comparison

The present results of the moments in x- and y-direction at central point are given in Table **4-3**. It should be noted that M_y is very small and the signs of M_x and M_y are opposite. These results coincide with the experimental observations in (Tan et al. 1989). In that paper, the moments in both x- and y-direction by 3D FEM and the solution by Tan et al. (1989) are the same positive sign, namely, the compression in the top and tension in the bottom, as would be expected. However, the experimental investigation disagrees with M_y obtained by Tan et al. (1989) and the 3D FEM; i.e. M_y is negative (i.e. the compression in the bottom and tension in the top). The trend can also be seen in the moment predictions of the proposed solution.

Table 4-3: Moments at central point

M_x (N-m/m)	M_y (N-m/m)
5.99E+03	-613.9807

As shown in Figure **4-3**, it is evident that the bending curvatures in both *x* and *y* directions are sagging. The curvature is directly related to the bending moment; therefore, M_x and M_y should be of the same sign. However, in Table **4-3**, the signs of M_x and M_y are opposite. This contradiction is due to the poor structural properties in the *y*-direction. The shear stiffness D_{Qy} in Table **4-1** is very low. Therefore, the deflections due to shear effect overcome the bending curvature in the *y*-direction. Thus, the deflection of the panel gives a net downward trend.

4.2.3 Convergence of Elastic Analysis

In uniformly distributed load cases, the infinite series solutions for Eq. **4.1** generally converge quickly; thus, a satisfactory accuracy can be obtained by considering only a few terms. Since the stress resultants and couples are obtained from the first derivatives of the slopes, q_x and q_y, the convergence of the infinite series expressions of the moments is less rapid.

Considering the same case as Section **4.2.2**, Table **4-4** shows the comparison of convergences of the central deflection and moments. The convergences of w, M_x, and M_y

are shown in Figures **4-5** through Figure **4-7** , respectively. As can be seen, in this uniformly distributed load case, the double Fourier expressions have a remarkable convergence of all the deflection and moments. In Table **4-4**, the convergence of these terms after m,n=13 has the difference only less than 1% in all deflection and moments.

Table 4-4: Comparison of convergence of w, M_x, and M_y

m,n =	w (mm)	Difference (%)	M_x (N-m/m)	Difference (%)	M_y (N-m/m)	Difference (%)
5	6.789		6048.20		-604.46	
7	6.736	0.79%	5962.60	1.44%	-620.97	2.66%
9	6.762	0.39%	6000.50	0.63%	-610.59	1.70%
11	6.747	0.22%	5980.00	0.34%	-616.85	1.01%
13	6.756	0.14%	5992.10	0.20%	-612.84	0.65%
15	6.750	0.09%	5984.20	0.13%	-615.49	0.43%
17	6.755	0.06%	5989.60	0.09%	-613.64	0.30%
19	6.752	0.04%	5985.70	0.07%	-614.97	0.22%
21	6.754	0.03%	5988.60	0.05%	-613.98	0.16%

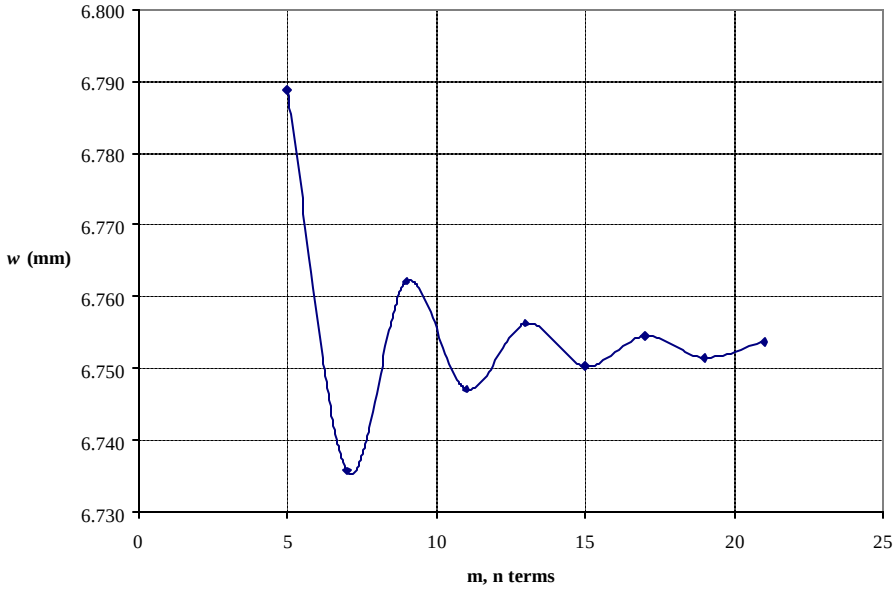

Fig. 4-5: Convergence of *w* at central point

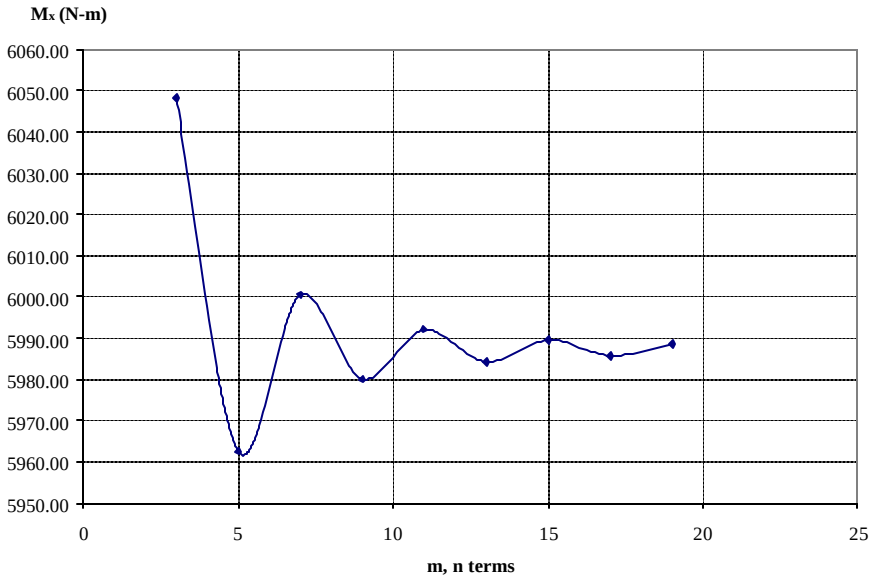

Fig. 4-6: Convergence of M_x at central point

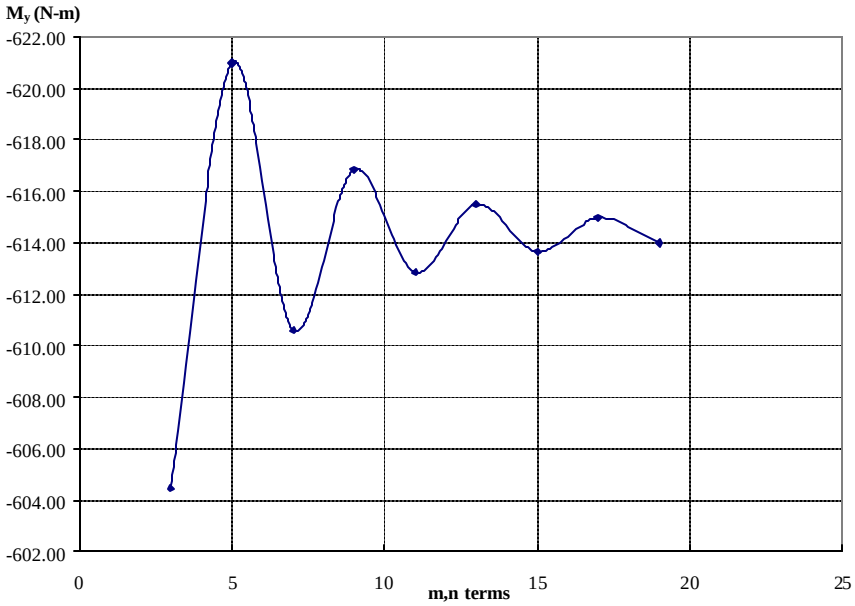

Fig. 4-7: Convergence of M_y at central point

It can be seen in Figure **4-5** and Table **4-4** that the deflection converges quickly. The difference between m, n=5 and 7 is already less than 1%. The difference for deflection between m,n=19 and 21 terms is only 0.03%. Even though m, n= 5 and 21, the difference is only 0.52%. Although moments are obtained from the first derivatives of the slopes, the convergences of the series expressions of moments in x- and y-direction are also very quick in this case. The differences for M_x and M_y between 19 and 21 terms are 0.05% and 0.16%, respectively. It is evident that more terms can be selected for the different loads and can lead to more accurate solutions. However, more terms means more computing cost. Therefore, according the convergence study in this Section, for the uniformly distributed loading, a solution that m and n are both equal to 21 terms is very good and it is employed in this study.

4.2.4 Conclusion

In the elastic analysis the solution with simply supported boundaries is corroborated by experimental results (Tan et al. 1989). Some new phenomena observed in experimental investigations of corrugated-core sandwich plates, but not found in previous numerical analysis, have been confirmed and reported. Experimentally obtained deflections and bending moments M_x agree very closely with the 3D finite element analysis and the solution by (Tan et al. 1989). However, the experimental results disagree with the moment M_y (y-direction is perpendicular to the corrugation.) obtained by 3D FEM and the solution by Tan where both M_x and M_y are positive. Experimental results (Tan et. al 1989) show that the signs of M_x and M_y are opposite and M_y is negative and very small. Nevertheless, these phenomena were shown in the present analysis. The negative moment does not occur in all the cases. This phenomenon relates to the geometric parameters and the induced elastic constants of the corrugated-core sandwich plate. The phenomenon of negative moment is discussed in Section 4.4.6, subsequently. The present solution for elastic linear analysis in this thesis significantly agrees with all the experimental investigations both in deflections and moments from (Tan et al. 1989).

4.3 Elasto-Plastic Analysis

The elastic analysis was introduced in previous Section **4.2**. The behavior before yielding occurs has been studied. The following section will discuss the elasto-plastic analysis. The incremental method is employed in the elasto-plastic analysis. Therefore, to obtain the incremental plastic moments, an iterative procedure is engaged. In the elasto-

plastic analysis, two iterations are employed. The outer loop is the load increment and the inner loop is to obtain the incremental plastic moments. The convergence can be achieved by setting up the criterion that the changes in the incremental plastic moments are sufficiently small.

4.3.1 Numerical Algorithm

For the elasto-plastic analysis, the incremental method and iterative procedure are employed in the numerical simulation. Now, let us recall the incremental governing equation, Eq. **3.63**, as follows:

$$[L]\{dJ\} = \{dR\} + \Delta\{dR\}$$

Since the boundary conditions remain simply supported, the incremental displacements and external uniformly distributed load can be expressed as:

$$\begin{aligned} dw &= \sum_{m=1}^{\infty}\sum_{n=1}^{\infty} dw_{mn} \sin\left(\frac{mp\,x}{a}\right)\sin\left(\frac{np\,y}{b}\right) \\ dq_x &= \sum_{m=1}^{\infty}\sum_{n=1}^{\infty} dA_{mn} \cos\left(\frac{mp\,x}{a}\right)\sin\left(\frac{np\,y}{b}\right) \\ dq_y &= \sum_{m=1}^{\infty}\sum_{n=1}^{\infty} dB_{mn} \sin\left(\frac{mp\,x}{a}\right)\cos\left(\frac{np\,y}{b}\right) \end{aligned} \qquad (\mathbf{4.8})$$

$$dq = \sum_{m=1}^{\infty}\sum_{n=1}^{\infty} dq_{mn} \sin\left(\frac{mp\,x}{a}\right)\sin\left(\frac{np\,y}{b}\right) \qquad (\mathbf{4.9})$$

We substitute Eq. **4.8** and Eq. **4.9** into Eq. **3.65**. This incremental simultaneous equation system is similar to Eq. **4.4** and can be arranged as:

$$[K]\{\Delta U\} = \{\Delta R\} + \{\Delta R^p\} \qquad (\mathbf{4.10})$$

Where $[K]$ is the same as in Eq. **4.4** and

$$\{\Delta U\} = \begin{Bmatrix} dw_{mn} \\ dA_{mn} \\ dB_{mn} \end{Bmatrix}; \{\Delta R\} = \begin{Bmatrix} 0 \\ 0 \\ dq_{mn} \end{Bmatrix}; \{\Delta R^p\} = \begin{Bmatrix} \frac{\partial(dM_x^p)}{\partial x} + \frac{\partial(dM_{xy}^p)}{\partial y} \\ \frac{\partial(dM_{xy}^p)}{\partial x} + \frac{\partial(dM_y^p)}{\partial y} \\ 0 \\ \\ \end{Bmatrix}$$

To solve the algebraic system, Eq. **4.10**, the incremental displacements can be obtained by substituting these coefficients into Eq. **4.8**. Thus, we add these increments to the previous state of displacements and find the current displacement. Furthermore, the current moments can be obtained by the constitutive equations.

However, one thing should be noted that the plastic moment vector, $\{dM^p\}$, which must be unknown at any increment, simply appears in the equations as an additional lateral load in the governing equation. Therefore, $\{\Delta R^p\}$ is unknown in the governing equation, Eq. **4.10**. Let us recall Eq. **3.60** as follows:

$$\{dM^p\} = [C^e]\frac{\{a\}\{a\}^T[C^e]\{dc\}}{\{a\}^T[C^e]\{a\} + H}$$

We can obtain the plastic moments $\{dM^p\}$ from Eq. **3.60**. However, because the plastic moments are unknown at any increment, it is necessary to employ an iterative procedure to find $\{dM^p\}$ and $\{\Delta R^p\}$ in this analysis.

Before yielding occurs, there are no plastic moments. Thus, at the first load loop for the first iteration, when yielding just occurs, the plastic moments $\{dM^p\}$ can be assumed to be zero. Then, by solving Eq. **4.10** with the assumed $\{dM^p\}$ and using iterative procedure, the incremental displacements can be obtained and the vector $\{dM^p\}$ can be determined. Eq. **4.10** is the governing equation of the elasto-plastic analysis of the sandwich plate bending problems. $\{\Delta R^p\}$, in right-hand side of these simultaneous equations, depends on the incremental plastic moments which are unknown but can be found by an iterative procedure. With respect to the iterative procedure, it should be noted that the increments of the plastic moments are related to the increments of the plastic bending strains, which are related to the increments of the total bending strains shown in Eq. **3.60**. The main advantage in this procedure is that only $\{\Delta R^p\}$ in Eq. **4.10** changes during the incremental procedure.

4.3.2 Numerical Procedure

There are many options for the iterative sequence to be employed. The most generally applicable methods are direction iteration, the Newton-Raphson method, tangential stiffness method, and the initial stiffness method. In this analysis the initial

stiffness method is employed. This method has been widely applied in elasto-plastic analysis with finite element and boundary element methods. For the initial stiffness method, the stiffness matrix, [*K*] in Eq. **4.10**, is the same at each stage. This has the immediate advantage of significantly reducing the computing cost per iteration but reduces the convergent rate, as can be seen from Figure **4-8** .

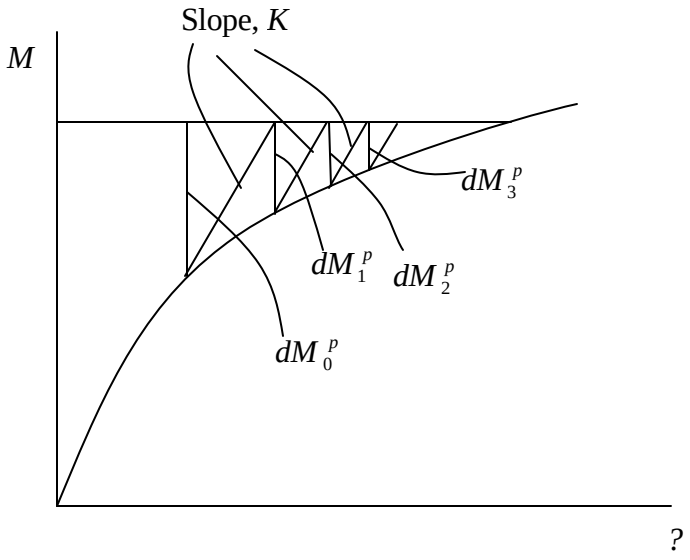

Fig. 4-8: Initial stiffness solution algorithm

The solution procedure of the initial stiffness method can be summarized as:

(1) Apply a load q and calculate the corresponding elastic bending strains $\{J\}^e$ using the linear stress analysis procedure.

(2) Determine moments $\{M\}$ and shear forces $\{Q\}$ corresponding to $\{J\}^e$ by Eq. **3.6** to Eq. **3.10**. Define a load which gives the elastic limit at the central point of the plate by using Eq. **3.26**.

(3) Update q, w, $\{J\}^e$, $\{M\}$, and $\{Q\}$ for the onset of yielding at a central point.

(4) Apply a load increment dq and assume $\{dM^p\}$ =0. If returned from step 11, the final value of $\{dM^p\}$ from last increment can be chosen as a first approximation.

(5) Evaluate $\{dc\}$ by Eq. **4.10**, the assumed $\{dM^p\}$ and the load increment.

(6) Evaluate the corresponding increments of moments $\{dM\}$ and shear forces $\{dQ\}$ by Eq. **3.36**.

(7) Add $\{dM\}$ to $\{M\}$ and check yielding using Eq. **3.26**. If the point has yielded at the start of the increment, calculate $\left\{d\bar{c}^p\right\}$ by Eq. **3.53**.

(8) Using $\left\{d\bar{c}^p\right\}$ calculate $\{dM^p\}$ by Eq. **3.60**.

(9) Check convergence. Convergence occurs if changes in $\{dM^p\}$ are sufficiently small. If convergence was not achieved replace assumed $\{dM^p\}$ by calculated $\{dM^p\}$ and return to step 5.

(10) If convergence has been obtained, update w, $\{q\}$, $\{M\}$. $\{Q\}$, q, and define the corresponding value of M_0. In a case of hardening, the yield moment should be update too.

(11) Return to step 4 unless $q = P_{max}$ or predetermined maximum number of iterations has been reached.

An outline of the program procedure is provided in Figure **4-9**. In elastic analysis, the deformations and loading are directly solved by the corresponding load step until the

yielding occurs. The incremental method is employed after yielding occurs. Two iteration loops are included in the post yield step. The inner loop is the iteration process. The convergence criterion determines when to terminate this inner iteration loop. The outer loop is the incremental loading loop.

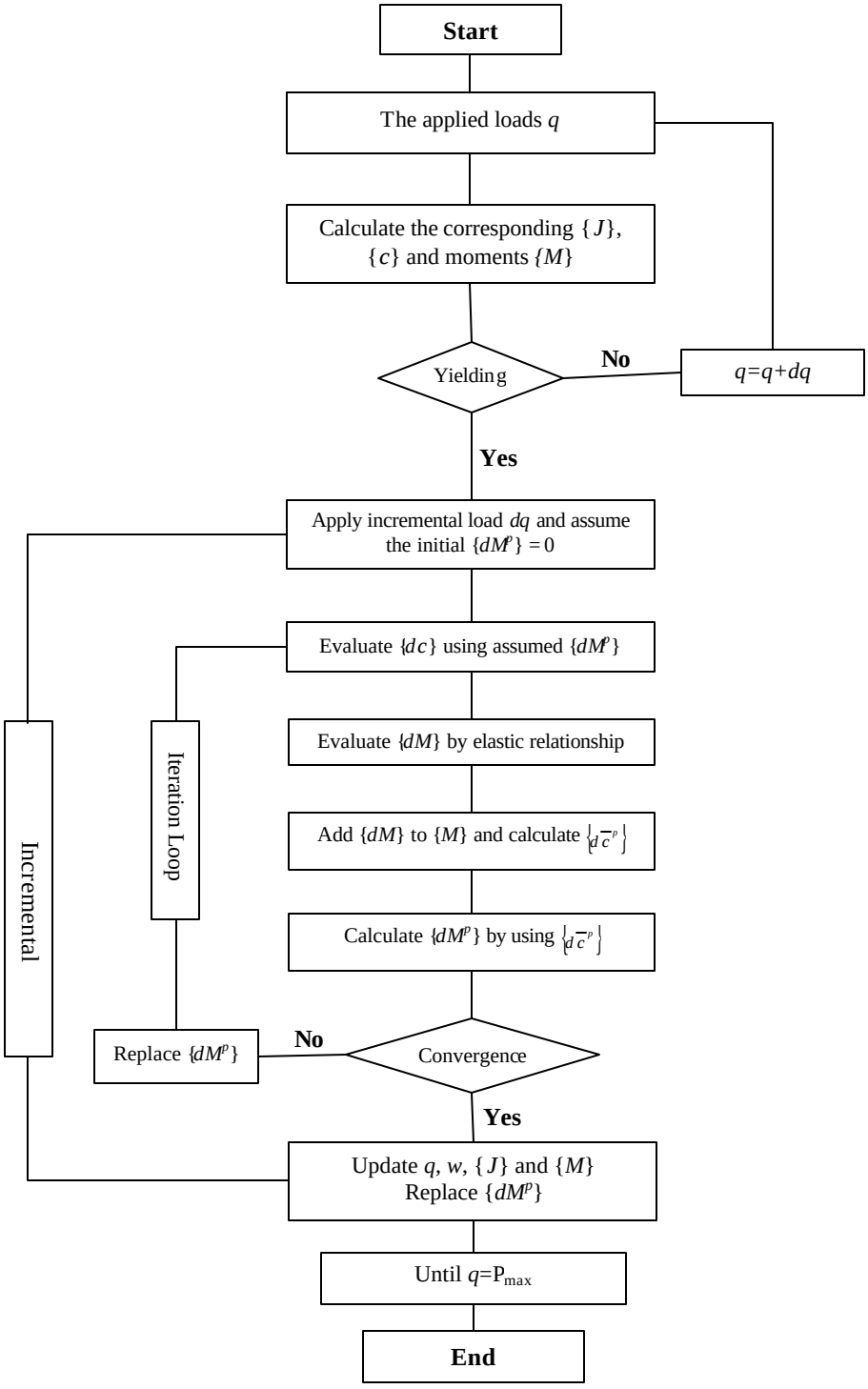

Fig. 4-9: Program organization for elasto-plastic application

4.3.3 Convergence Criterion

The iterative process is terminated when the numerical solution converges. In previous section it has been mentioned that the convergence occurs when changes in $\{dM^p\}$ are sufficiently small. Therefore, in this application we recommended the following convergence criteria. Let

$$E = \frac{\left\|\Delta dM^{p}_{(i)}\right\|}{\left\|dM^{p}_{(i+1)}\right\|} = \frac{\left\|dM^{p}_{(i+1)}\right\| - \left\|dM^{p}_{(i)}\right\|}{\left\|dM^{p}_{(i+1)}\right\|} \leq Tolerance \qquad (\mathbf{4.11})$$

Where i is the i^{th} iterations in the iterative procedure. Tolerance is a specified limit. Throughout the numerical analysis, the Tolerance is equal to 0.01. $\| \ \|$ is the norm of the vector inside the symbol and is defined as the following:

$$\left\|dM^{p}_{(i)}\right\| = \left[\sum_{j}\left(dM^{p}_{j\ (i)}\right)^2\right]^{\frac{1}{2}} \qquad (\mathbf{4.12})$$

Where the definition of i is the same as Eq. **4.11** and j is the j^{th} element of the vector $\{dM^p\}$.

4.3.4 Numerical Examples for Elastic Perfectly-Plastic Material

A MATLAB program was developed based on the above approach. The corrugated-core sandwich is made of steel. Throughout the analysis the Young's modulus of steel is 208 GPa, the yielding stress is 200 MPa and the Poison's ratio is 0.3. For the numerical examples, the depth of the corrugation, h_c, remains 0.1m throughout this

analysis. The elastic constants of a corrugated-core sandwich plate can be obtained from the formula in Appendix A.

In this elasto-plastic analysis the dimension of a rectangular plate is 6m by 2.1m. Due to the elastic-perfectly plasticity, we can use these initial orthotropic parameters in Appendix A for the whole plastic analysis. For a hardening case, these orthotropic parameters vary at each stage. In this analysis, trial functions that m and n equal to 21 for w, q_x, and q_y and the increments are selected. The reason has been discussed in Section **4.2.3**. Figure **4-10** shows the behavior of elastic perfectly-plastic structures. When the material reaches the yielding moment, it can not take any more moment. M_0 in Figure **4-10** is the yielding moment of the uniaxial test.

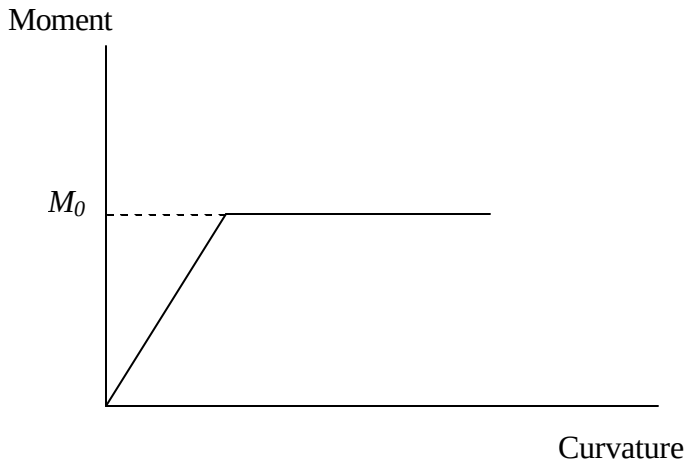

Fig. 4-10: Elastic Perfectly-Plastic Behavior

In this numerical analysis, the geometric parameters are h_c/t_c=10, t_c/t_f=1.0, and p/h_c=1.0. These stiffness constants obtain by the formula in Appendix A according to these geometric parameters. Table **4-5** shows the comparison of stiffness constants, yield loads, and yield deflections. The yield load and deflection is the corresponding load and deflection when yield occurs. In this table only corrugation angle a varies in the range from 60^0 to 90^0.

It can be seen in Table **4-5** that increasing the corrugation angle by increments of 10 degrees will increase the bending stiffness D_x by less than 5% and increase D_y increase by less than 0.5% and will not increase D_{xy}, whereas there is a significant decrease in the value of D_{Qx} and D_{Qy}, especially for D_{Qy} by the corrugation angle increments. D_{Qy} decreases more than 30%. The decreases of D_{Qx} and D_{Qy} cause the overall plate stiffness to reduce. The bending stiffness D_x increases because the flat part of the trough and crown of the corrugation increase when the corrugation angle is larger. Therefore, the moment of inertia of the cross section is increasing.

It also can be found that the yield load increases about 3% to 5% but the yield deflection decreases more than 30% by the corrugation angle increments of 10 degrees. The yield load increases due to the increase of flexural stiffness. In these cases, the bending stiffness D_x and D_y increase marginally. The yielding is the flexural effect. Therefore, as the flexural stiffness increases the yield load also increases.

Table 4-5: Comparison of stiffness constants, yielding loadings, and deflections

p/h_c	t_c/t_f	a	D_x	% Change	D_y	% Change	D_{xy}	D_{Qx}	% Change	D_{Qy}	% Change	w_0 (mm)	% Change	p_0 (N/m^2)	% Change
1	1	60	1.92E+07	~	1.53E+07	~	1.15E+07	7.81E+08	~	1.07E+08	~	9.97E+00	~	5.23E+05	~
		70	2.01E+07	4.95%	1.53E+07	0.33%	1.15E+07	7.44E+08	-4.63%	4.80E+07	-55.14%	1.33E+01	33.39%	5.36E+05	2.58%
		80	2.10E+07	4.42%	1.54E+07	0.26%	1.15E+07	7.02E+08	-5.72%	2.88E+07	-40.00%	1.76E+01	31.95%	5.56E+05	3.77%
		90	2.19E+07	4.23%	1.54E+07	0.33%	1.15E+07	6.55E+08	-6.74%	1.92E+07	-33.33%	2.32E+01	32.08%	5.86E+05	5.23%

$$\%Change = \frac{a(i) - a(i-1)}{a(i-1)}$$

The elasto-plastic analysis of corrugated-core sandwich plates on variations of corrugation angle on deflections at the central point is shown in Figure **4-11**. The central deflection increases with increasing corrugation angle. The central deflection behavior after yielding maintains a straight line but the slope is different from the behavior in elastic stage and the slope in elasto-plastic stage is smaller than in elastic stage. The reason that the slope in elasto-plastic is smaller than in elastic stage is that after yield occurs, the stiffness of the plate reduces. In this figure, we can also find that the yielding loading is also a somewhat increase with increasing corrugation angle.

Consequently, from Table **4-5** and Figure **4-11** it is demonstrated that although the higher corrugation angle has a better flexural stiffness, the deflections are larger due to the drastic decrease in D_{Qy}. The detail of the effect of geometric parameters and stiffness is discussed subsequently.

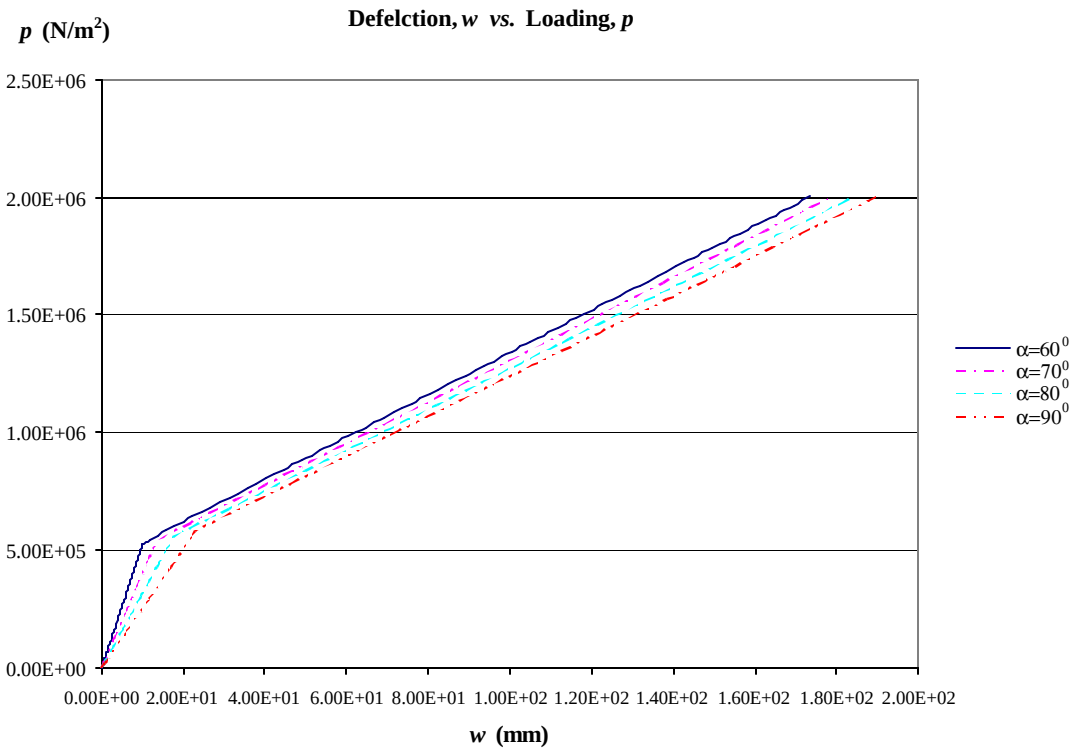

Fig. 4-11: Central deflection *vs*. Loading

Figures **4-12** through **4-13** are the moment vs. curvature diagrams in the *x*- and *y*-directions, respectively. In these figures, it is shown that the moments in *x*- and *y*-directions remain unchanged after approaching a certain value. The trend satisfies the elastic perfectly-plastic behavior of the material used in this analysis. Both moments in the *x*- and *y*-directions do not reach the uniaxial yielding moment in the analysis, respectively. This is a two-dimensional behavior and the yielding occurs when the moment combinations attain the yielding surface, i.e. these moment combinations satisfy Eq. **3.26**.

As discussed previously, with an increasing corrugation angle, the flexural stiffnesses increase slightly. In these two figures, the final moments, which are the moment combinations when yielding occurs, for higher degree of corrugation angles in *x*- and *y*-directions are somewhat higher. However, these differences are very small. Therefore, the corrugation angles do not affect significantly the flexural moments.

Also it was found that the moments in the *y*-direction are higher that those in *x*-direction. This is due to the length contribution. In this analysis, the length is 6m and the width is 2.1m. The length is almost three times the width. Because the values of flexural stiffnesses shown in Table **4-5** in the *x*- and *y*-directions have only slight differences, the effect of the length becomes more important. Due to the drastic decrease in D_{Qy}, the deflection of high degree of the corrugation angle becomes larger and meanwhile the curvature increases. This also can be seen in Figure **4-12** and Figure **4-13**.

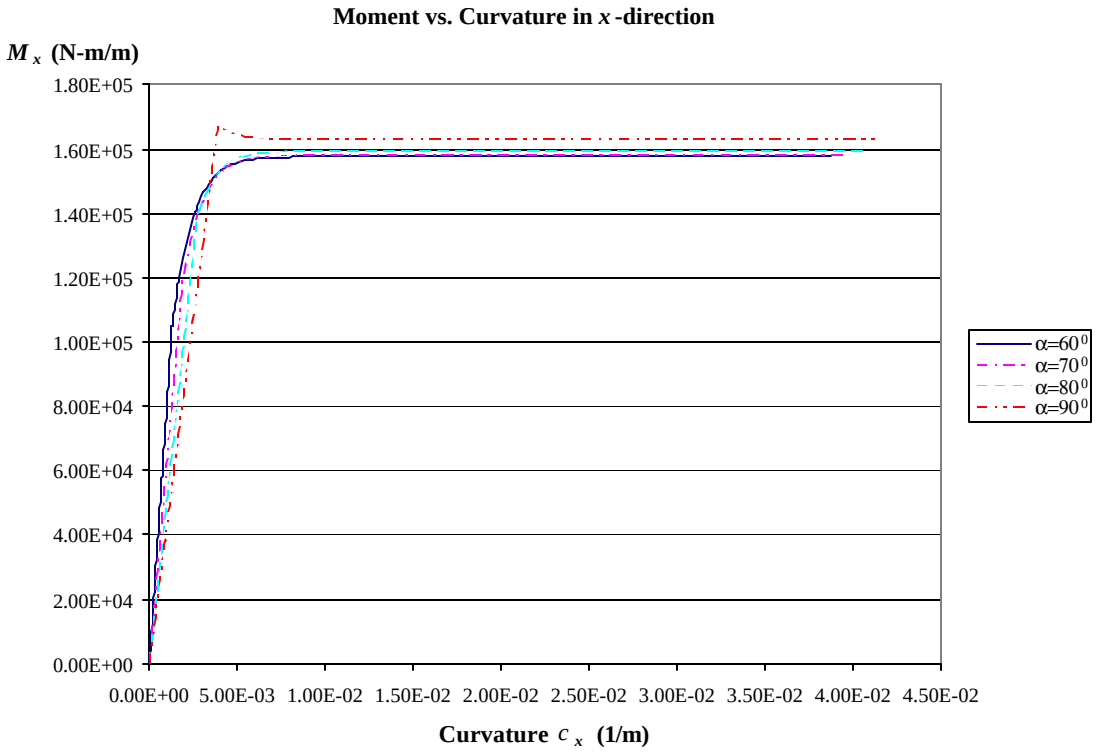

Fig. 4-12: Moment *vs.* Curvature in *x*-direction

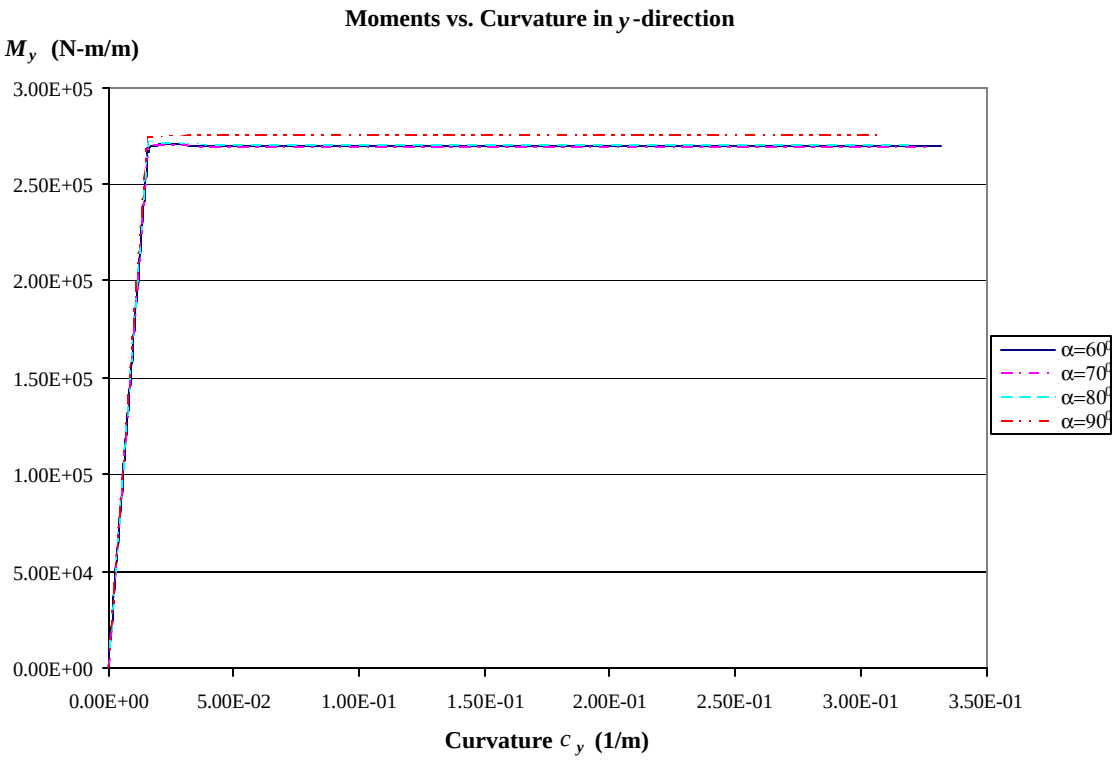

Fig. 4-13: Moment *vs.* Curvature in *y*-direction

It can be seen in Fig. 4-11, 4-12, and 4-13 that when yielding occurs, the deflection and moments in *x*- and *y*-directions increase as the corrugation angle increases. The deflection at the central point increased by more than 30% for every 10^0 increment in the corrugation angles between 60^0 and 90^0. However, the uniform load increased by about 3% to 5% in the same range of corrugation angles. Increasing the corrugation angle by increments of 10 degrees caused the moment in the *x*-direction at the central point to increase by about 12% to 20%, and the moment in the *y*-direction at the central point to increase by less than 1%.

The reason that the moment in the *x*-direction increased for larger corrugation angles is that the first moment area increased. The first moment areas of the face plates for a unit width are constant. For the larger corrugation angles, however, the contribution to the first moment area from the inclined parts of corrugation increases. That means that the areas of the crown and trough increase for larger corrugation angles, but the area of inclined parts of corrugation decreases. The increases from crown and trough are more than the decreases from the corrugation. Also, the crown and trough are farther from the central plane than and it contributes more to the flexural stiffness. Consequently, the bending capacity when yield occurs is higher for larger corrugation angles. This also happens to the moment in the *y*-direction for the same reason. However, although the flexural stiffness increases for larger corrugation angles, the deflection also increases. Although the flexural rigidity increases for larger corrugation angles, the shear stiffnesses decrease more than the flexural stiffnesses. The deflection contributed by transverse shears causes the deflection to increase.

4.3.5 Conclusions

The elasto-plastic analysis of a corrugated-core sandwich plate is developed, herein. In this section, an elastic perfectly-plastic behavior of the corrugated-core sandwich plate has been studied. Since comparable studies have not been made on the elasto-plastic analysis of the corrugated-core sandwich plate bending problem, a comparison of the results with the previous researches is not possible.

The behavior of the corrugated-core sandwich plate has been discussed in this section. The trends of moments in *x*- and *y*-direction in this analysis are satisfied the elastic perfectly-plastic behavior. It is demonstrated that the iterative method for finding the incremental plastic moments converges. The convergence of the iterative procedure is quite quick. The convergence can be achieved just only 4 to 6 iterations in this analysis.

4.4 Geometric Parameters Analysis

Figure **4-14** is the corrugation unit. *t* is the thickness and the subscripts *c* and *f* are the core and facing respectively. *2p* is the distance between central lines of two adjacent crowns. α is the corrugation angle. h_c is the depth of the corrugation and *h* is the depth of the plate. In Figure **4-14** it can be found that several geometric parameters relate to the stiffness of a corrugated-core sandwich plate. To discuss the geometric parameters in this section, a hard-type simply supported rectangular corrugated core sandwich plates with the dimensions 6m x 2.1m is considered. The intensity of the uniform load is taken to be 10 KN/m^2. These above properties remain the same throughout Section **4.4**. We vary

different geometric parameters associated with stiffness of corrugation and stiffness of facing plates and study their coupling effect.

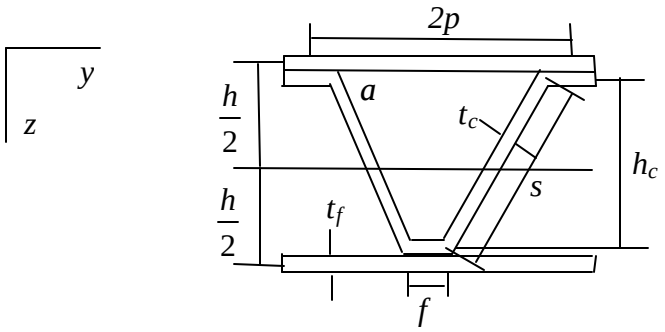

Fig. 4-14: Corrugation unit

The primary geometric parameters affecting the behavior of the plate are the corrugation angle (a), core sheet to facing sheet thickness ratio (t_c/t_f), the pitch to core depth ratio (p/h_c) and the core depth to core thickness ratio (h_c/t_c). Therefore, in this study these geometric parameters are analyzed. The corrugation angles vary from 60^0 to 90^0 with the increment of 10 degrees. The ratios of core sheet to facing sheet thickness are 0.6, 1.0, and 1.25. The pitch to core depth ratios are 1.0, 1.2, and 1.4. The ratios of the core depth to core thickness are 10, 20, and 40. Table **4-6,** Table **4-7**, and Table **4-8** show the results of the conducted numerical investigations for the certain h_c/t_c=10, 20, and 40, respectively, and various a, t_c/t_f, and p/h_c.

In general, the moment in the stiffer direction is larger than that in the weak direction. It can be shown in Table **4-6** that, although the stiffness in *x*-direction is stronger than these in *y*-direction, the moments in *x*-direction are smaller than these in *y*-direction in all cases. This is because the length in *x*-direction is almost three times that in *y*-direction. However, it also can be shown in Table **4-7** and Table **4-8** that in some cases the moments in *x*-direction are larger than these in *y*-direction in the same dimensions as Table **4-6**. Comparing these cases that M_x is greater than M_y, it can be found that with a tremendously increasing value of ratio, D_{Qx}/D_{Qy}, the moments in *x*-direction become greater than the moments in *y*-direction although the length in *x*-direction is almost three times that in *y*-direction. Therefore, in the case that the overall stiffness is little different in *x*-direction from in *y*-direction, the length effect is the key factor for the moments. Otherwise, in the case that the ratio D_{Qx}/D_{Qy} is irrelevantly high, the length effect is eliminated due to the stronger stiffness.

Table 4-6: Comparison of various geometric parameters for simply support, $\frac{h_c}{t_c}$ =10

a	t_c/t_f	p/h_c	D_x (N-m)	D_y (N-m)	D_{xy} (N-m)	D_{Qx} (N-m)	D_{Qy} (N-m)	w (mm)	M_x (N-m/m)	M_y (N-m/m)
60	0.6	1	3.20E+07	2.81E+07	2.14E+07	7.14E+08	2.95E+08	0.095	1.91E+03	5.16E+03
		1.2	3.22E+07	2.82E+07	2.14E+07	5.09E+08	1.36E+08	0.115	1.97E+03	5.11E+03
		1.4	3.23E+07	2.82E+07	2.14E+07	3.81E+08	7.53E+07	0.145	2.08E+03	5.03E+03
	1	1	1.92E+07	1.53E+07	1.15E+07	6.41E+08	2.47E+08	0.164	1.95E+03	5.18E+03
		1.2	1.93E+07	1.53E+07	1.15E+07	4.57E+08	1.07E+08	0.191	2.01E+03	5.14E+03
		1.4	1.95E+07	1.53E+07	1.15E+07	3.42E+08	6.03E+07	0.228	2.10E+03	5.09E+03
	1.25	1	1.58E+07	1.19E+07	8.91E+06	6.20E+08	2.16E+08	0.209	1.98E+03	5.18E+03
		1.2	1.60E+07	1.19E+07	8.91E+06	4.42E+08	9.71E+07	0.238	2.04E+03	5.15E+03
		1.4	1.61E+07	1.19E+07	8.91E+06	3.31E+08	5.39E+07	0.280	2.12E+03	5.10E+03
70	0.6	1	3.30E+07	2.82E+07	2.14E+07	6.32E+08	1.01E+08	0.127	2.05E+03	5.07E+03
		1.2	3.30E+07	2.82E+07	2.14E+07	4.58E+08	6.08E+07	0.160	2.18E+03	4.96E+03
		1.4	3.30E+07	2.82E+07	2.14E+07	3.47E+08	3.91E+07	0.204	2.38E+03	4.81E+03
	1	1	2.01E+07	1.53E+07	1.15E+07	5.67E+08	8.50E+07	0.203	2.07E+03	5.12E+03
		1.2	2.01E+07	1.53E+07	1.15E+07	4.11E+08	4.80E+07	0.249	2.19E+03	5.04E+03
		1.4	2.01E+07	1.53E+07	1.15E+07	3.12E+08	3.26E+07	0.297	2.33E+03	4.95E+03
	1.25	1	1.67E+07	1.19E+07	8.91E+06	5.49E+08	1.21E+08	0.227	2.05E+03	5.17E+03
		1.2	1.67E+07	1.19E+07	8.91E+06	3.98E+08	4.45E+07	0.299	2.21E+03	5.07E+03
		1.4	1.68E+07	1.19E+07	8.91E+06	3.02E+08	2.94E+07	0.356	2.35E+03	4.99E+03
80	0.6	1	3.39E+07	2.83E+07	2.14E+07	5.66E+08	4.92E+07	0.178	2.32E+03	4.88E+03
		1.2	3.37E+07	2.83E+07	2.14E+07	4.16E+08	3.45E+07	0.220	2.51E+03	4.73E+03
		1.4	3.36E+07	2.83E+07	2.14E+07	3.19E+08	2.46E+07	0.272	2.77E+03	4.52E+03
	1	1	2.10E+07	1.54E+07	1.15E+07	5.08E+08	4.25E+07	0.262	2.29E+03	5.01E+03
		1.2	2.09E+07	1.54E+07	1.15E+07	3.73E+08	2.88E+07	0.316	2.45E+03	4.90E+03
		1.4	2.08E+07	1.54E+07	1.15E+07	2.86E+08	2.06E+07	0.382	2.66E+03	4.76E+03
	1.25	1	1.76E+07	1.20E+07	8.91E+06	4.91E+08	3.91E+07	0.314	2.31E+03	5.05E+03
		1.2	1.75E+07	1.20E+07	8.91E+06	3.61E+08	2.70E+07	0.371	2.46E+03	4.96E+03
		1.4	1.74E+07	1.19E+07	8.91E+06	2.77E+08	1.94E+07	0.440	2.64E+03	4.84E+03
90	0.6	1	3.47E+07	2.83E+07	2.14E+07	5.09E+08	3.01E+07	0.238	2.69E+03	4.63E+03
		1.2	3.45E+07	2.83E+07	2.14E+07	3.79E+08	2.23E+07	0.290	2.95E+03	4.42E+03
		1.4	3.43E+07	2.83E+07	2.14E+07	2.93E+08	1.68E+07	0.352	3.27E+03	4.16E+03
	1	1	2.19E+07	1.54E+07	1.15E+07	4.57E+08	2.52E+07	0.339	2.61E+03	4.84E+03
		1.2	2.16E+07	1.54E+07	1.15E+07	3.40E+08	1.92E+07	0.397	2.80E+03	4.71E+03
		1.4	2.14E+07	1.54E+07	1.15E+07	2.63E+08	1.48E+07	0.467	3.03E+03	4.55E+03
	1.25	1	1.85E+07	1.20E+07	8.91E+06	4.42E+08	2.43E+07	0.390	2.61E+03	4.92E+03
		1.2	1.82E+07	1.20E+07	8.91E+06	3.29E+08	1.78E+07	0.461	2.80E+03	4.79E+03
		1.4	1.80E+07	1.20E+07	8.91E+06	2.54E+08	1.40E+07	0.531	2.99E+03	4.67E+03

Table 4-7: Comparison of various geometric parameters for simply support, $\frac{h_c}{t_c}$=20

a	t_c/t_f	p/h_c	D_x (N-m)	D_y (N-m)	D_{xy} (N-m)	D_{Qx} (N-m)	D_{Qy} (N-m)	w (mm)	M_x (N-m/m)	M_y (N-m/m)
60	0.6	1	1.32E+07	1.13E+07	8.56E+06	3.48E+08	3.47E+07	0.338	2.10E+03	5.03E+03
		1.2	1.33E+07	1.13E+07	8.56E+06	2.63E+08	1.43E+07	0.536	2.50E+03	4.72E+03
		1.4	1.34E+07	1.13E+07	8.56E+06	2.06E+08	8.74E+06	0.732	2.94E+03	4.38E+03
	1	1	8.39E+06	6.44E+06	4.84E+06	3.28E+08	2.45E+07	0.547	2.15E+03	5.07E+03
		1.2	8.48E+06	6.44E+06	4.84E+06	2.48E+08	1.02E+07	0.823	2.53E+03	4.82E+03
		1.4	8.54E+06	6.44E+06	4.84E+06	1.94E+08	5.66E+06	1.178	3.08E+03	4.45E+03
	1.25	1	7.04E+06	5.08E+06	3.80E+06	3.22E+08	2.15E+07	0.670	2.18E+03	5.08E+03
		1.2	7.13E+06	5.08E+06	3.80E+06	2.43E+08	9.34E+06	0.964	2.54E+03	4.88E+03
		1.4	7.19E+06	5.09E+06	3.80E+06	1.91E+08	5.14E+06	1.364	3.07E+03	4.55E+03
70	0.6	1	1.37E+07	1.13E+07	8.56E+06	3.32E+08	1.07E+07	0.640	2.81E+03	4.52E+03
		1.2	1.37E+07	1.13E+07	8.56E+06	2.52E+08	5.99E+06	0.940	3.56E+03	3.93E+03
		1.4	1.37E+07	1.13E+07	8.56E+06	1.98E+08	3.89E+06	1.261	4.38E+03	3.29E+03
	1	1	8.87E+06	6.46E+06	4.84E+06	3.13E+08	8.17E+06	0.935	2.79E+03	4.69E+03
		1.2	8.87E+06	6.46E+06	4.84E+06	2.37E+08	4.78E+06	1.312	3.41E+03	4.28E+03
		1.4	8.88E+06	6.46E+06	4.84E+06	1.87E+08	3.14E+06	1.735	4.15E+03	3.78E+03
	1.25	1	7.52E+06	5.10E+06	3.80E+06	3.07E+08	7.79E+06	1.064	2.76E+03	4.79E+03
		1.2	7.52E+06	5.10E+06	3.80E+06	2.33E+08	5.92E+06	1.249	3.01E+03	4.64E+03
		1.4	7.53E+06	5.10E+06	3.80E+06	1.83E+08	2.96E+06	1.948	4.06E+03	3.99E+03
80	0.6	1	1.42E+07	1.14E+07	8.56E+06	3.13E+08	5.02E+06	1.055	4.00E+03	3.66E+03
		1.2	1.41E+07	1.14E+07	8.56E+06	2.39E+08	3.37E+06	1.377	4.85E+03	2.99E+03
		1.4	1.40E+07	1.13E+07	8.56E+06	1.89E+08	2.43E+06	1.697	5.69E+03	2.33E+03
	1	1	9.31E+06	6.48E+06	4.84E+06	2.95E+08	4.15E+06	1.435	3.80E+03	4.11E+03
		1.2	9.24E+06	6.48E+06	4.84E+06	2.25E+08	2.86E+06	1.840	4.52E+03	3.62E+03
		1.4	9.19E+06	6.48E+06	4.84E+06	1.78E+08	2.11E+06	2.252	5.26E+03	3.12E+03
	1.25	1	7.96E+06	5.12E+06	3.80E+06	2.90E+08	4.05E+06	1.580	3.68E+03	4.31E+03
		1.2	7.89E+06	5.12E+06	3.80E+06	2.21E+08	2.74E+06	2.042	4.40E+03	3.87E+03
		1.4	7.84E+06	5.11E+06	3.80E+06	1.75E+08	1.99E+06	2.520	5.15E+03	3.40E+03
90	0.6	1	1.46E+07	1.14E+07	8.56E+06	2.92E+08	2.91E+06	1.501	5.43E+03	2.67E+03
		1.2	1.45E+07	1.14E+07	8.56E+06	2.24E+08	2.20E+06	1.787	6.18E+03	2.08E+03
		1.4	1.44E+07	1.14E+07	8.56E+06	1.78E+08	1.68E+06	2.089	6.96E+03	1.45E+03
	1	1	9.76E+06	6.50E+06	4.84E+06	2.75E+08	2.64E+06	1.929	4.96E+03	3.46E+03
		1.2	9.61E+06	6.49E+06	4.84E+06	2.11E+08	1.92E+06	2.377	5.78E+03	2.91E+03
		1.4	9.51E+06	6.49E+06	4.84E+06	1.68E+08	1.51E+06	2.764	6.47E+03	2.43E+03
	1.25	1	8.41E+06	5.13E+06	3.80E+06	2.70E+08	2.55E+06	2.128	4.83E+03	3.75E+03
		1.2	8.27E+06	5.13E+06	3.80E+06	2.07E+08	1.87E+06	2.613	5.60E+03	3.26E+03
		1.4	8.16E+06	5.12E+06	3.80E+06	1.65E+08	1.43E+06	3.098	6.36E+03	2.78E+03

Table 4-8: Comparison of various geometric parameters for simply support, $\frac{h_c}{t_c}$ =40

a	t_c/t_f	p/h_c	D_x (N-m)	D_y (N-m)	D_{xy} (N-m)	D_{Qx} (N-m)	D_{Qy} (N-m)	w (mm)	M_x (N-m/m)	M_y (N-m/m)
60	0.6	1	5.98E+06	5.01E+06	3.79E+06	1.54E+08	3.54E+06	1.745	3.11E+03	4.26E+03
		1.2	6.02E+06	5.01E+06	3.79E+06	1.17E+08	1.45E+06	3.173	4.79E+03	2.94E+03
		1.4	6.05E+06	5.01E+06	3.79E+06	9.13E+07	8.00E+05	4.548	6.46E+03	1.62E+03
	1	1	3.92E+06	2.94E+06	2.21E+06	1.49E+08	2.51E+06	2.621	3.15E+03	4.41E+03
		1.2	3.96E+06	2.94E+06	2.21E+06	1.13E+08	1.09E+06	4.561	4.72E+03	3.34E+03
		1.4	3.99E+06	2.94E+06	2.21E+06	8.85E+07	6.00E+05	6.618	6.45E+03	2.14E+03
	1.25	1	3.32E+06	2.34E+06	1.75E+06	1.48E+08	2.17E+06	3.129	3.21E+03	4.46E+03
		1.2	3.36E+06	2.34E+06	1.75E+06	1.12E+08	9.70E+05	5.293	4.73E+03	3.50E+03
		1.4	3.39E+06	2.34E+06	1.75E+06	8.77E+07	5.60E+05	7.505	6.35E+03	2.47E+03
70	0.6	1	6.22E+06	5.02E+06	3.79E+06	1.47E+08	1.14E+06	3.657	5.60E+03	2.41E+03
		1.2	6.22E+06	5.02E+06	3.79E+06	1.12E+08	6.36E+05	5.092	7.40E+03	1.01E+03
		1.4	6.22E+06	5.02E+06	3.79E+06	8.78E+07	4.15E+05	6.226	8.80E+03	-7.58E+01
	1	1	4.15E+06	2.95E+06	2.21E+06	1.43E+08	9.30E+05	5.019	5.36E+03	3.03E+03
		1.2	4.16E+06	2.95E+06	2.21E+06	1.08E+08	5.25E+05	7.088	7.19E+03	1.80E+03
		1.4	4.16E+06	2.95E+06	2.21E+06	8.51E+07	3.41E+05	8.877	8.76E+03	7.43E+02
	1.25	1	3.56E+06	2.35E+06	1.75E+06	1.41E+08	8.21E+05	5.866	5.44E+03	3.19E+03
		1.2	3.56E+06	2.35E+06	1.75E+06	1.07E+08	4.85E+05	8.103	7.16E+03	2.12E+03
		1.4	3.56E+06	2.35E+06	1.75E+06	8.43E+07	3.28E+05	10.030	8.64E+03	1.20E+03
80	0.6	1	6.44E+06	5.04E+06	3.79E+06	1.39E+08	5.52E+05	5.402	8.16E+03	6.13E+02
		1.2	6.41E+06	5.04E+06	3.79E+06	1.06E+08	3.62E+05	6.504	9.53E+03	-4.51E+02
		1.4	6.38E+06	5.03E+06	3.79E+06	8.36E+07	2.63E+05	7.322	1.05E+04	-1.20E+03
	1	1	4.38E+06	2.96E+06	2.21E+06	1.34E+08	4.73E+05	7.435	7.95E+03	1.52E+03
		1.2	4.34E+06	2.96E+06	2.21E+06	1.03E+08	3.19E+05	9.065	9.39E+03	5.46E+02
		1.4	4.32E+06	2.96E+06	2.21E+06	8.10E+07	2.29E+05	10.470	1.06E+04	-2.71E+02
	1.25	1	3.78E+06	2.36E+06	1.75E+06	1.33E+08	4.48E+05	8.394	7.89E+03	1.90E+03
		1.2	3.75E+06	2.36E+06	1.75E+06	1.02E+08	2.99E+05	10.400	9.45E+03	9.34E+02
		1.4	3.72E+06	2.35E+06	1.75E+06	8.02E+07	2.20E+05	11.960	1.06E+04	1.88E+02
90	0.6	1	6.66E+06	5.05E+06	3.79E+06	1.29E+08	3.24E+05	6.687	1.03E+04	-7.45E+02
		1.2	6.59E+06	5.05E+06	3.79E+06	9.92E+07	2.82E+05	7.072	1.06E+04	-1.05E+03
		1.4	6.54E+06	5.04E+06	3.79E+06	7.88E+07	1.87E+05	8.029	1.17E+04	-1.93E+03
	1	1	4.60E+06	2.97E+06	2.21E+06	1.25E+08	3.00E+05	9.186	1.02E+04	3.70E+02
		1.2	4.53E+06	2.96E+06	2.21E+06	9.61E+07	2.18E+05	10.520	1.13E+04	-4.09E+02
		1.4	4.48E+06	2.96E+06	2.21E+06	7.63E+07	1.69E+05	11.560	1.21E+04	-9.89E+02
	1.25	1	4.01E+06	2.36E+06	1.75E+06	1.24E+08	2.87E+05	10.430	1.02E+04	8.12E+02
		1.2	3.93E+06	2.36E+06	1.75E+06	9.52E+07	2.13E+05	11.960	1.13E+04	8.61E+01
		1.4	3.88E+06	2.36E+06	1.75E+06	7.56E+07	1.64E+05	13.270	1.22E+04	-5.21E+02

4.4.1 Ratios of Core Depth to Thickness, $\frac{h_c}{t_c}$

In this section, the effects of ratios of core depth to thickness h_c/t_c are discussed from Table **4-6,** Table **4-7**, and Table **4-8**. It is seen that with an increasing h_c/t_c value the stiffness of the corrugated-core sandwich plate decrease in these tables. In this analysis, the depth of corrugation h_c is a constant. Thus, with an increasing value of h_c/t_c, the thickness of the core sheet becomes thinner and the stiffness of the corrugated-core sandwich plate also declines.

Comparing Table **4-6** for h_c/t_c=10 with Table **4-7** for h_c/t_c=20, we can find that by an increment of 10 for h_c/t_c, the elastic constants, D_x, D_y, and D_{xy}, decline about 55% to 60% and D_{Qx} decreases about 35% to 50% but D_{Qy} declines about 90%. The difference between Table **4-7** and Table **4-8** for h_c/t_c=40, we noted that the elastic constants, D_x, D_y, D_{xy}, and D_{Qx} decreases about 55% by an increasing h_c/t_c value for 20, and D_{Qy} declines still about 90%. Therefore, with an increasing value of the h_c/t_c ratio, the values of the stiffness of the corrugated-core sandwich decrease mitigated.

Comparing the deflections in these tables, it can be found that due to the decrease of the stiffness, the deflection increases with an increasing value of h_c/t_c. Although the deflection increases as several times as the lower value of h_c/t_c, the deflections of the higher value of h_c/t_c are still remarkably small. For the moments in these tables, we noted that when value the of h_c/t_c increases, the moments in x-direction increase but the moments in y-direction decrease. This is due to the difference of stiffness between x- and

y-direction increases by an increasing value of h_c/t_c. This phenomenon has been discussed previously.

4.4.2 Corrugation Angle, *a*

The effect of corrugation angle of a corrugated-core sandwich plate is discussed subsequently. The geometric parameters in this section are h_c/t_c=10, t_c/t_f=0.6, and p/h_c=1 and the corrugation angle, a, is varied. It can be shown in Table **4-9** that with an increasing corrugation angle, the bending stiffness D_x and D_y increase only marginally and D_{xy} almost remains unchanged, whereas there are significant decreases in the values of D_{Qx} and D_{Qy} causing the overall plate stiffness to decrease. Increasing the corrugation angle by increments of 10 degrees, D_{Qx} decreases about 10% and D_{Qy} decreases mitigated from 60% to 40%. We also noted that the deflection can increase several times with only increasing the degree of the corrugation angle.

Table 4-9: Comparison of various ratios a for h_c/t_c=10, t_c/t_f=0.6, and p/h_c =1.0

a	t_c/t_f	p/h_c	D_x (N-m)	% Change	D_y (N-m)	% Change	D_{xy} (N-m)	% Change	D_{Qx} (N-m)	% Change	D_{Qy} (N-m)	% Change	w (mm)	% Change	M_x (N-m/m)	% Change	M_y (N-m/m)	% Change
60	0.6	1	3.20E+07	~	2.81E+07	~	2.14E+07	~	7.14E+08	~	2.95E+08	~	0.095	~	1.91E+03	~	5.16E+03	~
70			3.30E+07	2.97%	2.82E+07	0.25%	2.14E+07	0.00%	6.32E+08	-11.51%	1.01E+08	-65.70%	0.127	34.56%	2.05E+03	7.56%	5.07E+03	-1.88%
80			3.39E+07	2.70%	2.83E+07	0.18%	2.14E+07	0.00%	5.66E+08	-10.43%	4.92E+07	-51.41%	0.178	40.09%	2.32E+03	13.07%	4.88E+03	-3.67%
90			3.47E+07	2.63%	2.83E+07	0.21%	2.14E+07	0.00%	5.09E+08	-10.03%	3.01E+07	-38.83%	0.238	33.56%	2.69E+03	15.88%	4.63E+03	-5.18%

$$\%Change = \frac{a(i) - a(i-1)}{a(i-1)}$$

4.4.3 Ratios of Core to Facing Plate Thickness, $\frac{t_c}{t_f}$

In this section, the effect of the ratio t_c/t_f is discussed. Because the corrugation height h_c is 0.1m and the certain ratio of h_c/t_c, the thickness of the core sheet is determined. The geometric parameters in this section are h_c/t_c=10, α=60^0, and p/h_c=1 and the ratio, t_c/t_f, is varied. Table **4-10** is the comparison of various t_c/t_f for h_c/t_c=10, α=60, and p/h_c =1.0. It can be found in the table that with an increasing value of t_c/t_f the stiffness of the corrugated-core sandwich plate decreases. As the ratio of t_c/t_f increases for a particular value of t_c, the thickness of the facing sheet, t_f, becomes thinner, and this causes the plate to be less stiff.

With an increasing t_c/t_f ratio 0.6 to 1.0, D_x decreases about 40% and D_y and D_{xy} decrease about 45%, but D_{Qx} decreases about 10% and D_{Qy} decreases about 16%. For an increasing t_c/t_f ratio 1.0 to 1.25, D_x decreases about 17% and D_y and D_{xy} decrease about 22%, but D_{Qx} decreases about 3% and D_{Qy} decreases about 12%. In these cases when the t_c/t_f ratio increases the t_f become thinner. And for a corrugated-core sandwich plate, the face sheets take most of the flexural load. Therefore, the t_c/t_f ratio affects the flexural stiffness more than the shear stiffness.

Table 4-10: Comparison of various ratios t_c/t_f for h_c/t_c=10, a =60, and p/h_c =1.0

a	p/h_c	t_c/t_f	D_x (N-m)	% Change	D_y (N-m)	% Change	D_{xy} (N-m)	% Change	D_{Qx} (N-m)	% Change	D_{Qy} (N-m)	% Change	w (mm)	% Change	M_x (N-m/m)	% Change	M_y (N-m/m)	% Change
60	1	0.6	3.20E+07	~	2.81E+07	~	2.14E+07	~	7.14E+08	~	2.95E+08	~	0.095	~	1.91E+03	~	5.16E+03	~
		1	1.92E+07	-40.08%	1.53E+07	-45.70%	1.15E+07	-46.14%	6.41E+08	-10.25%	2.47E+08	-16.39%	0.164	73.49%	1.95E+03	2.05%	5.18E+03	0.29%
		1.25	1.58E+07	-17.73%	1.19E+07	-22.32%	8.91E+06	-22.65%	6.20E+08	-3.31%	2.16E+08	-12.60%	0.209	27.38%	1.98E+03	1.59%	5.18E+03	0.10%

$$\%Change = \frac{\frac{t_c}{t_f}(i) - \frac{t_c}{t_f}(i-1)}{\frac{t_c}{t_f}(i-1)}$$

4.4.4 Ratios of Pitch to Core Depth, $\frac{p}{h_c}$

It can be shown in Table **4-6**, Table **4-7,** and Table **4-8** that as the ratios p/h_c increase the D_x and D_y increase marginally and the D_{xy} remains unchanged. However, the shear stiffnesses, D_{Qx} and D_{Qy}, decrease drastically especially the D_{Qy}. The geometric parameters in this section are h_c/t_c=10, a=60^0, and t_c/t_f=0.6 and the ratio, p/h_c, is varied. Table **4-11** shows the certain cases obtained from Table **4-6** for the comparison of various ratios p/h_c. It can be shown in Table **4-11** that the D_{Qy} reduces about 45% to 55% and the D_{Qx} reduces about 25% to 30% by an incremental ratio, 0.2, of p/h_c. The deflection increases about 21% to 25% by an incremental value, 0.2, of p/h_c. It can be seen that as the p/h_c ratio increases the deflection at the center of the corrugated-core sandwich plate increases and the stiffness of the plate decreases. This is because as the p/h_c ratio increases there are fewer corrugations in the plate for a given width of the plate, and this causes the plate to be less stiff.

Table 4-11: Comparison of various ratios p/h_c for h_c/t_c=10, a =60, and t_c/t_f=0.6

a	t_c/t_f	p/h_c	D_x (N-m)	% Change	D_y (N-m)	% Change	D_{xy} (N-m)	D_{Qx} (N-m)	% Change	D_{Qy} (N-m)	% Change	w (mm)	% Change	M_x (N-m/m)	% Change	M_y (N-m/m)	% Change
60	0.6	1	3.20E+07	~	2.81E+07	~	2.14E+07	7.14E+08	~	2.95E+08	~	0.095	~	1.91E+03	~	5.16E+03	~
		1.2	3.22E+07	0.53%	2.82E+07	0.04%	2.14E+07	5.09E+08	-28.72%	1.36E+08	-53.91%	0.115	21.34%	1.97E+03	3.57%	5.11E+03	-0.99%
		1.4	3.23E+07	0.37%	2.82E+07	0.04%	2.14E+07	3.81E+08	-25.12%	7.53E+07	-44.69%	0.145	26.07%	2.08E+03	5.57%	5.03E+03	-1.66%

$$\%Change = \frac{\frac{p}{h_c}(i) - \frac{p}{h_c}(i-1)}{\frac{p}{h_c}(i-1)}$$

It should be noted that with an increasing p/h_c the D_x increases; however, for theses cases that the corrugation angles are greater than 80 degree, the D_x decrease with an increasing p/h_c shown in Table **4-12**.

Table 4-12: Comparison of various ratios p/h_c for h_c/t_c=10, a =80, and t_c/t_f=0.6

a	t_c/t_f	p/h_c	D_x (N-m)	D_y (N-m)	D_{xy} (N-m)	D_{Qx} (N-m)	D_{Qy} (N-m)	w (mm)	M_x (N-m/m)	M_y (N-m/m)
80	0.6	1	3.39E+07	2.83E+07	2.14E+07	5.66E+08	4.92E+07	0.178	2.32E+03	4.88E+03
		1.2	3.37E+07	2.83E+07	2.14E+07	4.16E+08	3.45E+07	0.220	2.51E+03	4.73E+03
		1.4	3.36E+07	2.83E+07	2.14E+07	3.19E+08	2.46E+07	0.272	2.77E+03	4.52E+03

This phenomenon is discussed subsequently. According to Figure **4-14**, the D_x can be expressed as follows:

$$D_x = E_c I_c + E_f I_f = E_c \left(I_c + I_f \right) \tag{**4.13**}$$

From the geometry of the corrugated-core cross-section, moments of inertia for face sheets and core sheet can be expressed as follows:

$$I_f = 2\left[2p \times t_f \times \left(\frac{h}{2} \right)^2 \right] \tag{**4.14**}$$

$$\begin{aligned} I_c &= 2\left[f \times t_c \times \left(\frac{h_c}{2} \right)^2 \right] + \frac{2 \times t_c \times s^3}{12} \sin^2 q \\ &= \frac{f \times t_c \times h_c^2}{2} + \frac{2 \times t_c \times h_c^3}{12 \sin q} \end{aligned} \tag{**4.15**}$$

$$I_{c1} = \frac{f \times t_c h_c^2}{2}; I_{c2} = \frac{2 \times t_c \times h_c^3}{12 \sin q} \tag{**4.16**}$$

Where:

E_c Young's modulus of the core sheet

E_f Young's modulus of face sheets

In these following cases, the depth of corrugation h_c remains 0.1m, h_c/t_c equals to 10, and t_c/t_f remains 0.6. The calculated results of moment of inertia on various p/hc and a can be found in Table **4-13**. It can be shown that the moment of inertia increases with an increasing corrugation angle and p/h_c for a given width, $2p$. However, the increasing rates of moments of inertia for the corrugation angles greater than 80 degree are less than the increasing rates of the corrugation pitches. Therefore, with an increasing value of p/h_c, moments of inertia decrease for these cases that the corrugation angles are greater than 80 degree.

Table 4-13: Comparison of moments of inertia on various p/h_c and a

p/h_c	a	I_c		I_f	I_c+I_f	$(I_c+I_f)/2p$
		I_{c1}	I_{c2}			
1	60	1.057E-06	9.623E-07	1.070E-05	1.272E-05	6.361E-05
	70	1.590E-06	8.868E-07	1.070E-05	1.318E-05	6.590E-05
	80	2.059E-06	8.462E-07	1.070E-05	1.361E-05	6.805E-05
	90	2.500E-06	8.333E-07	1.070E-05	1.404E-05	7.019E-05
1.2	60	1.557E-06	9.623E-07	1.284E-05	1.536E-05	6.401E-05
	70	2.090E-06	8.868E-07	1.284E-05	1.582E-05	6.592E-05
	80	2.559E-06	8.462E-07	1.284E-05	1.625E-05	6.771E-05
	90	3.000E-06	8.333E-07	1.284E-05	1.668E-05	6.949E-05
1.4	60	2.057E-06	9.623E-07	1.499E-05	1.800E-05	6.430E-05
	70	2.590E-06	8.868E-07	1.499E-05	1.846E-05	6.594E-05
	80	3.059E-06	8.462E-07	1.499E-05	1.889E-05	6.747E-05
	90	3.500E-06	8.333E-07	1.499E-05	1.932E-05	6.899E-05

4.4.5 Effects of length, *a*, and width, *b*

The geometric parameters in this section are h_c/t_c=10, p/h_c=1.0, a=60^0, and t_c/t_f=0.6. In this study, the uniformly distributed load is kept 10 kN/m^2. Various lengths, the corrugation direction, and widths, the direction normal to corrugation, are discussed subsequently. Table **4-14** is the comparison of deflections and moments with various length, *a*, and width, *b*. In the table, *a* and *b* are varied from 2.1m, 4m, and 6m, respectively.

Table 4-14: Comparison of central deflections and moments with various length

a (m)	b (m)	D_x	D_y	D_{xy}	D_{Qx}	D_{Qy}	w (mm)	M_x (N-m/m)	M_y (N-m/m)
6	2.1	1.92E+07	1.53E+07	1.15E+07	6.41E+08	2.47E+08	0.164	1.95E+03	5.18E+03
4.2							0.137	2.34E+03	4.41E+03
2.1							0.054	2.50E+03	1.89E+03
2.1	2.1						0.054	2.50E+03	1.89E+03
	4.2						0.111	4.79E+03	1.68E+03
	6						0.126	5.33E+03	1.45E+03

It can be seen in Table **4-14** that in the fixed value of the width or length, by increasing length or width, the corresponding deflection increases. It is also seen that decreasing the plate span in one direction not only decrease the deformation but also changes the bending moments. In fact, decreasing the plate span in one direction influences the moments in the same manner as increasing the rigidity in that direction, e.g., decreasing the span in the *x*-direction, *a*, increases M_x whereas M_y is decreased. The effect of increasing stiffness in one direction has the same effect as changing the plate span.

4.4.6 Discussion of negative moments in the direction normal to the corrugation

In previous sections, we can find that the negative moments in the direction normal to corrugation (or y-direction) do not occur in all cases. According to the moment-displacement relation, the negative moment might occur only when the slope in y-direction q_y is negative. Therefore, from Eq. **4.4**, we can obtain the coefficients of slope q_y as following form:

$$B_{mn} = \frac{K_{21}K_{13} - K_{11}K_{23}}{K_{11}K_{22} - K_{21}K_{12}} w_{mn} \tag{4.17}$$

According to the condition inducing the negative moment in previous paragraph, we can write:

$$B_{mn} < 0 \tag{4.18}$$

For corrugated-core sandwich plates, in general, the shear stiffness D_{Qx} is irrelevantly higher than other stiffness. Therefore, according to the denominator in Eq. **4.17** and the elastic constants of the corrugated-core sandwich plate, we can find:

$$\begin{aligned} & K_{11}K_{22} - K_{21}K_{22} \\ & = \left[D_{xx}\left(\frac{mp}{a}\right)^2 + \frac{D_{xy}}{2}\left(\frac{np}{b}\right)^2 + D_{Qx} \right]\left[D_{yy}\left(\frac{np}{b}\right)^2 + \frac{D_{xy}}{2}\left(\frac{mp}{a}\right)^2 + D_{Qy} \right] \\ & - \left[\left(\frac{D_{xy}}{2} + D_{xx}u_y \right)\left(\frac{mnp^2}{ab}\right) \right]^2 > 0 \end{aligned} \tag{4.19}$$

Because Eq. **4.19** is always positive, the numerator in Eq. **4.19** should be negative and Eq. **4.18** can be satisfied. Thus,

$$K_{21}K_{13} - K_{11}K_{23} < 0 \tag{4.20}$$

Substituting Eq. **4.5** and Eq. **4.6** into Eq. **4.20**, we can obtain:

$$\left[D_{xx}\left(\frac{mp}{a}\right)^2+\frac{D_{xy}}{2}\left(\frac{np}{b}\right)^2+D_{Qx}\right]\left[D_{Qy}\left(\frac{np}{b}\right)\right]-\left[\left(\frac{D_{xy}}{2}+D_{xx}u_y\right)\left(\frac{mnp^2}{ab}\right)\right]\left[D_{Qx}\left(\frac{mp}{a}\right)\right]<0 \qquad \textbf{(4.21)}$$

The above equation can be written as:

$$\left[D_{xx}\left(\frac{mp}{a}\right)^2+\frac{D_{xy}}{2}\left(\frac{np}{b}\right)^2+D_{Qx}\right]\left[D_{Qy}\left(\frac{np}{b}\right)\right]<\left[\left(\frac{D_{xy}}{2}+D_{xx}u_y\right)\left(\frac{mnp^2}{ab}\right)\right]\left[D_{Qx}\left(\frac{mp}{a}\right)\right] \qquad \textbf{(4.22)}$$

Rearranging the above equation, we can obtain:

$$\frac{\left[\frac{D_{xy}}{2D_{Qy}}+\frac{D_{xx}u_y}{D_{Qy}}\right]\left(\frac{mp}{a}\right)^2}{\left[\frac{D_{xx}}{D_{Qx}}\left(\frac{mp}{a}\right)^2+\frac{D_{xy}}{2D_{Qx}}\left(\frac{np}{b}\right)^2+1\right]}>1 \qquad \textbf{(4.23)}$$

We note that the moments in the *y*-direction are negative only when the elastic constants and dimensions of the plate satisfy Eq. **4.23**. It can be seen that Eq. **4.23** relates to the dimensions and elastic constants of the corrugated-core sandwich plate. For the denominator in Eq. **4.23**, as can be known that the shear stiffness D_{Qx} is irrelevantly high in corrugated-core sandwich plates; consequently, the ratios D_{xx}/D_{Qx} and D_{xy}/D_{Qx} are very small. For the numerator in Eq. **4.23**, the situation that *m* and *n* is equal to 1 is discussed. If the length, *a*, is less than *p*, Eq. **4.23** is easily satisfied because the ratio, *p*/*a*, is greater than 1. In general, the D_{xx}/D_{Qy} and D_{xy}/D_{Qy} ratios causing the negative moments in y-direction could be different if *a*, length in *x*-direction or corrugation direction, changes.

The ratios of D_{xx}/D_{Qy} and D_{xy}/D_{Qy} are discussed subsequently. In these cases, the length in corrugation direction, *a*, is 6m. The comparison of elastic constants ratios for these cases that the moments in *y*-direction are negative in Table **4-8** is shown in Table **4-**

15. As mentioned previously, the D_{xx}/D_{Qx} and D_{xy}/D_{Qx} ratios are very small in all the cases shown in Table **4-15**. It can also be found that only in these cases that the ratio D_{xx}/D_{Qy} is greater than 16 and the ratio D_{xy}/D_{Qy} is greater than 9, the coefficients of q_y are negative and M_y is negative. The ratios D_{xx}/D_{Qy} and D_{xy}/D_{Qy} that cause the moment in y-direction to be negative relates to the dimensions of the plate. Consequently, higher ratio of h_c/t_c, higher degree of corrugation angle a, and higher p/h_c value can cause the ratios of these above elastic constants, D_{xx}/D_{Qy} and D_{xy}/D_{Qy}, to be higher due to the lower D_{Qy} and can cause the moment in y-direction to be negative.

According the above analysis, we noted that only in the relatively high values of D_{xx}/D_{Qy} and D_{xy}/D_{Qy} ratios and shorter length in corrugation direction, the negative moments in y-direction might occur. Furthermore, only either D_{xx} or D_{xy} are relatively larger than D_{Qy} or the shear stiffness D_{Qy} is relatively low, the ratios, D_{xx}/D_{Qy} and D_{xy}/D_{Qy}, become relatively high. In these cases the stiffness in the x-direction or corrugation direction is extremely higher than that in y-direction due to the irrelevantly high D_{Qx} and low D_{Qy}. Therefore, the most bending resistance is taken by x-direction and that causes the moment in y-direction to be relatively small or even become negative.

Table 4-15: Comparison of elastic constant for negative-moment cases

h_c/t_c=40 a=6m b=2.1m

α	t_c/t_f	p/h_c	D_x (N-m)	D_y (N-m)	D_{xy} (N-m)	D_{Qx} (N-m)	D_{Qy} (N-m)	D_{xx}	D_{xx}/D_{Qx}	D_{xy}/D_{Qx}	D_{xx}/D_{Qy}	D_{xy}/D_{Qy}
70	0.6	1.4	6.22E+06	5.02E+06	3.79E+06	8.78E+07	4.15E+05	6.71E+06	0.076	0.043	16.16	9.14
80	0.6	1.2	6.41E+06	5.04E+06	3.79E+06	1.06E+08	3.62E+05	6.89E+06	0.065	0.036	19.05	10.48
		1.4	6.38E+06	5.03E+06	3.79E+06	8.36E+07	2.63E+05	6.87E+06	0.082	0.045	26.13	14.43
	1	1.4	4.32E+06	2.96E+06	2.21E+06	8.10E+07	2.29E+05	4.60E+06	0.057	0.027	20.12	9.64
90	0.6	1	6.66E+06	5.05E+06	3.79E+06	1.29E+08	3.24E+05	7.15E+06	0.055	0.029	22.09	11.71
		1.2	6.59E+06	5.05E+06	3.79E+06	9.92E+07	2.82E+05	7.08E+06	0.071	0.038	25.11	13.46
		1.4	6.54E+06	5.04E+06	3.79E+06	7.88E+07	1.87E+05	7.03E+06	0.089	0.048	37.64	20.32
	1	1.2	4.53E+06	2.96E+06	2.21E+06	9.61E+07	2.18E+05	4.81E+06	0.050	0.023	22.12	10.14
		1.4	4.48E+06	2.96E+06	2.21E+06	7.63E+07	1.69E+05	4.76E+06	0.062	0.029	28.20	13.06
	1.25	1.4	3.88E+06	2.36E+06	1.75E+06	7.56E+07	1.64E+05	4.11E+06	0.054	0.023	25.00	10.64

4.4.7 Conclusions

The primary geometric parameters affecting the behavior of the plate, such as the corrugation angle (a), core sheet to facing sheet thickness ratio (t_c/t_f), the pitch to core thickness ratio (p/h_c), and the core depth to core thickness ratio (h_c/t_c), and the width and length of the plate have been discussed in previous sections. It is demonstrated that the h_c/t_c and t_c/t_f control the effect of the flexural stiffness and h_c/t_c, t_c/t_f, a, and p/h_c affect the shear stiffness more. In this section we noted that the h_c/t_c affects both flexural and shear stiffnesses and with an increasing h_c/t_c ratio, the stiffness might decrease more than 50% in D_x, D_y, D_{xy}, and D_{Qx} and about 90% in D_{Qy}. The ratio h_c/t_c and corrugation angle a are highly sensitive to D_{Qy} at higher values of this ratio. It is also seen that in a short length or width the plate become stiffer.

According to this analysis of different geometric parameters, the central plate deflection is affected significantly by the core in this corrugated-core sandwich plate. The shear stiffness strongly influences the central deflection of these plates. It also can be seen that high shear stiffness stiffens the plate even though the flexural rigidities are marginally increased. Also, the effect of increasing plate stiffness has the same effect as shortening the panel length.

The negative moments in the direction normal to the corrugation do not occur in all the corrugated-core sandwich plates. Only in these cases that the stiffness of the plate in corrugation direction is extremely higher than that in the direction normal to

corrugation, the negative moments might occur. The most bending resistance is taken by *x*-direction and that cause the moment in *y*-direction to be relatively small or even become negative. The stiffness of the corrugated-core sandwich plate is determined by the flexural and shear stiffnesses. In general, the flexural stiffnesses in both *x*- and *y*-direction do not have a significant discrepancy. However, the shear stiffnesses are affected significantly by the above discussed geometric parameters. To prevent the extremely weak shear stiffness in *y*-direction, the higher degrees of corrugation angle, higher values of the p/h_c ratio, and lower values of the t_c/t_f ratio should be avoided.

Chapter 5

Conclusions

5.1 Introduction

One of the main goals of this study was to develop an accurate and powerful method for a complicated elasto-plastic problem. The Reissner-Mindlin plate theory was employed to formula the elasto-plastic plate bending representation. The linear elastic analysis is well-known and straightforward. In the elasto-plastic analysis, the general Galerkin method and incremental method were employed to construct a powerful algorithm to solve these difficult problems. Also, the iterative procedure was engaged to find the incremental plastic moments $\{dM^p\}$. Convergence occurs if changes in $\{dM^p\}$ are sufficiently small.

In this numerical study, the elastic perfectly-plastic analysis has been analyzed. The other main goal is the analysis of effects of geometric parameters for a corrugated core and various lengths and widths of these plates. The relationship between geometry and the stiffness of the corrugated-core sandwich plate was studied.

5.2 Conclusions

The elasto-plastic analysis of a corrugated-core sandwich plate has been developed in this study. The developed study can be applied in both elastic perfectly-

plastic and strain-hardening behaviors. However, due to currently absent experimental data of the post yield behavior of corrugated-core sandwich plates, in these numerical studies, only the behaviors of elastic perfectly-plastic material were analyzed in this work.

The modified yield surface based on Ilyushin and Hill's yield criteria for the structurally orthotropic plate can theoretically work well. The convergence of the elasto-plastic analysis is achieved quickly in this study. In general, the convergence is achieved in only five or six iterations.

Also, a comprehensive stress analysis for corrugated-core plates is developed. The effects of geometric parameters and various lengths and widths of corrugated-core sandwich plates with all simply supported boundary conditions on the plate behavior and strength were studied. These geometric parameters such as the ratios of core sheet to facing sheet thickness (t_c/t_f), the pitch to core thickness (p/h_c), the core depth to core thickness (h_c/t_c), and corrugation angle (α), are analyzed and discussed. The central deflection of the corrugated-core plate is significantly affected by the corrugated core in this study. It also can be seen that high shear stiffness stiffens the plate even though the flexural rigidities are marginally increased. The effect of increasing plate stiffness has the same effect as shortening the panel length or width.

Some new phenomena observed in experimental investigations of corrugated-core sandwich plates, but not found in previous numerical analysis, have been confirmed and reported. In particular, our investigation has strengthened some experimental results

obtained in (Tan et al. 1989) which lacked supported from 3D FEM, and the other analytical solutions. The present analytical solution agrees with all the experimental investigations both for the deflections and the bending moments in (Tan et al. 1989).

In this study, it was shown that the negative moments in the *y*-direction do not happen in all cases. The negative moments can be obtained only for significantly high stiffness ratios D_x/D_{Qy} and D_{xy}/D_{Qy}, and lower values of D_{Qy}. Therefore, to avoid the negative moment in the *y*-direction, higher corrugation angle a and higher h_c/t_c and p/h_c ratios should not be used.

According to this analysis, some recommendations for the selection of the geometric parameters of corrugated-core sandwich plates have been made. It is found that lower ratios of some geometric parameters such as h_c/t_c, t_c/t_f, and p/h_c make the plate stronger. However, this will result in an increasing amount of material in the structure. Therefore, better corrugated-core sandwich plates should have the following properties: t_c is identical to t_f, the corrugation angle a is between 45^0 and 70^0, the ratio h_c/t_c is around 20, and the ratio p/h_c is between 1 and 1.2.

5.3 Recommendations for Future Work

The numerical study of the elasto-plastic analysis in this research focuses on perfectly-plastic behavior although the developed research can be applied to strain-hardening behavior. It is necessary to do experiments to verify the structural behavior

after yielding occurs. These experiments relate to the post yielding behaviors and the orthotropic parameters of plasticity described in Appendix B should be taken in the future studies.

The displacement-strain relationship of this elasto-plastic study is based on the small deflection theory. In general, when yielding occurs, the deflection might be large enough to consider the effects of high order terms in displacement-strain relationship. Therefore, in future work, combining both geometric and material nonlinearities is another important issue and the von Karmam stress-strain relation might be one of the options to be applied in the elasto-plastic analysis to consider the geometric nonlinearity. However, the mathematical complexity due to combination of the high order terms of the displacement-strain relationship and material nonlinearity might be very difficult to solve.

In this study, an assumption that the whole cross-section yields simultaneously is made to simplify the calculation and complexity of the mathematical model in this analysis. In realty, the yielding occurs layer by layer through the whole cross-section. The layer-by-layer analysis can be done by FEM. However, the employed method in this study has the mathematical complexity corresponding to the realty, i.e., layer-by-layer analysis. In the future research, if the complexity caused by layer-by-layer analysis can be solved, the more accurate and more closed to realty answer can be obtained.

In this research, only the deflection at the central point was calculated, and moments in the x- and y-directions at the central point were calculated to check the yielding of the plate. However, the yielding at other points on this plate was not checked. It is known that the whole plate should show gradual plastification until some failure mechanism is achieved. In the future, it is necessary to determine the spread of plastic behavior in the whole plate, i.e. considering yielding at other points in the plate. The resistant curve in Fig. 4-11 is bilinear. In realty, when considering the entire plastic behavior of the plate, the real shape of the function after the first yielding occurs should be a curve, instead of the straight line.

Bibliography

Allen, H. G. (1969). "Analysis and design of structural sandwich panels." *Pergamon, Oxford, U.K.*

Banerjee, P. K., and Butterfield, R. (1981). "Boundary element methods in engineering science." *McGraw-Hill, New York*.

Bennett, J. A. (1971). "Nonlinear vibration of simply supported angle ply laminated plates." *AIAA J.*, 9, 1997-2003.

Bird, J. (1991). "Laser welded steel sandwich panels." *DRA TM 91221*.

Budiansky, B. (1959). "A reassessment of deformation theories of plasticity." *Journal of Applied Mechanics*, 26, 259-264.

Calcote, L. R. (1968). "Introduction to Continuum Mechanics." *Van Nostrand Reinhold Company, New York*.

Chakrabarty, J. (1987). "Theory of plasticity." *McGraw-Hill, New York*.

Davies, J. M. (2001). "Lightweight sandwich construction." *Blackwell Science, Iowa, USA*.

Doltsinis, I. (2000). "Elements of plasticiity: Theory and Computation." *WIT Press, UK*.

Folie, G. M. (1971). "The behavior and analysis of orthotropic sandwich plates." *Build. Sci.*, 57-67.

Forbes, A. T. (1989). "Strength tests on laser welded corrugated steel sandwich panels." *ARE TM 89215*.

Fung, T. C., Tan, K. H., and Lok, T. S. (1993). "Analysis of G-core sandwich plate decking." *Proc., 3rd Int. Offshore and Polar Engrg. Conf.,*, 4, 244-249.

Fung, T. C., Tan, K. H., and Lok, T. S. (1994). "Elastic constants for Z-core sandwich panels." *IJ. Struct. Engrg., ASCE*, 120(10), 3046-3055.

Fung, T. C., Tan, K. H., and Lok, T. S. (1996). "Shear stiffness DQx for C-core sandwich panels." *J. Struct. Engineering, ASCE*, 122(8), 958-966.

Giri, J., and Smitses, G. J. (1980). "Deflection Response of General Laminates Composite Plates to In-Plane and Transverse Loads." *Fiber Science and Technology*, 13, 225-242.

Gough, G. S., Elam, C. F., and de Bruyne, N. D. (1940). "The Stabilization of a Thin Sheet by a Continuous Supporting Medium." *J. Roy. Aero. Soc., Jan.*, 44, 12-43.

Hill, R. (1950). "The Mathematical Theory of Plasticity." *Clarendo, Oxford*.

Hu, L. W. (1956). "Studies on plastic flow of anistropic metals." *J. Appl. Mech., Sept*.

Holston, A. (1971). "Laminated orthotropic plates under transverse loading." *AIAA J.*, 9, 520-522.

Jensen, W. R., Falby, W. E., and Prince, N. (1966). "Matrix analysis methods for anisotropic inelastic structures." *AFFDL TR 65-220*.

Kachanov, L. M. (1971). "Foundations of the Theory of Plasticity." *North-Holland company, New York*.

Karam, V. J., and Telles, J. C. F. (1992). "The BEM applied to plate bending elastoplastic analysis using Reissner's theory." *Engineering analysis with boundary elements*, 9(4), 351-357.

Karbhari, V. M. (1997). "Appication of composite materials to the renewal twenty-first century infratructure." *Proceedings of the eleventh international conference on composite materials, Australian composite structures society, RMIT, Fishermens Bend, Melbourne, Australia*.

Kattan, M. R. (1995). "Steel sandwich construction for ships- a reality?" *Proceedings of the third international conference on sandwich construction, September 1995, Southampton, UK*.

Koiter, W. T. (1953). "Stress-strain relations, uniqueness and variational theorems for elastic-plastic materials with a singular yield surface." *Quarterly of applied mathematics*, 11, 350-354.

Koiter, W. T. (1960). "General theorems for elastic-plastic solids." *Progress in solid mechanics*, 1, 167-221.

Kujala, P., and Tuhkuri, J. (1995). "All-steel corrugated core sandwich panels for ship structures." *Proceedings of the third international conference on sandwich construction, September 1995, Southampton, UK*.

Libove, C., and Batdorf, S. B. (1948). "A general small-deflection theory for flat sandwich plates." *NACA TN 1526*.

Libove, C., and Hubka, R. E. (1951). "Elastic constants for corrugated core sandwich plates."

Lok, T. S., and Cheng, Q. H. (2000). "Elastic stiffness and behavior of truss-core sandwich panel." *J. Struct. Engineering, ASCE,* 126(5), 552-559.

Lubliner, J. (1990). "Plasticity Theory." *Macmillan, New York*.

MATLAB. (2000). "Using MATLAB, Version 6." *The Math Works, Inc.*

Marcal, P. V., and King, I. P. (1967). "Elastic-plastic analysis of two-dimensional stress system by the finite element method." *Int. J. Mech. Sci*, 9, 143-155.

Martine, J. B., Reddy, B. D., Griffin, T. B., and Bird, W. W. (1987). "Applications of mathematical programming concepts to incremental elastic-plastic analysis." *Eng. Struct.*, 9, July, 171-176.

Marsico, T. A., Denney, P. E., and Furio, A. (1993). "Laser welding of lightweight structural steel panels." *Proceedings of the laser materials processing* conference, ICALEO'93, Olrando.

Mendelson, A. (1983). "Plasticity : theory and application." *Macmillan, New York*.

Mindlin, R. D. (1951). "Influence of rotatory interia and shear in flexural motion of isotropic, elastic plates." *J. Appl. Mech*, 18, 1031-1036.

Montague, P., and Norris, C. (1987). "Spot-welded, corrugated-core, sandwich steel panels subjected to lateral load." *Steel Structures, Proc. Interational Conference on Steel and Aluminium Structures, Cardiff, UK, July*, 8-10.

Moshaiov, A., and Vorus, W. S. (1986). "Elasto-plastic plate bending analysis by boundary element method with initial plastic moments." *Int. J. Solids Structures*, 22(11), 1213-1229.

Niyogi, A. K. (1973). "Nonlinear Bending Of Rectangular Orthotropic Plates." *Int. J. Solid Structures*, 9, 1133-1139.

Noor, A. K., Burton, W. S., and Bert, C. W. (1996). "Computational models for sandwich panels and shells." *Applied Mechanics Reviews*, 49(3), 155-199.

Norris, C., Montague, P., and Tan, K. H. (1989). "All-steel structural panels to carry lateral load; experimental and theoretical behavior." *The Structural Engineer*, 67.

Oden, J. T. (1969). "Finite element applications in nonlinear structural analysis." *Proc. Symp. On Application of Finite Element Methods in Civil Engineering, Vanderbilt University, Tennessee*.

Olszak, W., and Urbanowski, W. (1956). "The plastic procential and generalized distortion energy in the theory of non-homogeneous anisotropic elastic-plastic bodies." *Arch. Mech. Stos.*, 4(8).

Owen, D. R. J., and Figueiras, J. A. (1983a). "Anisotropic elasto-plastic finite element analysis of thick and thin plates and shells." *International journal for numerical methods in engineering*, 19, 541-566.

Owen, D. R. J., and Figueiras, J. A. (1983b). "Elasto-plastic analysis of anisotropic plates and shells by the semiloof element." *International journal for numerical methods in engineering*, 9, 521-539.

Owen, D. R. J., and Hinton, E. (1980). "Finite elements in plasticity: theory and practice." *Pineridge Press, U.K.*

Pagano, N. J. (1970). "Exact solutions for rectangular bidirectional composites and sandwich plates." *J. Composite Mater.*, 4, 20-34.

Plantema, F. J. (1966). "Sandwich construction: the bending and buckling of sandwich beams, plates and shells." *Willey, New York*.

Reissner, E. (1945). "The effect of transverse shear deformation on the bending of elastic plate." *J. Appl. Mech*, 12, 69-76.

Shames, I. H., and Cozzarelli, F. A. (1992). "Elastic and Inelastic Stress Analysis." *Prentice Hall, New Jersey*.

Shi, G., and Voyiadjis, C. Z. (1992). "A simple non-layered finite element for the elasto-plastic analysis of shear flexible plates." *International journal for numerical methods in engineering*, 33, 85-99.

Stein, M., and Mayers, J. (1950). "A small-deflection theory for curved sandwich plates." *NACA TN 2017*.

Tan, K. H., Montague, P., and Norris, C. (1989). "Steel sandwich panels: finite element, closed solution, and experimental comparisons, on 6m x 2.1m panel." *Structural Engineer, London*, 67(9), 159-166.

Telles, J. C. F., and Brebbia, C. A. (1979). "On the application of the boundary element method to plasticity." *Applied Mathematical Modelling*, 3, 446-470.

Telles, J. C. F. (1983). "Boundary element method applied to inelastic problems." *Spring-Verlag, New York*.

Telles, J. C. F., and Carrer, J. A. M. (1991). "Implicit procedures for the solution of elastioplastic problems by the boundary element method." *Mathematical and Computer Modelling*, 15, 303-311.

Valliappan, S., Boonlaulohr, P., and Lee, I. K. (1976). "Non-linear analysis for anisotropic materials." *International journal for numerical methods in engineering*, 10, 597-606.

Ventsel, E., and Krauthammer, T. (2001). "Thin Plates and Shells." *Marcel Dekker, New York*.

Vinson, J. R. (1999). "The behavior of sandwich structures of isotropic and composite materials." *Technomic Publ, Lancaster PA*.

Vinson, J. R. (2001). " Sandwich structures." *Applied Mechanics Reviews*, 54(3), 201-214.

Whang, B. (1969). "Elasto-plastic orthotropic plates and shells." *Proc. Symp. On Application of Finite Element Methods in Civil Engineering, Vanderbilt University, Tennessee*.

Whitney, J. M. (1969). "Bending-extensional coupling in laminated plates under transverse loading." *J. Composite Mater.*, 3, 20-28.

Whitney, J. M., and Leissa, A.W. (1970). "Analysis of a simply supported laminated anisotropic rectangular plate." *AIAA J.*, 8, 28-33.

Wiernicki, J. C., Liem, F., Woods, G. D., and Furio, A. J. (1991). "Structural analysis method for lightweight metallic corrugated-core sandwich panels subjected to blast loads." *Naval Engineers Journal*, May.

Williams, D., Leggett, D. M. A., and Hopkins, H. G. (1941). "F lat Sandwich Panels under Compressive End Loads." *A.R.C., R&M 1987*.

Zenkert, D. (1995). "An introduction to sandwich construction." *EMAS Publications, West Midlands, U.K.*

Zienkiewicz, O. C., Valliappan, S., and King, I. P. (1969). "Elasto-plastic Solutions of Engineering Problems, 'Initial Stress', Finite Element Approach." *Int. J. num. Mech. Engng*, 1(1), 75-100.

Appendix A

ELASTIC CONSTANTS

The dimensions of the corrugation unit are defined in Figure **A-1**. To analyze a corrugated-core sandwich plate seven physical constants, D_x, D_y, D_{xy}, D_{Qx}, D_{Qy}, u_x and u_y, are required. Precise formulas for evaluating these constants of corrugated-core sandwich panels are given by Libove and Hubka (1951).

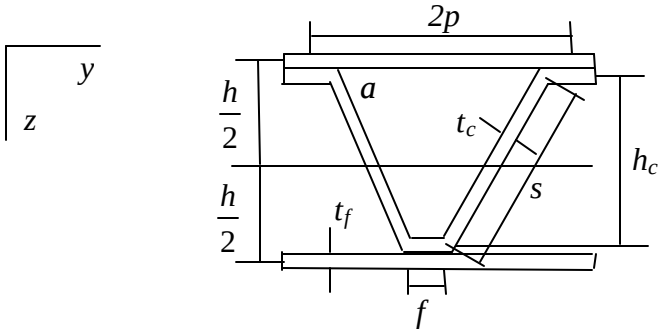

Fig. A-1: Dimensions of the corrugation unit

$$D_x = E_c I_c + E_f I_f \qquad \textbf{(A.1)}$$

$$D_y = \frac{E_f I_f}{1 - u_f^2 \left(1 - \frac{E_f I_f}{D_x}\right)} \qquad \textbf{(A.2)}$$

$$u_x = u_f, u_y = u_f \frac{D_y}{D_x} \tag{A.3}$$

$$D_{xy} = 2G_f I_f ; G_f = \frac{E_f}{2(1+u_f)} \tag{A.4}$$

$$I_f = 2\left[2p \times t_f \times \left(\frac{h}{2}\right)^2\right] \tag{A.5}$$

$$\begin{aligned} I_c &= 2\left[f \times t_c \times \left(\frac{h_c}{2}\right)^2\right] + \frac{2 \times t_c \times s^3}{12} \sin^2 q \\ &= \frac{f \times t_c \times h_c^2}{2} + \frac{2 \times t_c \times h_c^3}{12 \sin q} \end{aligned} \tag{A.6}$$

Where subscripts f and c refer to facings and core of the sandwich plate, respectively; A_c and I_c are the core area and the moment of inertia of the cross-section of the core parallel to yz plane taken about centroidal axis of corrugation cross section per unit width of corrugation; I_f is the moment of inertia per width of the faces considered as membranes, with respect to the sandwich middle surface.

$$D_{Qy} = \frac{ShE_c}{1-u_c^2}\left(\frac{t_c}{h_c}\right)^3$$

$$D_{Qx} \approx \frac{G_c t_c h^2}{pl} = \frac{G_c t_c^2}{\overline{A}_c}\left(\frac{h}{p}\right)^2$$

$$\overline{A}_c = \frac{lt_c}{p}$$

Where S is non-dimensional parameter depending upon the geometry of cross-section of the corrugation and given in graphs prepared by Libove and Hubka (1951) and l is the length of one corrugation-leg center line shown in Figure **A-2**.

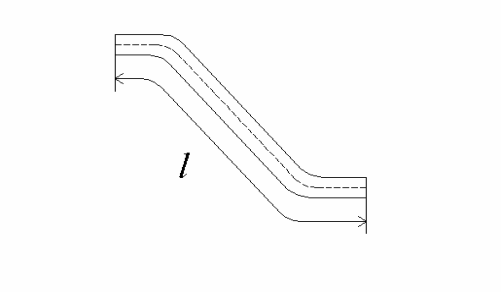

Fig. A-2: One corrugation leg

Appendix B

ORTHOTROPIC PARAMETERS OF PLASTICITY

Initial parameters $A_{11}^0, A_{12}^0, A_{22}^0, A_{33}^0$

The equivalent moment is defined as:

$$\overline{M}^2 = \frac{A_{11}}{2} M_x^2 - A_{12} M_x M_y + \frac{A_{22}}{2} M_y^2 + 3A_{33} M_{xy}^2 \qquad \textbf{(B.1)}$$

The orthotropic parameters in Eq. **B.1**, $A_{11}, A_{12}, A_{22}, A_{33}$, can be determined from the yield stress in various directions. The initial parameters, $A_{11}^0, A_{12}^0, A_{22}^0, A_{33}^0$, are obtained by successively permitting all moments in the yield criterion equal to zero except the considered one. The approach is similar to the one suggested by (Whang 1969).

Let M_{x0}, M_{y0} are the uniaxial yield bending moments in the x and y directions, respectively. M_{xy0} is the yield twisting moment. Those yield moments can be determined by the uniaxial pure bending tests for a strip-beams cut from the sandwich plate in the adopted direction. Therefore, the tests in the direction of corrugation, x-axis, and in the direction perpendicular to the corrugation, y-axis, as well as from the twisting test are necessary. Moreover, one more test is needed for determining the fourth parameter, namely, a uniaxial bending test for a strip beam cut from given sandwich plate at an angle q from the x axis. Let the corresponding uniaxial bending moment is M_{q0}.

By successively letting all the moments in Eq. **B.1** be equal to zero and letting $\overline{M}_0$ be the equivalent initial uniaxial yield moment in the y direction, i.e., setting $\overline{M}_0 = M_{y0}$, we obtain

$$A_{22}^0 = \frac{2\overline{M}_0^2}{M_{y0}^2} = 2 \qquad \textbf{(B.2)}$$

It is assumed that whenever the equivalent moment reaches the yield moment M_0 the whole cross section plastifies simultaneously. This assumption has been discussed in section 3.3.

Similarly,

$$A_{11}^0 = \frac{2\overline{M}_0^2}{M_{x0}^2} = 2\left(\frac{\overline{M}_0}{M_{x0}}\right)^2 \qquad \textbf{(B.3)}$$

$$A_{33}^0 = \frac{\overline{M}_0^2}{3M_{xy0}^2} = \frac{1}{3}\left(\frac{\overline{M}_0}{M_{xy0}}\right)^2 \qquad \textbf{(B.4)}$$

As mentioned in previous paragraph, to obtain A_{12}^0, it is necessary to conduct one more test for a strip beam cut at angle q from the x aixs shown in Figure **B-1** and subjected to pure bending due to the moment M_q. Thus, the following relations take place

$$M_x = M_q \cos^2 q$$

$$M_y = M_q \sin^2 q \qquad \textbf{(B.5)}$$

$$M_{xy} = M_q \cos q \sin q$$

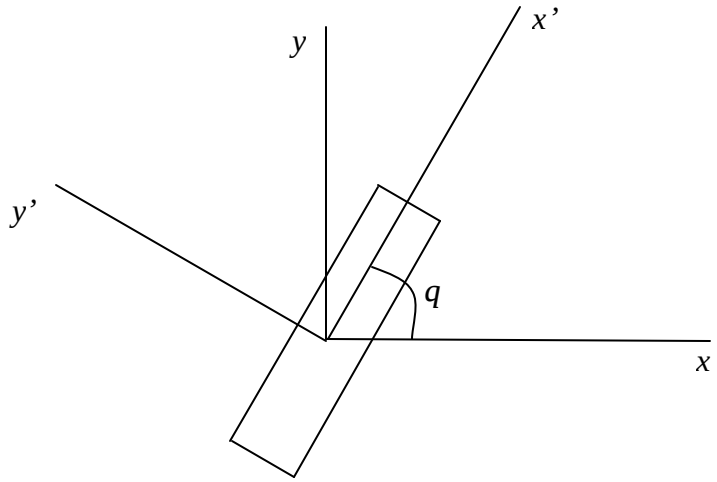

Fig. B-1: Strip beam in q **direction for** A_{12}^0

Substituting Eq. **B.5** into Eq. **B.1**, the equivalent yield moment reduces to

$$\overline{M}_0^2 = M_{q0}^2 \left[\frac{A_{11}^0}{2}\cos^2 q + \frac{A_{22}^0}{2}\sin^2 q - \left(\frac{A_{11}^0}{2} + A_{12}^0 + \frac{A_{22}^0}{2} - 3A_{33}^0 \right)\sin^2 q \cos^2 q \right] \quad \textbf{(B.6)}$$

Now, let $q=45^0$, thus Eq. **B.6** brings to the following form

$$8\overline{M}_0^2 = M_{045}^2 \left(A_{11}^0 + A_{22}^0 - 2A_{12}^0 + 6A_{33}^0 \right) \quad \textbf{(B.7)}$$

When Eq. **B.2,** Eq. **B.3,** and Eq. **B.4** are substituted into Eq. **B.7**, the coefficient A_{12}^0 can finally be expressed as

$$A_{12}^{0} = 1 + \left(\frac{\overline{M}_0}{M_{x0}}\right)^2 + \left(\frac{\overline{M}_0}{M_{xy0}}\right)^2 - \left(\frac{2\overline{M}_0}{M_{045}}\right)^2 \qquad \textbf{(B.8)}$$

The calculations of those uniaxial yield moments used in previous equations have been derived in section 3.3.1. In Eq. **B.7** and Eq. **B.8**, we have the bending yield moment at 45 degree from x axis. In reality, M_{045} is an independent parameter. However, for simplicity, we will make an assumption that Eq. **B.9**

$$M_{045} = \frac{1}{2}\left(M_{x0} + M_{y0}\right) \qquad \textbf{(B.9)}$$

Subsecquent parameters $A_{11}, A_{12}, A_{22}, A_{33}$

Since for a strain-hardening material, the equivalent moment and the uniaxial yield moments vary, A_{11}, A_{12}, A_{22} and A_{33} should vary also. To consider a pure bending of the strip beam cut from the plate in x direction, the strip beam is subjected to the moment M_x. Let the corresponding maxium bending moment reached by this strip beam be M_x^m. Similarly, for a test in the y direction, the maximum bending moment is M_y^m. The plastic deformations that correspond to the above moments are c_x^p and c_y^p, respectively. Let the strain-hardening relations be linear with the slops of H_x and H_y as shown in Figure **B-2** . The plastic work done by the above moments in x axis and y axis should be the same.

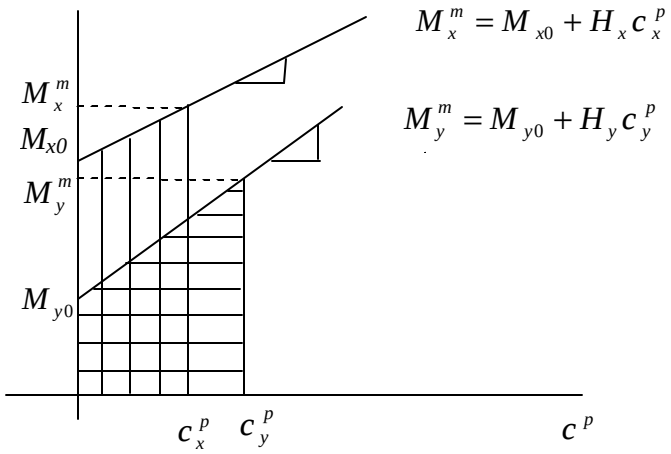

Fig. B-2: Moment vs. plastic curvature curve in *x* and *y* directions

The plastic work done by M_x^m can be expressed as

$$W_x^p = \frac{1}{2} c_x^p \left(M_x^m + M_{x0} \right) \tag{B.10}$$

c_x^p can be expressed as

$$c_x^p = \frac{M_x^m - M_{x0}}{H_x} \tag{B.11}$$

Substituting c_x^p into Eq. **B.11**, we can obtain

$$W_x^p = \frac{\left(M_x^m \right)^2 - \left(M_{x0} \right)^2}{2H_x} \tag{B.12}$$

Similarly, the plastic work in terms of M_y^m is

$$W_y^p = \frac{\left(M_y^m \right)^2 - \left(M_{y0} \right)^2}{2H_y} \tag{B.13}$$

By equating Eq. **B.12** and Eq. **B.13**, M_x^m becomes

$$\left(M_x^m\right)^2 = \frac{H_x}{H_y}\left[\left(M_y^m\right)^2 - M_{y0}\right] + M_{x0}^2 \qquad \textbf{(B.14)}$$

Let $\overline{M} = M_y^m$, we obtain

$$A_{22} = 2\left(\frac{\overline{M}}{M_y^m}\right)^2 = 2 \qquad \textbf{(B.15)}$$

$$A_{11} = 2\left(\frac{\overline{M}}{M_x^m}\right)^2 = \frac{2\overline{M}^2}{\frac{H_x}{H_y}\left(\overline{M}^2 - M_{y0}^2\right) + M_{x0}^2} \qquad \textbf{(B.16)}$$

Similarly,

$$A_{33} = \frac{\overline{M}}{3\left(M_{xy}^m\right)^2} = \frac{\overline{M}^2}{3\left[\frac{G_p}{H_y}\left(\overline{M}^2 - M_{y0}^2\right) + M_{xy0}^2\right]} \qquad \textbf{(B.17)}$$

$$A_{12} = 1 + \frac{A_{11}}{2} + 3A_{33} - \frac{4\overline{M}^2}{\frac{H_{45}}{H_y}\left(\overline{M}^2 - M_{y0}^2\right) + M_{450}^2} \qquad \textbf{(B.18)}$$

Where G_p and H_{45} are the linear strain-hardening slopes corresponding to M_{xy}^m vs. c_{xy}^p and M_{45}^m vs. c_{45}^p, respectively.

VITA

Wan-Shu Chan

Place, data of birth

- Taipei, Taiwan, 1971

Education

- Ph.D. in Civil Engineering, The Pennsylvania State University, 2004
- M.Sc. in Structural Engineering, National Cheng-Kung University, Taiwan, 1996
- B.Sc. in Civil Engineering, National-Cheng Kung University, Taiwan, 1994

Employment

- Research Assistant, Pennsylvania State University, 2001 ~ 2004
- Civil Engineer, Taipei City Government, 1998 ~ 2001
- Lieutenant/ Facilities Engineering Officer, R.O.C. Air Force, 1996 ~ 1998

Publications

- Wan-Shu Chang, E. Ventsel, T. Krauthammer, J. John *Nonlinear analysis of corrugated-core sandwich plates with various boundary conditions*. (Submitted for publication in the journal Computers & Structures)
- Wan-Shu Chang, E. Ventsel, T. Krauthammer, J. John, *Bending behavior of corrugated-core sandwich plates*. (Submitted for publication in the journal Composite Structures)
- Wan-Shu Chang, J. John, E. Ventsel, T. Krauthammer, *Investigation of behavior of corrugated-core sandwich plates*. (Accepted by 11th Int. Conference of Composites/NANO Engineering, Aug. 8-14, 2004)
- E. Ventsel, T.Krauthammer, J.John, Wan-Shu Chang, *Nonlinear analysis of corrugated sandwich plates*, 9th annual Int. Conference of Composite Engineering, San-Diego CA, Jun 29-Jul 8 2002.